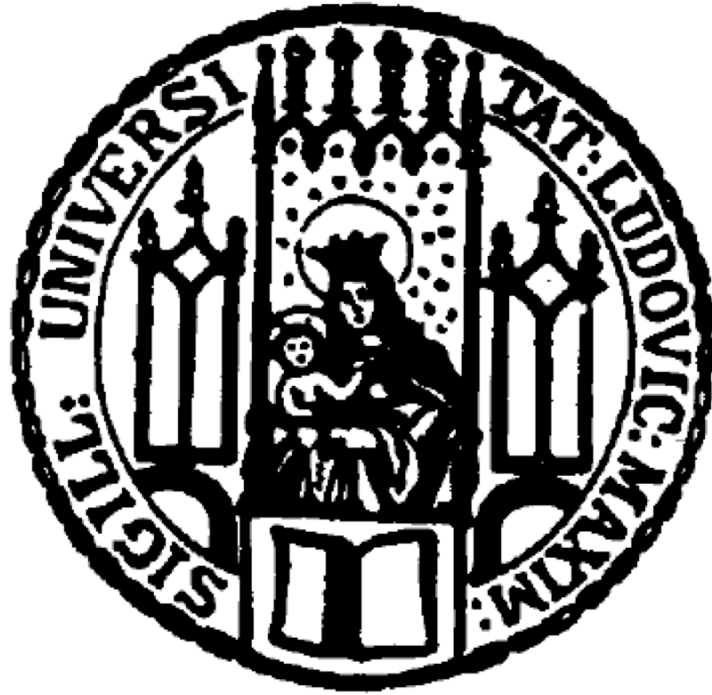


**Some *ABCA3* mutations elevate ER stress and initiate apoptosis of lung epithelial cells**



Nina Weichert

Aus der Kinderklinik und Kinderpoliklinik  
im Dr. von Haunerschen Kinderspital  
der Ludwig-Maximilians-Universität München  
Direktor: Prof. Dr. med. Dr. sci. nat. Christoph Klein

**Some *ABCA3* mutations elevate ER stress and initiate  
apoptosis of lung epithelial cells**

Dissertation  
zum Erwerb des Doktorgrades der Humanmedizin  
an der Medizinischen Fakultät der  
Ludwig-Maximilians-Universität zu München

Vorgelegt von  
Nina Weichert  
aus Heidelberg  
2011

**Mit Genehmigung der Medizinischen Fakultät  
der Universität München**

1. Berichterstatter: Prof. Dr. Matthias Griese

2. Berichterstatter: Prof. Dr. Dennis Nowak

Mitberichterstatter: Priv. Doz. Dr. Angela Abicht

Prof. Dr. Michael Schleicher

Mitbetreuung durch den

promovierten Mitarbeiter: Dr. Suncana Kern

Dekan: Herr Prof. Dr. med. Dr. h. c. Maximilian Reiser,  
FACR, FRCR

Tag der mündlichen Prüfung: 24.11.2011

*Diese Arbeit widme ich meiner Mutter*

# Table of Contents

<b>1. Abstract</b> .....	<b>1</b>
<b>2. Zusammenfassung</b> .....	<b>2</b>
<b>3. Introduction</b> .....	<b>3</b>
<b>3.1 Pediatric interstitial lung disease</b> .....	<b>3</b>
3.1.1 Epidemiology of pILD .....	3
3.1.2 Classification of pILD .....	4
3.1.3 Genetic surfactant dysfunction disorders .....	5
3.1.4 Clinical diagnostics and therapy of pILD .....	6
3.1.5 Prognosis of pILD .....	6
<b>3.2 ATP- binding cassette protein A3 (ABCA3)</b> .....	<b>7</b>
3.2.1 ABC transporters .....	7
3.2.2 General on the ABCA3 protein .....	8
3.2.3 Function of ABCA3 .....	8
3.2.3.1 Localization and lamellar body biogenesis .....	8
3.2.3.2 ABCA3 is a lipid transporter .....	9
3.2.3.3 Categorization of ABCA3 mutations .....	9
3.2.4 ABCA3 in lung disease .....	10
3.2.4.1 Early and late onset of lung disease .....	10
3.2.4.2 Genotype-phenotype interplay .....	11
3.2.4.3 Outer stressor .....	11
3.2.4.4 Histopathological pattern .....	11
3.2.4.5 Therapy .....	12
3.2.5 ABCA3 mutations in this study.....	12
<b>3.3 How misfolded proteins disturb cell homeostasis</b> .....	<b>14</b>
3.3.1 Function of the endoplasmic reticulum .....	14
3.3.2 Induction of the quality control system by unfolded proteins .....	15
3.3.3 Induction of apoptosis .....	17
<b>3.4 ER stress and apoptosis contribute to disease pathogenesis</b> .....	<b>18</b>
<b>3.5. An objective</b> .....	<b>20</b>
<b>4. Materials</b> .....	<b>21</b>
<b>4.1 Chemicals</b> .....	<b>21</b>
<b>4.2 Equipment</b> .....	<b>21</b>
<b>4.3 Enzymes and kits</b> .....	<b>22</b>
<b>4.4 Primers</b> .....	<b>23</b>

<b>4.5 Vectors</b> .....	<b>24</b>
<b>4.6 Antibodies</b> .....	<b>25</b>
<b>4.7 Bacterial strains and cell lines</b> .....	<b>27</b>
<b>5. Methods</b> .....	<b>27</b>
<b>5.1 Molecular biological methods</b> .....	<b>27</b>
5.1.1 Cloning strategy: Generation of pUB6- <i>ABCA3-HA</i> vector .....	27
5.1.2 Site-directed point mutagenesis.....	28
5.1.3 DNA- sequencing .....	29
5.1.4 <i>E.coli</i> DH5 culture .....	29
5.1.5 Generation of competent <i>E.coli</i> DH5 .....	29
5.1.6 Transformation of <i>E.coli</i> DH5 .....	30
5.1.7 Plasmid-DNA isolation .....	30
5.1.8 Restriction .....	30
<b>5.2 Mamalian cell culture</b> .....	<b>31</b>
5.2.1 Media and growth conditions .....	31
5.2.2 Mycoplasma testing .....	31
5.2.3 Transfection of A549 cells.....	31
<b>5.3 Biochemical methods</b> .....	<b>31</b>
5.3.1 Whole cell lysates preparation .....	31
5.3.2 Crude membrane preparation.....	32
5.3.3 Determination of protein concentration .....	32
5.3.4 Deglycosylation-assay .....	32
5.3.5 SDS-Polyacrylamide Gel Electrophoreses (SDS-PAGE) .....	33
5.3.6 Western Blotting.....	33
5.3.7 Liposome preparation and NBD-lipid uptake .....	34
5.3.8 RNA isolation from A549 cells .....	34
5.3.9 RT-PCR .....	34
5.3.10 Densitometric analysis of the intensity of protein and DNA bands .....	35
5.3.11 Immunofluorescence.....	35
5.3.12 FACS analyses .....	36
5.3.13 Statistical analyses .....	36
<b>6. Results</b> .....	<b>37</b>
<b>6.1 Creating a model system to analyse the effect of ABCA3 mutations on alveolar type II cells' homeostasis</b> .....	<b>37</b>
6.1.1 Generation of pUB6- <i>hABCA3</i> vector and site-directed point mutagenesis.....	37
6.1.2 Optimization of transfection procedure in A549 cell line .....	39
<b>6.2 General characterization of R43L, R280C and L101P ABCA3 mutations</b> .....	<b>40</b>

6.2.1 Localization and trafficking.....	41
6.2.2 ABCA3 WT and mutant protein processing and maturation in A549 cells.....	44
6.2.3 Glycosylation of ABCA3 protein.....	45
6.2.4 Functional assay.....	46
6.2.5 Biogenesis of LAMP3 <sup>+</sup> vesicles induced by ABCA3-WT protein expression.....	47
<b>6.3 Induction of ER stress by mutant ABCA3 expression.....</b>	<b>48</b>
6.3.1 L101P and R280C mutations upregulate ER stress marker BiP.....	49
6.3.2 ABCA3 mutants influence expression of Hsp90.....	50
6.3.3 No influence on calnexin expression by ABCA3 mutations.....	50
6.3.4 L101P and R280C mutations increase susceptibility of A549 cells to ER stress...	51
<b>6.4 L101P and to a lesser extent R280C mutation induce apoptosis of A549 cells ...</b>	<b>54</b>
6.4.1 Annexin V/PI staining.....	54
6.4.2 GSH decrease.....	55
6.4.3 Caspase 3 activation.....	55
<b>6.5 Prolonged ER stress leads to apoptosis through caspase 4 activation in A549 cells expressing R280C and L101P mutations.....</b>	<b>58</b>
<b>6.6 Epithelial-mesenchymal transition in A549 cells expressing ABCA3 defect proteins.....</b>	<b>59</b>
6.6.1 Induction of epithelial-mesenchymal transition in A549 cell line.....	60
6.6.2 Induction of epithelial-mesenchymal transition in A549 cells expressing ABCA3 defect protein.....	61
<b>7. Discussion.....</b>	<b>64</b>
7.1 General characterization of the <i>ABCA3</i> mutations R43L, R280C and L101P.....	64
7.2 Induction of ER stress and UPR system by <i>ABCA3</i> mutants.....	67
7.3 Induction of apoptotic cell death by <i>ABCA3</i> mutations.....	68
7.4 EMT in alveolar type II cells overexpressing <i>ABCA3</i> mutations.....	69
7.5 Conclusion.....	71
7.6. Future directions.....	72
<b>8. References.....</b>	<b>73</b>
<b>9. List of tables.....</b>	<b>79</b>
<b>10. List of figures.....</b>	<b>80</b>
<b>11. Danksagung.....</b>	<b>82</b>
<b>12. Publication list.....</b>	<b>83</b>

## List of Abbreviations

$\alpha$ 1-AT	$\alpha$ 1 antitrypsin
A549	human type II lung adenocarcinoma epithelial cell line
ABCA1	ATP binding cassette A1
ABCA3 transporter	ATP-binding cassette A3 transporter
ABCA4	ATP binding cassette A4
AIP	acute interstitial pneumonia
ASK1	apoptosis signaling-regulating kinase 1
ATF6	activating transcription factor 6
ATF4	activating transcription factor 4
ATP	adenosine triphosphate
BAL	broncho-alveolar lavage
BiP	binding protein= GRP78
BIP	bronchiolitis obliterans with interstitial pneumonia
bp	base pair
BSA	bovine serum albumin
Ca <sup>2+</sup>	calcium
cAMP	cyclic adenosine monophosphate
Cer	ceramid
CFTR	Cystic Fibrosis transmembrane conductance regulator
CHOP	CEBP homology protein= growth arrest and DNA damage inducible gene 153
Cl <sup>-</sup>	chloride
COP	cryptogenic organizing pneumonia
DAPI	4',6-Diamidin-2'-phenylindol-dihydrochloride
DIP	desquamative interstitial pneumonia
DLCO	diffusing capacity of the lung for carbon monoxide
DNA	deoxyribonucleotid acid
DPLD	diffuse parenchymal lung disease
DPPC	dipalmitoyl phsophatidylcholine
DTT	dithiothreitol
ECAD	e-cadherin
ECL	enhanced chemiluminescence

ECMO	extracorporeal membrane oxygenation
E.coli	escherichia coli
EEA-1	early endosome antigen-1
EDTA	ethylenediaminetetraacetic acid
eIF2 $\alpha$	eukaryotic translation initiation factor 2 $\alpha$
EMT	epithelial-mesenchymal transition
ER	endoplasmatic reticulum
ERAD	ER-associated degradation
ERS	European Respiratory Society
FACS	fluorescence activated cell sorting
FBS	fetal bovine serum
FEV1	1 second forced expiratory volume
FRET	fluorescence resonance energy transfer
FVC	forced vital capacity
GFP	green fluorescence protein
GIP	giant-cell interstitial pneumonia
GM130	golgi matrix protein of 130 kDa
GM-CSF	granulocyte-macrophage colony-stimulating factor
HA	hemagglutinin
hABCA3	human ABCA3
HDL	high-density lipids
HEPES	4-(2-hydroxyethyl)-1-piperazineethanesulfonic acid
Hsp90	heat shock protein 90
HRCT	high-resolution computer tomography
HRP	horseradish peroxidase
hXBP1	hybrid XBP1
IL-1 $\beta$	interleucin 1 $\beta$
ILD	interstitial lung disease
IPF	idiopathic pulmonary fibrosis
IPP	idiopathic pulmonary pneumonitis
IRE1	ionsitol-requiring enzyme 1
JNK	c-Jun Nh2-terminal kinase
LAMP3	anti-human CD 63
LB	lamellar body
LIP	lymphoid interstitial pneumonia

LPC	lysophosphatidylcholin
mRNA	messenger ribonucleic acid
NaCl	natrium chloride
NSIP	nonspecific interstitial pneumonia
OD	optical density
OLB	open lung biopsy
PAGE	polyacrylamide gel electrophoresis
PAP	pulmonary alveolar proteinosis
PBS	phosphate buffered saline
PC	phosphatidylcholine
PE	phosphatidylethanolamine
PERK	ER resident transmembrane protein kinase
PFT	pulmonary function test
PG	phosphatidylglycerol
PI	phosphatidylinositol
pILD	pediatric interstitial lung disease
PS	phosphatidylserine
PVDF	polyvinyldiene fluoride
RB-IP	respiratory-bronchiolitis interstitial pneumonia
RDS	respiratory distress syndrome
RNA	ribonucleic acid
ROS	Reactive oxygen species
RPMI	Rosewell Park Memorial Insitute: cell culture medium
rRNA	ribosomal ribonucleic acid
RSV	respiratory synsytial virus
RT-PCR	reverse transcriptase polymerase chain reaction
SD	standard deviation
SDS	sodium dodecyl sulphate
SFTPB	mutation in the SP-B gene
SFTPC	mutation in SP-C gene
siRNA	small interfering ribonucleic acid
SM	sphingomyeline
SP-B	surfactant protein B
SP-C	surfactant protein C
sXBP1	spliced XBP1
TBB	transbronchial biopsy

TBS	tris-buffered saline
Tfb	transformation buffer
TGF- $\beta$	tissue growth factor- $\beta$
TLC	total lung capacity
TM	tunicamycin
TNF- $\alpha$	tumor necrose factor- $\alpha$
UIP	usual interstitial pneumonia
UPR	unfolded protein response
uXBP1	unspliced XBP1
VATB	video-assistant thoracic biopsy
wt	wild type
XBP1	X-box-binding protein 1
YFP	yellow fluorescence protein

## 1. Abstract

Mutations in the gene coding for the ATP binding cassette protein A3 (ABCA3) are known as the most frequent genetic cause of fatal neonatal respiratory distress syndrome and chronic interstitial lung disease (ILD) of children. ABCA3 transporter is localized to the limiting membrane of lamellar bodies, organelles for assembly and storage of pulmonary surfactant in alveolar epithelial type II cells. It transports surfactant phospholipids into lamellar bodies and is essential for their biogenesis. *ABCA3* mutations can result in either functional defects of the correctly localized ABCA3 or trafficking/folding defects where mutated ABCA3 remains in the endoplasmic reticulum (ER).

This study showed previously not examined cellular dysfunction in cultured lung epithelial A549 cells overexpressing the three ABCA3 mutations R43L, R280C and L101P. All three mutations were found in children with ABCA3-associated lung disease either with fatal neonatal respiratory distress syndrome (L101P and R43L) or chronic pediatric ILD (R280C). Cell biology of R43L and R280C mutations was studied here for the first time. L101P mutation was used as a known example of the trafficking/folding defect leading to the ER retention of ABCA3 protein.

Human lung epithelial A549 cells were transfected with vectors containing wild type ABCA3 or one of the three ABCA3 mutant forms, R43L, R280C and L101P, C-terminally tagged with YFP or hemagglutinin-tag. Localization/trafficking properties were analyzed by immunofluorescence and ABCA3 deglycosylation. Uptake of fluorescent NBD-labeled lipids into lamellar bodies was used as a functional assay. ER stress and apoptotic signaling were examined through RT-PCR based analyses of XBP1 splicing, immunoblotting or FACS analyses of stress- and apoptosis-proteins, Annexin V surface staining and determination of the intracellular glutathion level. Induction of epithelial-mesenchymal transition (EMT) was assessed by immunoblotting.

It was demonstrated that two *ABCA3* mutations, which affect ABCA3 protein trafficking/folding and lead to partial (R280C) or complete (L101P) retention of ABCA3 in the ER compartment, can elevate ER stress and susceptibility to it and induce apoptosis in A549 cells. A549 cells expressing L101P additionally gain a mesenchymal phenotype. R43L mutation, resulting in a functional defect of the properly localized ABCA3, had no effect on intracellular stress and apoptotic signaling.

These data suggest that expression of partially or completely ER localized ABCA3 mutant proteins induce raised intracellular stress and apoptotic cell death of the affected cells, which are factors that might contribute to the pathogenesis of genetic ILD via a fatal ER-stress/apoptosis/fibrogenesis-axis.

## 2. Zusammenfassung

Mutationen im ATP-Bindekassetten-Protein A3 (ABCA3) sind die häufigsten bekannten genetischen Ursachen für schwere Atemnotsyndrome bei Neugeborenen und für chronische interstitielle Lungenerkrankungen (ILD) im Kindesalter. Der ABCA3-Transporter ist in der äußeren Membran von Lamellarkörperchen lokalisiert, dem Speicherort von Surfactant in Alveolar Typ II Zellen. Er transportiert Phospholipide in die Lamellarkörperchen und ist essentiell für deren Bildung. *ABCA3* Mutationen zeigen entweder einen funktionellen Defekt des korrekt lokalisierten ABCA3 Proteins oder einen Transport-/Proteinfaltungs-Defekt des mutierten ABCA3 Proteins, welches im Endoplasmatischen Retikulum (ER) verbleibt.

Diese Studie zeigt die zuvor noch nicht untersuchten zellulären Fehlfunktionen der Lungenepithelzellen A549, welche die drei ABCA3 Mutationen R43L, R280C und L101P überexprimieren. Alle drei Mutationen wurden bei Kindern mit einer ABCA3-assoziierten Lungenerkrankung gefunden. Diese Kinder waren entweder an einem schweren neonatalen Atemnotsyndrom (L101P und R43L) oder einer chronischen kindlichen ILD (R280C) erkrankt. Zellbiologische Untersuchungen der R43L und R280C Mutationen wurden in dieser Studie zum ersten Mal durchgeführt. Die L101P Mutation wurde als bekanntes Beispiel eines Transport-/Proteinfaltungs-Defektes verwendet, der zu einer Akkumulation des ABCA3 Proteins im ER führt.

Humane Lungenepithelzellen A549 wurden mit Vektoren transfiziert, die das ABCA3-WT Protein oder eine der drei ABCA3 Mutationen R43L, R280C und L101P, C-terminal fusioniert mit einem YFP oder Hämagglutinin-Tag, enthalten. Lokalisations-/Transport-Eigenschaften wurden mittels Immunfluoreszenz und eines Deglykosylierungs-Assays analysiert. Die Aufnahme von fluoreszierenden NBD-markierten Lipiden in Lamellarkörperchen wurde als funktioneller Assay angewandt. ER Stress und Apoptosesignale wurden untersucht anhand von RT-PCR basierenden Messungen des XBP1-Splicing, Immunoblotting und FACS-Analysen von Stress-/Apoptose-Proteinen, Annexin V-Färbung und Bestimmung des intrazellulären Glutathion-Gehaltes. Die Induktion der epithelialen-mesenchymalen Transformation wurde anhand von Immunoblotting bemessen.

Es zeigte sich, dass in A549 Zellen die zwei *ABCA3* Mutationen, die Transport/Faltung des ABCA3 Proteins beeinflussen, zu partiellem (R280C) oder vollständigem (L101P) Verbleiben von ABCA3 im ER führen, ER Stress sowie die Anfälligkeit dafür erhöhen und Apoptose induzieren. A549 Zellen, die L101P überexprimieren, erlangten zusätzlich einen mesenchymalen Phänotyp. Die R43L Mutation zeigte einen funktionellen Defekt des richtig lokalisierten ABCA3 Proteins und hatte keinen Effekt auf intrazellulären Stress und Apoptosesignale.

Diese Daten lassen vermuten, dass die Expression von teilweise oder vollständig im ER verbleibendem mutiertem ABCA3 Protein in den betroffenen Zellen erhöhten intrazellulären Stress und Apoptose verursacht und damit ein Faktor ist, der zu der Pathogenese genetischer ILD über eine ER-Stress/Apoptose/Fibrogenese-Achse beitragen kann.

### 3. Introduction

#### 3.1 Pediatric interstitial lung disease (pILD)

Interstitial lung disease (ILD) in infants and children, also called diffuse parenchymal lung disease (DPLD), comprises a heterogeneous group of rare respiratory disorders affecting the pulmonary interstitium (1). Some entities are unique to children (1). These disorders are associated with high morbidity and mortality (2). Limited by the rarity of pediatric interstitial lung disease (pILD), these disorders are still poorly investigated and understood. Common characteristics of pILD are respiratory symptoms such as dyspnea, tachypnea, cyanosis, cough, wheezing and haemoptysis, that persist longer than three months, accompanied by abnormal pulmonary function tests (PFTs), impaired gas exchange, frequent respiratory infections and infiltrates on the chest x-ray (1,3).

##### 3.1.1 Epidemiology of pILD

To date, epidemiological analysis of pILD is difficult to obtain and the development of prospective trials requires a systematic multicenter cooperation. Current knowledge is based on case reports presenting patients' clinical features and course of disease. The estimative prevalence of ILDs in children is much lower than reported in adults (4-7): A national survey in the United Kingdom and Ireland revealed an estimated prevalence of 3,6 cases/million (4). A study conducted in Germany assessed an incidence of 1,32 new cases of pILD per 1 million of children per year (2). Parental consanguinity is confirmed in pILD in 7 % (8). Furthermore, in reviewing the family history it was shown that siblings suffered from similar disease in 10 %, suggesting a genetic influence (8). One main group of pILD is related to genetic surfactant dysfunction (2,9, Fig.1). Among these genetic surfactant abnormalities mutations in the *ABCA3* gene are most frequent (2).

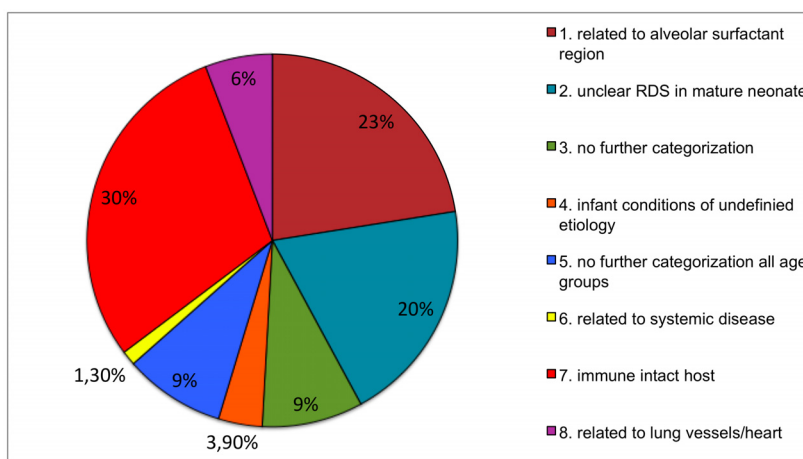


**Fig.1:** Distribution of pediatric ILD in Germany. pILD are classified into two groups: entities occurring in infants (1-4) and at all ages (5-8). In infants, surfactant dysfunction disorders are the most prevalent entities, whereas *ABCA3* mutations were the most frequent mutations in genes leading to surfactant abnormalities. According to (2)

### 3.1.2. Classification of pILD

Many attempts were made on an accurate classification scheme of pILD. For a long time, pILD was tried to fit into the adult's classification. Limited by different disease frequency, histopathological features and clinical outcome a direct adaption of the adult scheme failed.

A novel classification scheme of pILD was proposed by Deutsch and coworkers (10). For that multicenter study lung biopsies of 187 affected children less than 2 years old were collected from 1999 to 2004 in North America. Deutsch and coworkers provide a categorization scheme of almost all known entities in pILD (Fig.2). It mainly comprises two groups: entities prevalent in infants and entities in all ages. As shown in Figure 2 both groups consists of four subgroups. In entities seen in neonates and infants, the subgroups contain diffuse developmental disorders, alveolarization abnormalities, specific conditions of undefined etiology and surfactant disorders. Essential for surfactant production are the genes for the surfactant protein B and C gene (*SFTPB* and *SFTPC*) and the ATP-binding cassette protein A3 (*ABCA3*) gene. Therefore, abnormalities in these genes are involved in surfactant dysfunction and cause respiratory disease. Entities at all ages include disorders related to systemic diseases, in immune-intact hosts, in immunocompromised hosts and disorders masquerading as ILD.

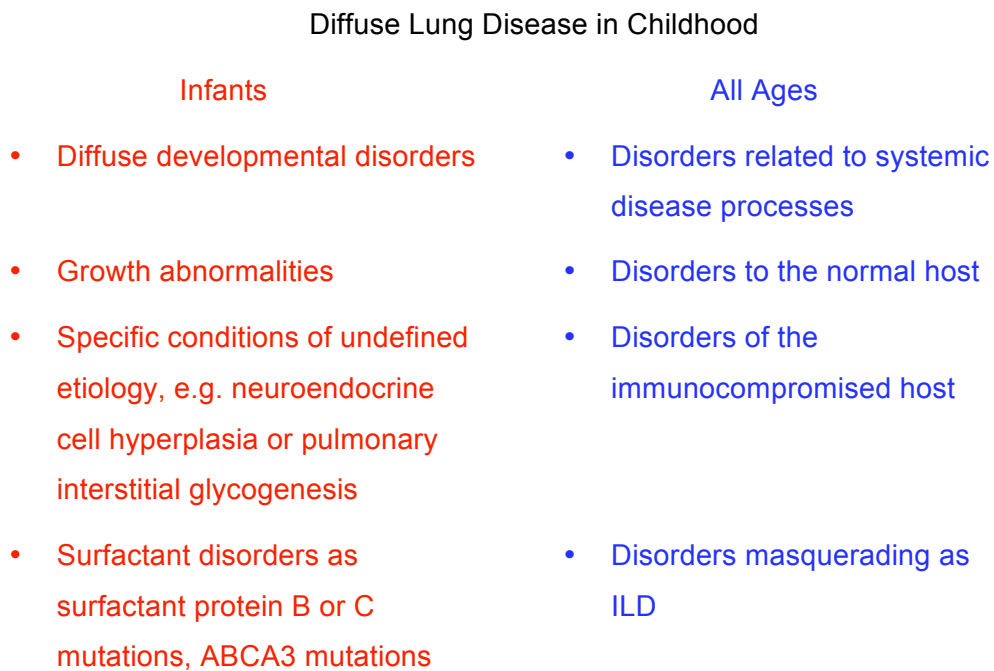


**Fig.2:** Classification of diffuse lung disease in children. This scheme provides a categorization of almost all known diffuse pediatric lung disease entities two groups: entities prevalent in infants and occurring at all ages. According to (10).

### 3.1.3 Genetic surfactant dysfunction disorders

Pulmonary surfactant is a complex mixture of 90 % lipids (mostly phospholipids) and 10 % surfactant-specific proteins A-D (11). It forms a film at the alveoli-air interface to reduce surface tension in the alveoli and to prevent alveolar collapse at the end of expiration. Alveolar type II cells (AT II) produce the surfactant mixture, which is stored within 120-180 lamellar bodies until it is secreted (12-14). Lamellar bodies (LB) are characterized by multiple lamellar structures and one surrounding outer membrane (15, Fig.3).

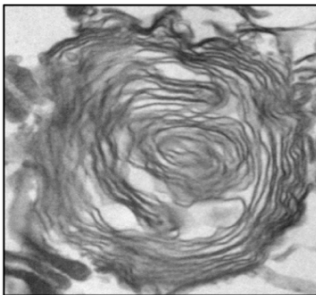


**Fig.3:** A representative electron micrograph of a lamellar body in A549 cells (provided by our research group). LBs show many regular concentric lamellae and appear like "onion-skin" (diameter: 0.1-2.4  $\mu\text{m}$ ).

Mutations in the genes encoding for surfactant protein B (SP-B) and C (SP-C) as well as for the ATP-binding cassette protein A3 (ABCA3) were found in genetic surfactant deficiency syndromes (16-22). In 1993, for the first time a genetic mechanism for fatal respiratory distress syndrome (RDS) was discovered in a full-term infant. An autosomal recessively inherited mutation in the SP-B gene (*SFTPB*) was identified to be the underlying cause for surfactant protein B deficiency and genetic respiratory disease (23). Since then, an increasing number of mutations in *SFTPB* have been identified in full-term infants presenting with severe RDS and a rapid progressive and fatal course (24-26). Also mutations in the SP-C gene (*SFTPC*) have been identified in newborns with RDS, but usually in *SFTPC*-associated lung disease, disease onset occurs later than in neonatal period and patients present with a more chronic clinical course (16,18).

Recently in 2004, when mutations in *SFTPB* or *SFTPC* have been excluded in newborns with neonatal lung disease unresponsive to exogenous surfactant, mutations in the *ABCA3* gene were recognized as a cause of lethal RDS and imbalance in surfactant composition (22, 27). Today, mutations in the *ABCA3* gene are known to cause not only fatal neonatal RDS but also chronic pILD in older children with a milder course (21). With more than 500 identified mutations, *ABCA3* deficiency is the most frequent known cause of genetic ILD today (own unpublished data, 22, 27, 28).

### **3.1.4 Clinical diagnostics and therapy of pILD**

Clinical signs and symptoms like hypoxia, tachypnea, dyspnea, retractions, failure to thrive, crackles, cough, wheeze and frequent respiratory infections are observed in infants and children with suspected diffuse parenchymal lung disease, but clinical presentation varies from asymptomatic to severe respiratory distress (29). As a first diagnostic study when plain chest x-ray provides insufficient insight, a high-resolution CT (HRCT) can show the most common feature of widespread ground-glass opacities, secondary honeycomb, interlobular septal and air wall thickening and fibrotic lesions (29). Lung biopsy and the histological analysis of lung tissue are often indispensable and crucial for the final diagnosis of pILD (8). According to the latest data and the increasing number of genetic pILD (2, 30, 31), the diagnostic workup of newborns and infants with probable genetic-associated lung disease should also include a DNA blood sample testing for mutations in the genes encoding for SP-C, SP-B and ABCA3.

The current treatment of pILD is based on the clinical experience from small case series in children and from clinical trials in adults. Affected newborns with severe respiratory distress onset directly after birth require mechanical ventilation and application of exogenous surfactant. Generally, therapy aims for the suppression of inflammation and prevention of fibrogenesis (29). Over half of the patients receive systemic steroids and a minor group profits additionally from further immunosuppressive, anti-inflammatory or anti-fibrotic drugs as hydroxychloroquine, azathioprine and methotrexate for weeks, months or years (2, 10). As children are sometimes unresponsive to drug-therapy, the ultimate option is lung transplantation. Today controlled clinical trials in children are conducted for evidence based treatment recommendations.

### **3.1.5 Prognosis of pILD**

Today morbidity and mortality in pILD is pretty high, but also varying between different entities. The overall mortality in pILD is around 15% and 21% (9, 29). Whereas better prognosis and lower mortality is reported for children with neuroendocrine cell hyperplasia of infancy or pulmonary interstitial glycogenesis, other forms of pILD, especially genetic surfactant deficiency syndromes, are associated with worse outcome. Particularly for ABCA3-related lung disease mortality is pretty high (10, 22).

## 3.2 ATP- binding cassette protein A3 (ABCA3)

### 3.2.1 ABC transporters

ABCA3 is a member of the large family of the ATP-binding cassette (ABC) transporters. The ABC transporters, including family A-F, are transmembrane proteins that utilize energy of ATP hydrolysis to drive the transport of a variety of substrates across biological cellular or intracellular membranes (32, 33). The ABC family shares a common structure. It is characterized by the full transporter structure with 12 transmembrane domains, two cytoplasmic ATP-binding sides and various conserved motives (Fig.4).

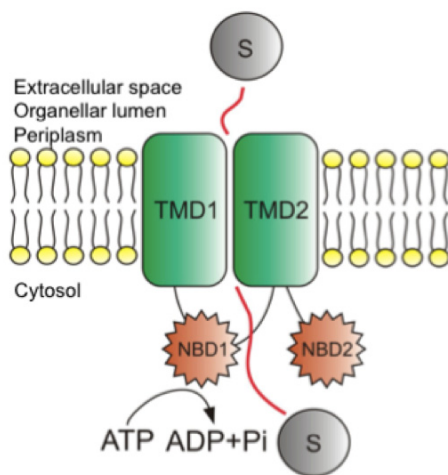


**Fig.4:** Structure of an ABC-transporter: Representative of the twelve transmembrane domains (TMD), here two TMDs are shown (TMD1 and TMD2) with the two cytoplasmic nucleotide-binding domains (NBD1 and NBD2). ATP-hydrolysis drives the transport of the substrates (S) (According to (34)).

In humans, the A subfamily consists of the members ABCA1 to ABCA13. Many members play similar roles especially in lipid transport. For example, ABCA1 and ABCA4 transport cholesterol and phosphatidylethanolamine, respectively (35-37).

Several members of the ABC superfamily are well known for their role in inherited disorders (38). Particularly, the most frequent genetic lung disease named cystic fibrosis is caused by mutations in *ABCC7* gene, encoding for CFTR. In the A subfamily not only ABCA3 deficiency is recognized as a cause for genetic disease, also other members have been known for associated inherited disorders before. For example, mutations in the human *ABCA1* gene cause Tangier disease with the accumulation of cholesterol, HDL deficiency, early onset of arteriosclerosis and peripheral neuropathy and mutations in the human *ABCA4* gene cause Stargardt's macular dystrophy (36, 37, 39, 40).

### 3.2.2 General on the ABCA3 protein

First, ABCA3 protein was found in thyroid tissue (33), followed by a wide variety of other tissue as brain, heart, kidney, stomach, pancreas and platelets. However, its highest protein expression levels are found in lung tissue, particularly in alveolar type II cells (41-43). The expression level of ABCA3 is developmentally regulated, increases prior to birth and is upregulated in a glucocorticoid-dependent manner *in vitro* (41, 43, 44).

The ABCA3 protein is encoded by a single gene mapped to human chromosome 16p13.3 with a size of 80 kB, transcribed into 6500bp mRNA and translated into a 1704 amino acid protein (45). Mutations in *ABCA3* gene are inherited in an autosomal-recessive manner. According to the general structure of an ABC transporter, ABCA3 consists of 12 transmembrane domains, two extracellular loops (EL) and two nucleotide-binding domains (NBD) (Fig.5).

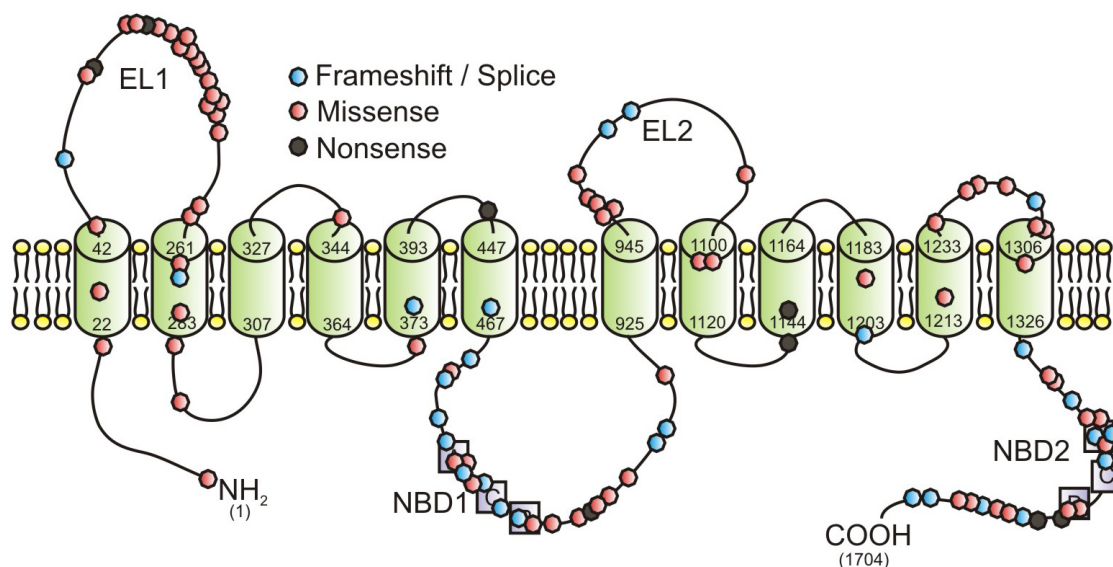


**Fig.5:** Structure of the ABCA3 transporter in a lipid bilayer membrane (yellow): According to the general structure of an ABC transporter, ABCA3 is a transporter with 12 transmembrane domains (green), two extracellular loops (EL) and two nucleotide-binding domains (NBD). More than 500 mutations are identified, some of them are colored blue (frameshift mutation), red (missense mutation) or black (nonsense mutation) in this scheme. The author of this model is Dr. Suncana Kern, she provided it to our research group and I use it with her permission.

### 3.2.3 Function of ABCA3

#### 3.2.3.1 Localization and lamellar body biogenesis

ABCA3 is highly expressed in alveolar type II cells (ATII) and localizes to the limiting membrane of lamellar bodies (LBs) (41, 42), intracellular organelles for assembly and storage of pulmonary surfactant. ABCA3 protein plays a key role in the biogenesis of LBs

and is crucial for their morphology. In electron microscope studies of healthy lungs, LBs appear as “onion-skin” like, regular concentric arranged lamellae (Fig.3). In children with *ABCA3* mutations, LB morphology is abnormal (22). Immature LBs with “tightly packed concentric membranes” (46) show small electro-dense bodies within, appearing as “fried-egg” inclusions (46-48). This LB-morphology is characteristic for *ABCA3* deficiency and LB morphology can be an indicator to distinguish between the entities of genetic surfactant dysfunction disorders. Whereas in SP-B deficiency large and disorganized composite bodies and multiple vesicular inclusions appear (49, 50), in SP-C deficiency vesicular bodies with aggregates of small vesicles with electro-dense cores can be observed (51-53).

Furthermore, *ABCA3* protein is not only essential for LB morphology but also for their formation. In *Abca3* knock-out mice presenting with acute respiratory failure normal and mature LBs are absent and mice die within hours after birth (54-56). Moreover, in *in vitro* studies, the *ABCA3* overexpression in kidney cells (HEK293 cells) induces *de novo* synthesis of lamellar body-like vesicles (57).

#### **3.2.4.2 ABCA3 is a lipid transporter**

*ABCA3* expression is not only essential for biogenesis of mature LBs as the intracellular organelle for assembly and storage of surfactant, but is also responsible for the composition and homeostasis of pulmonary surfactant. *ABCA3* is a lipid transporter, which drives the transmembrane translocation of surfactant phospholipids from the cytoplasm into LBs. *In vitro* studies show that *ABCA3* overexpression promotes the uptake of natural choline-phospholipids into LBs (58, 59). When *ABCA3* expression is down-regulated by siRNA, phosphatidylcholine, sphingomyelin and cholesterol uptake are significantly decreased (57). Furthermore, in human and mice with *ABCA3* deficiency, phosphatidylcholine species and phosphatidylglycerol are dramatically reduced in bronchoalveolar lavage and lung tissue, respectively (27, 54, 60). Thereby surfactant mixture loses its function and surface tension is increased (27). Since the last steps in SP-B and SP-C processing occur inside of functional LBs, *ABCA3* deficiency in human and mouse leads to accumulation of SP-B and SP-C precursors and lack of mature forms (28, 55, 60).

##### **3.2.3.1.1 Categorization of ABCA3 mutations**

Mutations in the *ABCA3* gene are classified into two categories (61): Type I mutations are characterized by abnormal intracellular *ABCA3* protein localization and impaired

intracellular ABCA3 protein trafficking. In type II mutations, the ABCA3 transporter shows decreased ATP-binding capacity/ decreased ATP-hydrolysis activity but proper trafficking to LBs. Table 1 gives an overview of mutations that were found in patients and which have been analyzed and classified in *in vitro* studies before.

**Table 1:** Overview of ABCA3 mutations examined in previous studies *in vitro*.

Type I (abnormal localization)	Type II (impaired ATP-hydrolysis)
L101P (57, 61)	N568D (57, 59, 61)
L982P (61)	G1221S (57, 61)
W1142X (61)	L1580P (61)
Q1591P (61)	E292V (34, 61)
L1553P (61)	E690K (62)
Ins1518fs/ter1519 (61)	T1114M (62)
Q215K (34)	

### 3.2.4 ABCA3 in lung disease

#### 3.2.4.1 Early and late onset of lung disease

Current data show that ABCA3 mutations are the most frequent known cause of genetic ILD. In 2004, ABCA3 mutations were discovered in full-term neonates with fatal neonatal lung disease and symptoms of surfactant deficiency occurring shortly after birth (22). Morbidity and mortality in these ABCA3-related surfactant deficiency syndromes is pretty high (10). Recently, mutations in ABCA3 gene have also been associated with chronic lung disease in older children (21, 66, 68, 71), demonstrating that children with ABCA3 mutations can also survive well beyond infancy to early adulthood with a diagnosis of pILD. Currently, an increasing number of case reports about patients with ABCA3 deficiency is published and raises the number of identified ABCA3 mutations (21, 22, 27, 28, 46, 48, 63-73). To the date, our research group knows more than 500 mutations, including some unpublished data. Similar to SP-C deficiency, ABCA3-related lung disease is complex and heterogeneous in histopathology and symptom severity. The disease onset varies from directly after birth, early in infancy or later in childhood, sometimes following the exposure to environmental stressors (71). However, the exact mechanism leading to the milder phenotype in pILD caused by ABCA3 mutation compared with the lethal cause in RDS is not yet known.

#### **3.2.4.2 Genotype-phenotype interplay**

Some data show a genotype-phenotype correlation in lung disease caused by *ABCA3* mutations, suggesting that patients with a type I homozygous *ABCA3* mutation or with type I / type II compound heterozygous mutations die within the neonatal period, whereas patients with a type II homozygous *ABCA3* mutation survive beyond neonatal period and occur with milder phenotype (21, 22). In contrast, some clinical experience on *ABCA3*-related lung disease is inconsistent with the idea of a genotype-phenotype correlation (47, 48, 62, 66, unpublished data from our research group), demonstrating a significant phenotypic heterogeneity of lung disease associated with *ABCA3* mutations from fatal RDS to milder course in pILD that is independent from genotype. However, the mechanism leading to phenotypic heterogeneity of lung disease associated with *ABCA3* deficiency is still poorly understood.

#### **3.2.4.3 Outer stressor**

Since the variety of clinical appearance in *ABCA3* deficient patients can not completely be explained by the genotype-phenotype correlation, clinical experience suggests a link between the late onset of genetic ILD and exposure to outside stress factors, such as respiratory infections and cigarette smoke (71), speculating that outer stressors accelerated the patients' underlying disease course.

#### **3.2.4.4 Histopathological pattern**

Hyperplastic alveolar type II cells, accumulation of alveolar macrophages and proteinaceous material in distal air spaces characterize the histological pattern in patients with *ABCA3* deficiency (22, 47). In further course of the disease, interstitial thickening and fibroblast proliferation in interstitial spaces are found in the histological pattern (46, 47). Lung biopsy findings show the histology of CPI (chronic pneumonitis of infancy), DIP (desquamative interstitial pneumonia), NSIP (nonspecific interstitial pneumonia), PAP (pulmonary alveolar proteinosis) and pulmonary fibrosis, whereas DIP is seen in the majority of the patients (47).

### 3.2.4.5 Therapy

To the date, there are no causative therapeutic options available for ABCA3-related surfactant deficiency. The therapeutic strategy concentrates on the reduction of symptoms and the limitation of inflammation and fibrogenesis. Oxygen application, mechanical ventilation and exogenous surfactant application can help to stabilize vital function temporarily in case of acute respiratory distress. Symptomatic treatment of ABCA3-related lung disease includes drugs, which are administered in the management of ILD as well like steroids and hydroxychloroquine (29). The ultimate therapeutic option in end-stage respiratory failure is lung transplantation.

### 3.2.4.6 ABCA3 mutations in this study

In this study, the clinically relevant ABCA3 mutations R43L, R280C and L101P, which either were found in newborns with respiratory distress syndrome (RDS) or in children with chronic pILD, were examined. Table 2 provides an overview on the patients, their clinical feature and outcome.

Brasch and colleagues reported from a full-term female newborn, delivered uneventfully after a normal pregnancy (28). Directly after birth she developed severe respiratory distress, required intense supportive care, mechanical ventilation and exogenous surfactant application and died at the age of 47 days. The patient had a sibling who has died briefly after birth from respiratory failure before. Analyzing the ABCA3 gene, which is inherited in an autosomal-recessive fashion, in the healthy parents and one healthy sibling showed that they are heterozygous for the G → T mutation at nucleotide 128 (first extracellular loop), which causes an R43L (Arg > Leu) amino acid substitution (Fig.6). Lung biopsy of the patient revealed chronic pneumonitis of infancy, absent ABCA3 protein expression, reduced mature SP-B expression (SP-C analysis not done) and electro-dense bodies in type II pneumocytes. Appropriate material for mutation analysis was not available from the patient. Furthermore, Somaschini (48) and Garmany (27) and coworkers, both reported from two full-term newborns that were compound heterozygote for the R43L mutation (R43L/R1482W and R43L/P264R, respectively) and had a similar clinical picture as the reported female patient above, including severe respiratory distress syndrome. Both newborns required intense supportive care. One patient died at the age of 30 days, the other patient received lung transplantation. The histological examination showed DIP and CIP, respectively (Table 2).

Unpublished data from our research group include a female patient, 15 years old, presenting with milder respiratory symptoms consistent with chronic pILD. She was found to

be heterozygote for the R280C mutation. Lung biopsy showed DIP. She is still alive and in a stable health condition that allows her an almost normal activity and life. None of her family members suffered from neonatal lung disease (Table 2). Besides, the R280C mutation was also found in a full-term male newborn, who suffered from unexplained respiratory distress within 24 hours after birth (27) (Table 2). Mechanical ventilation was insufficient and he died 2 days after delivery. He had no family history of neonatal lung disease. Lung tissue was not available.

The L101P mutation was found in two full-term newborns, siblings with consanguine parents, presenting with respiratory failure that occurred within hours after birth (48). Clinical and radiographic findings were consistent with surfactant deficiency and both newborns died within a month after birth. By sequencing analysis of the *ABCA3* gene, homozygous substitution of proline for leucine in codon 101 (L101P) was found in both infants (Fig.6). Lung tissue was not available.

While R43L and R280C mutations were examined in this study for the first time, L101P mutation was used as an example for a trafficking defect/ type I-mutation (22, 61).

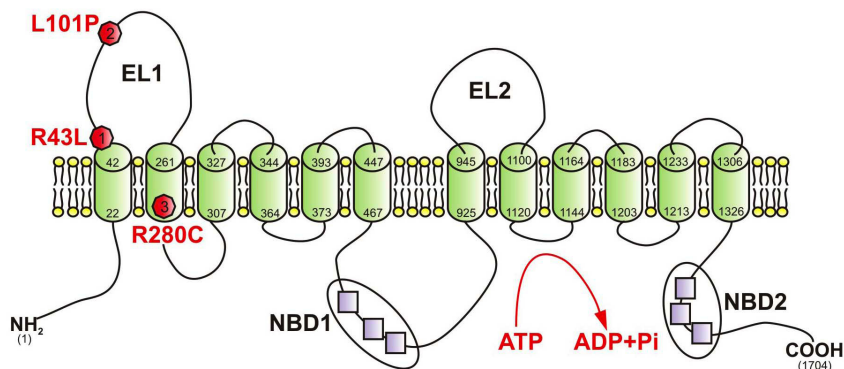


**Fig.6:** Localization of the *ABCA3* mutations R43L, R280C and L101P within the *ABCA3* transporter. R43L mutation is localized to the first extracellular loop at the border with the first transmembrane domain. L101P mutation localizes to the first extracellular loop. Depending on the topology software used, R280C mutation localizes either to the second transmembrane domain or to the second cytoplasmic loop. The author of this model is Dr. Suncana Kern, she provided it to our research group and I use it with her permission.

The identified missense mutations R43L, R280C and L101P involved highly conserved codons and were not detected in at least 100 control samples from racially or ethnically matched controls (22, 27, 28, 48).

**Table 2:** Characteristics of patients with *ABCA3* mutations analyzed in this study.

Patient No.	Gene/mutation	Phenotype	Family history/ Consanguinity	Histological findings	Outcome	Reference
1	n.a. Healthy parents + sibling heterozygous for R43L	RDS	yes/ no	CPI	Death at the age of 47 d	<i>Brasch et al., 2006 (28)</i>
2	R43L/P264R	RDS	yes/ n.d.	CPI	LTX	<i>Garmay et al., 2006 (27)</i>
3	R43L/R1482W	RDS	no/ n.d.	DIP	Death: 30 days after birth	<i>Somaschini et al., 2007 (48)</i>
4	R280C/wt	RDS	no/ n.d.	n.a.	Death: 2 days after birth	<i>Somaschini et al., 2007 (48)</i>
5	R280C/wt	Chronic pILD	no/ no	DIP	alive	Unpublished own data
6	L101P/L101P	RDS	yes/ yes	n.a.	Death in neonatal period	<i>Shulenin et al., 2004 (22)</i>
7	L101P/L101P	RDS	yes/ yes	n.a.	Death in neonatal period	<i>Shulenin et al., 2004 (22)</i>

Definition of abbreviations: RDS= respiratory distress syndrome, CPI= chronic pneumonitis of infancy, n.d.= not described, DIP= desquamative interstitial pneumonia, LTX= lung transplantation, n.a.= not available.

### 3.3 How misfolded proteins disturb cell homeostasis

#### 3.3.1 Role of the endoplasmic reticulum

The endoplasmic reticulum (ER) is an intracellular network of membranes consisting of interconnected tubules and vesicles with a wide variety of functions such as Ca<sup>2+</sup>-storage and -release, biosynthesis of secretory and membrane proteins, lipids and sterols, posttranslational modification of nascent polypeptides and their proper folding. Furthermore, proper protein folding of immature secretory and membrane proteins is a highly controlled process in the lumen of the ER. This procedure requires the presence of folding enzymes, quality control factors and chaperones that catalyze and assist in protein maturation and folding to their final confirmation (74). After further protein modification- and/or deglycosylation- processes the modified protein chains are transported into Golgi apparatus.

### 3.3.2 Induction of the quality control system by unfolded proteins

Failure of posttranslational protein modification and an increasing number of unfolded proteins retained within the ER lumen cause ER stress. Therefore, the ER offers a cytoprotective quality control mechanism named the unfolded protein response (UPR). The UPR system prevents the cell from unfolded defect proteins exit the ER and induces cellular adaption to disturbed cell homeostasis (74, 75). Three mechanisms regulate cellular adaption: first, general inhibition of protein translation to decrease the protein load in the ER, second, transcriptional induction of genes encoding chaperones to maintain the protein-folding capacity of the ER and third, the induction of proteins belonging to the ER-associated degradation (ERAD), that is responsible for the transport of misfolded proteins to the cytosol and subsequent degradation (76-79). If UPR fails to resolve ER stress and to restore cell homeostasis, apoptotic cell-death pathway is initiated (80).

In non stressed cells, the binding protein (BiP)- also named glucose regulated protein (GRP78)- binds to the three UPR signal transducers that are localized to ER membrane to maintain them in an inactive state (81, Fig.8). Upon ER stress and accumulation of unfolded proteins in the ER lumen, BiP is released from the three UPR sensors to assist in protein folding. Thus, UPR sensors are activated to induce the cellular adaption to disturbed cell homeostasis.

First UPR signal transducer, inositol-requiring enzyme 1 (IRE1), a transmembrane serine/ threonine receptor protein kinase, is activated upon accumulation of unfolded proteins in the ER lumen. IRE1 cleaves mRNA encoding for the basic leucine zipper transcription factor X-box binding protein 1 (XBP1), a key transcription factor of UPR elements, in the cytoplasm (82). The XBP1-mRNA is cleaved at two sites, the 5' and 3' fragments are ligated and a 26- base intron is cut off (82, Fig.7). The result is a translational frameshift and the active XBP1 transcription factor (83, 84). Active XBP1 is responsible for the transcription of genes encoding a wide variety of UPR elements such as chaperones and folding enzymes as well as ERAD elements (85, 86). Furthermore, IRE1 induces degradation of several mRNAs, thereby preventing the cells from a high protein load during ER stress (87).

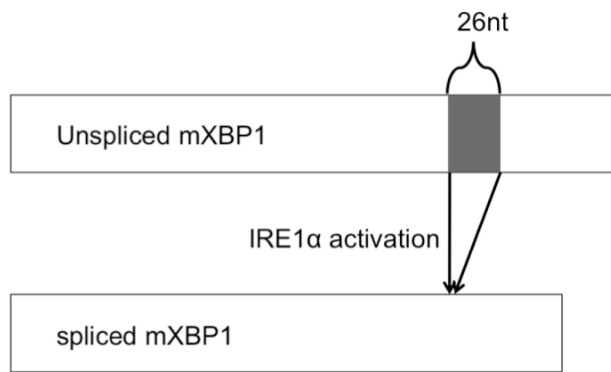


**Fig.7:** Schematic representation of the splicing of XBP1 mRNA: Upon ER stress, a 26-base intron (nt) is cut off by IRE1, 5' and 3' fragments are ligated, creating a translational frameshift and producing an active XBP1 transcription factor. (According to (84))

Second UPR sensor named activating transcription factor 6 (ATF6) regulates expression of genes encoding for ER quality control proteins (88).

Third UPR sensor is the ER resident transmembrane protein kinase (PERK), which induces mRNA translation of approximately one third of the genes encoding for UPR proteins and activates a translation factor (eIF2 $\alpha$ ) that attenuates protein synthesis in general and initiates translation of genes with pro-apoptotic function (89).

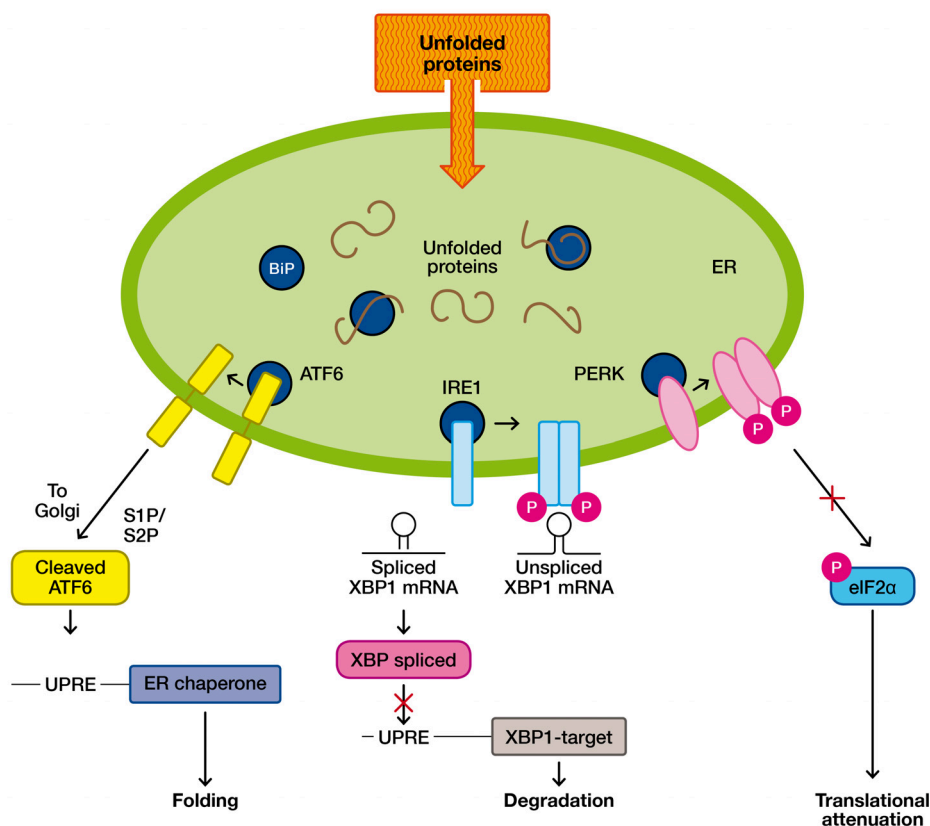


**Fig.8:** Overview of the UPR system and its elements. Upon the accumulation of unfolded proteins the UPR sensors ATF6, IRE1 and PERK are activated by the release of BiP and induce a variety of mechanisms for the cellular adaptation to a disturbed cell homeostasis: XBP1 splicing and activation as a transcription factor, upregulation of chaperones to assist in protein folding, induction of protein degradation and attenuation of general protein translation. (According to (90)).

### 3.3.3 Induction of apoptosis

Prolonged ER stress caused by accumulation of unfolded proteins in the ER lumen and the inability to restore cell homeostasis induces programmed cell death (=apoptosis). Apoptosis is a highly conserved cellular mechanism. It is essential for cell selection, cell homeostasis and tissue morphogenesis. A wide variety of stimuli can trigger cell surface death receptors (extrinsic pathway) or initiate the intrinsic pro-apoptotic pathway via mitochondria stimulation. Upon ER accumulation of misfolded proteins the three UPR sensors not only initiate cytoprotective mechanisms, but also contribute to the induction of programmed cell death via upregulation of pro-apoptotic proteins such as CHOP,  $Ca^{2+}$ -release, induction of mitochondrial stress (mitochondrial apoptosis) and ER stress (80).

Pro-apoptotic signals are transduced by a family of regulated proteolytic enzymes named caspases. Caspases are a family of highly conserved aspartate-specific cysteine proteases, which induce the pro-apoptotic pathway and contribute to the destruction of cell structures and mechanisms as well as to the deregulation of protein synthesis (91). The caspase-cascade is a complex signaling pathway. Most caspases are present in cells as longer inactive precursors and become sequentially activated by proteolytic cleavage through an active upstream caspase or through autocatalysis (91). In mammalian species, 15 known members are divided into two groups: initiator caspases, which are activated by death receptors, and effector caspases that cleave proteins involved in programmed cell death events. The activation of the down-stream executioner caspase 3 can be either conducted by the initiator caspase 9 that is activated in a mitochondria-dependent signaling way (mitochondrial apoptosis) by increased intracellular stress (92) or by caspase 8 that is activated through stimulation of the surface death receptor Fas. The executioner caspases 3, 6, 7 cleave proteins involved in DNA processing and several structural proteins.

Among the known caspases, mouse caspase 12 (homologous to human caspase 4), localized to the ER membrane, is specifically cleaved when ER stress increases by continuous accumulation of unfolded proteins and calcium imbalance (93, 94). Cleavage of caspase 12 leads to the activation of caspase 9 and caspase 3 (95, 96), resulting in apoptotic cell death, in a surface death receptor- and mitochondria-independent apoptotic signaling pathway (Fig.9).

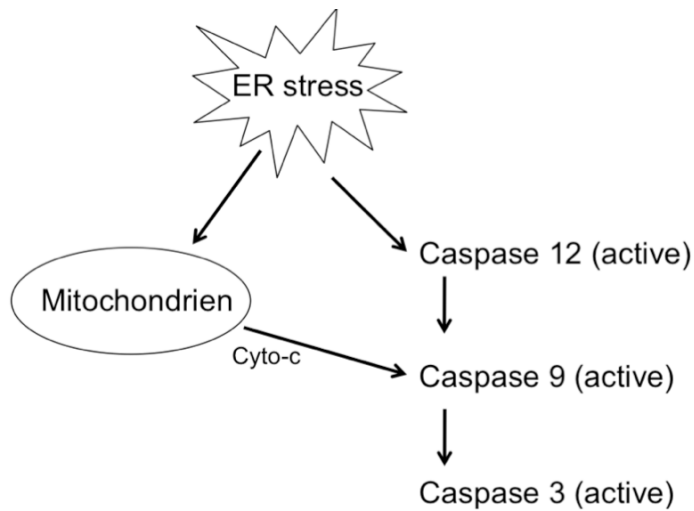


**Fig.9:** Scheme of the mechanism how ER stress causes apoptotic cell death: Increasing ER stress leads to the cleavage of the ER membrane-bound caspase 12 in mouse (homologous human caspase 4), which catalysis the cleavage of caspase 9. Active caspase-9 catalysis the cleavage of procaspase-3, thereby promoting the further conduction of apoptosis. (According to (96))

Vital cells generate and maintain an asymmetric double layer cell membrane of uncharged and charged phospholipids species. The negatively charged phosphatidylserines (PS) are mainly located in the inner leaflet facing the cytosol. During apoptosis, plasma membranes lose their feature of asymmetry by externalization of PS to the outer leaflet of the plasma membrane in a caspase-dependent way (97). Expression of PS on the cell surface is a signal for macrophages for phagocytosis. Furthermore, Annexin V binds to negatively charged PS on plasma membranes of apoptotic cells and can be used as a Molecular Imaging agent in visualizing apoptotic cells in patients and in *in vitro* studies (98, 99).

### 3.5 ER stress and apoptosis contribute to disease pathogenesis

Recent data show that prolonged accumulation of unfolded proteins within the ER accompanied by simultaneous failure of the UPR system contribute to the pathogenesis of several disorders, such as metabolic disease, atherosclerosis, neurodegenerative disease and conformational diseases (100-102). Furthermore, ER stress and apoptosis in alveolar type II cells play a role in lung disease, especially in pathogenesis of idiopathic pulmonary fibrosis (IPF) and genetic SP-C-associated pulmonary fibrosis (103-105). Moreover, in *in vitro* studies in lung epithelial A549 cells expressing SP-C mutations, which cause misfolding and aggregation of the SP-C pre-protein, ER stress increases, UPR is activated and apoptotic cell death is initiated (106).

Fibrosis is one of the hallmarks documented in ABCA3-associated lung disease (21,

68, 71). Today, it is known that idiopathic pulmonary fibrosis is not primarily connected to chronic and unresolved inflammation and fibrosis can occur without inflammation (107). Fibroblastic foci in the lung may underlie areas of unresolved chronic alveolar epithelial injury, ongoing lung repair and abnormal wound healing (29, 107, 108).

Under such conditions of epithelial micro-injury alveolar type II cells contribute significantly to the alteration of the normal lung architecture, aberrant tissue remodeling and fibrogenesis and induce activation and migration of fibroblasts (107). Recently, it was shown that ATII cells undergo epithelial-mesenchymal transition (EMT) under specific conditions and change their characteristics and morphology to a fibroblast-like feature (109). Thereby ATII may contribute to lung fibrogenesis as an additional source of myofibroblasts in the pathogenesis of ILD (110). Moreover, alveolar epithelial cells are responsible for the release of almost all pro-fibrotic cytokines and growth factors, such as TGF- $\beta$ 1, IL-1 $\beta$ , TNF- $\alpha$  and GM-CSF, and for the synthesis and release of enzymes that contribute to extracellular matrix (111, 112). TGF- $\beta$ 1 is the most aggressive pro-fibrotic growth factor among these mediators and the amount of TGF- $\beta$  is related to the extent of fibrosis and induction of myofibroblasts (113). Besides, TGF- $\beta$ 1 induce EMT in alveolar epithelial cells, which is characterized by the loss of epithelial marker E-Cadherin (ECAD), the gain of mesenchymal marker vimentin and transformation into myofibroblastic morphology (109, 114). In this way, alveolar type II cells can acquire fibroblast-like feature and play a role in the development of fibrosis in lung disease.

#### 4. An objective

ABCA3 protein is an ABC lipid transporter found in alveolar type II cells, where it localizes to the outer membrane of lamellar bodies which store surfactant. Current *in vitro* studies show that ABCA3 is essential for surfactant homeostasis and LB biogenesis. Mutations in the *ABCA3* gene are the most frequent known genetic cause of RDS in newborns and of late onset chronic ILD in children with a higher prevalence than mutations in *SPFTB* or *SPFTC*. Even though clinical experience suggests a link between the late onset of genetic ILD and exposure to outside stress factors, such as respiratory infections and cigarette smoke, contributing mechanisms leading to phenotypic heterogeneity remain unknown.

In order to elucidate mechanisms leading to pediatric ILD, I investigated the influence of three *ABCA3* mutations, R43L, R280C and L101P, found in children with surfactant deficiency and chronic ILD, on induction of ER stress, apoptosis and fibrogenesis in lung epithelial A549 cells.

## **4. Materials**

### **4.1 Chemicals**

In general, chemicals were obtained from Sigma-Aldrich (München, Germany) and Merck (Darmstadt, Germany). Special chemicals were purchased as follows: Agarose for DNA gel electrophoresis from SERVA (Heidelberg, Germany), D-PBS, trypsin-EDTA solution and FBS from PAA Laboratories GmbH (Pasching, Austria) and BSA from Paesel and Lorei (Duisburg, Germany). RPMI media was purchased from Sigma-Aldrich (München, Germany) and LB-Agar as well as LB-Bouillon were purchased from Merck (Darmstadt, Germany). Antibiotics kanamycin, ampicillin and tunicamycin were obtained from Sigma-Aldrich (München, Germany). Recombinant human Tumor Necrosis Factor  $\alpha$  (TNF- $\alpha$ ) was obtained from Invitrogen (Freiburg, Germany) and Recombinant human Tissue Growth Factor  $\beta$ 1 (TGF- $\beta$ 1) was obtained from R&D systems (Abingdon, England). Vectashield Hard and Set Mounting Media with DAPI was obtained from Vector Laboratories (Burlingame, CA, USA). NBD-labeled lipids phosphatidylcholine (C<sub>12</sub>-NBD-PC) and phosphatidylethanolamine (C<sub>12</sub>-NBD-PE) were purchased from Avanti Polar Lipids (Alabaster, AL) and other lipids from Sigma-Aldrich (München, Germany).

### **4.2 Equipment**

Fluorescence microscope Axiovert 135 obtained from Carl Zeiss (Oberkochen, Germany) was used for immunofluorescence analysis. The evaluation of pictures was performed with the help of the software AxioVision Release 4.7.1 (Carl Zeiss, Oberkochen, Germany). Olympus FluoView FV 1000 confocal microscope was used for the analysis of the NBD-lipid uptake.

BD FACSCanto II Flow Cytometer was used for the FACS assay and FACSDiva v6.1.3 for data analyses (BD Bioscience).

For the chemiluminescence detection Diana III camera system and for densitometric analysis software AIDA were purchased from Raytest (Straubenhardt, Germany). GraphPad Prism version 4 was obtained from GraphPad Software (La Jolla, CA, USA) for statistical analysis.

### 4.3 Enzymes and kits

Enzymes and kits were purchased as follows: QuickChange Site-directed Mutagenesis Kit for site directed point mutagenesis and PfuUltra™ Hotstart Polymerase were purchased from Stratagene (La Jolla, CA, USA). Restriction enzymes: KpnI, EcoRI, HindIII, ScaI, XbaI, XhoI, BglII, DpnI and the corresponding reaction buffers as well as EndoH and PNGaseF for deglycosylation assay were purchased from NewEngland BioLabs (Ipswich, MA, USA). T4-DNA ligase and corresponding reaction buffer were purchased from Fermentas (Burlington, Canada). DNA extraction from agarose gels was performed with the help of QIAquick Gel Extraction Kit (Qiagen, Hilde, Germany) and Ultrafree®-DA (Millipore, Billerica, MA, USA). Plasmid- DNA isolation was performed with either QIAprep Spin Miniprep Kit (Qiagen, Hilden, Germany) or with NucleoBond Xtra Midi EF from Macherey-Nagel (Düren, Germany). Cell culture was tested regularly for mycoplasma with the help of Venor GEM-Mykoplasma Detection Kit for conventional PCR.

High Pure RNA Isolation Kit and DNase I, RNase free from Roche (Mannheim, Germany) were used for RNA-isolation. SuperScript™III First Strand Synthesis System from Invitrogen (Freiburg, Germany) and Taq-polymerase from NewEngland BioLabs (Ipswich, MA, USA) were used for performance of RT-PCR.

Transfection was performed with the help of transfection reagent ExGen 500 from Fermentas (Burlington, Canada). Complete protease inhibitor cocktail was purchased from Roche (Basel, Schweiz). Determination of protein concentration was conducted with Bio-Rad Protein Assay Kit from Bio-Rad Laboratories (München, Germany). For SDS-Page and Western Blotting following buffers as well as precast gels were obtained from Invitrogen (Freiburg, Germany): NuPage® MOPS SDS Running Buffer (20x), NuPage® MES SDS Running Buffer (20x), NuPage® Tris-Acetate SDS Running Buffer (20x), GF® LDS Sample Buffer (4x), Transfer Buffer (20x), NuPage® 10 % Bis-Tris Gel, NuPage® 3-8 % Tris-Acetate Gel and 7 % Tris-Acetate Gel. Immobilon-P Transfer Membrane, a PVDF-membrane, was purchased from Millipore (Billerica, MA, USA). ECL and Hyperfilm™ ECL were obtained from GE-Healthcare (Buckinghamshire, UK). For the purpose of immunoblotting with anti-GFP antibody, the chemiluminescent immunodetection system WesternBreeze® was obtained from Invitrogen.

IntraPrep™ Permeabilization Reagent from Beckman Coulter (Fullerton, CA, USA) was used for preparing samples for flow cytometer analysis.

#### 4.4 Primers

All primers were purchased from Metabion International AG (Martinsried, Germany).

**Table 3:** List of primers for point mutagenesis or sequencing.

Primer name	Sequence
ABCA3.R43L.For	5'-CATCTGGCTCC <u>I</u> CTTGAAGATTC-3'
ABCA3.R43L.Rev	5'-GAATCTTCAAG <u>A</u> GGAGCCAGATG-3'
ABCA3.R280C.For	5'-CATTGCC <u>I</u> GTGCTGTCGTG-3'
ABCA3.R280C.Rev	5'-CACGACAGCAC <u>A</u> GGCAATG-3'
ABCA3.L101P.For	5'-CAGTGCGCAGGGCAC <u>C</u> TGTGATCAAC-3'
ABCA3.L101P.Rev	5'-GTTGATCACAG <u>G</u> TGCCCTGCGCACTG-3'
ABCA3.HA.For	5'-GCCGCGGGTACCATGGATTACCCATACGATGTTCCAGATTACGCTGCTGCTGTGCTCAGC-3'

**Table 4:** List of primers for RT-PCR.

Primer name	Sequence
XBP1.For.1	5'-AAACAGAGTAGCAGCTCAGACTGC-3'
XBP1.Rev.1	5'-TCCTTCTGGGTAGACCTCTGGGAG-3'
18srRNA.For.1	5'-TCAAGAACGAAAGTCGGAGG-3'
18srRNA.Rev.1	5'-GGACATCTAAGGGCATCACA-3'

## 4.5 Vectors

pEYFP-ABCA3-WT was a kind gift of the research group of Dr. Andreas Holzinger (Fig.10), pJET1/ABCA3-HA of my colleague Dr. M. Woischnik, puB6-hABCA3-HA-L101P of my colleague Eva Kaltenborn and pEGFP-N1-SPC-WT of Dr. Michael Beers. PuB6-V5-His/LacZ was purchased from Invitrogen (Freiburg, Germany) and pmax-GFP from AMAXA (Köln, Germany). Other vectors were generated in this study (Table 5).

**Table 5:** List of vectors.

Vector	Resistance in <i>E.coli</i> DH5 $\alpha$	Resistance in cells	Major characteristics	Size	Source
Pmax-GFP	kanamycin	none	Not suitable for making stable clones	3486 bp	AMAXA
pJET1/ABCA3-HA	ampicillin	Only effective in non transformed cells	HA tagged is fused to C-terminal end of ABCA3 gene	31228 bp	M. Woischnik
puB6/V5-His/LacZ	ampicillin	blasticidin	Contains gene for $\beta$ -galactosidase	8500bp	Invitrogen
pEYFP-ABCA3-WT	kanamycin	G418	Gene, encoding für YFP-protein, is fused to C-terminal end of ABCA3 gene	10146 bp	A. Holzinger
pEYFP-ABCA3-R43L	kanamycin	G418	Gene, encoding für YFP-protein, is fused to C-terminal end of ABCA3 gene	10146 bp	This study
pEYFP-ABCA3-R280C	kanamycin	G418	Gene, encoding für YFP-protein, is fused to C-terminal end of ABCA3 gene	10146 bp	This study
pEYFP-ABCA3-L101P	kanamycin	G418	Gene, encoding für YFP-protein, is fused to C-terminal end of ABCA3 gene	10146 bp	This study
puB6-hABCA3-HA-WT	ampicillin	blasticidin	HA tagged is fused to C-terminal end of ABCA3 gene	10542 bp	This study
puB6-hABCA3-HA-R43L	ampicillin	blasticidin	HA tagged is fused to C-terminal end of ABCA3 gene	10542 bp	This study
puB-hABCA3-HA-R280C	ampicillin	blasticidin	HA tagged is fused to C-terminal end of ABCA3 gene	10542 bp	This study
puB6-hABCA3-HA-L101P	ampicillin	blasticidin	HA tagged is fused to C-terminal end of ABCA3 gene	10542 bp	E. Kaltenborn
pcDNA4-TO-ABCA3-HA-WT	ampicillin	blasticidin	HA tagged is fused to C-terminal end of ABCA3 gene	n.a.	Provided by the group
pEGFP-N1-SPC-WT	kanamycin	neomycin	Gene, encoding für GFP-protein, is fused to C-terminal end of SP-C gene	5371bp	M. Beers

n.a.: not available

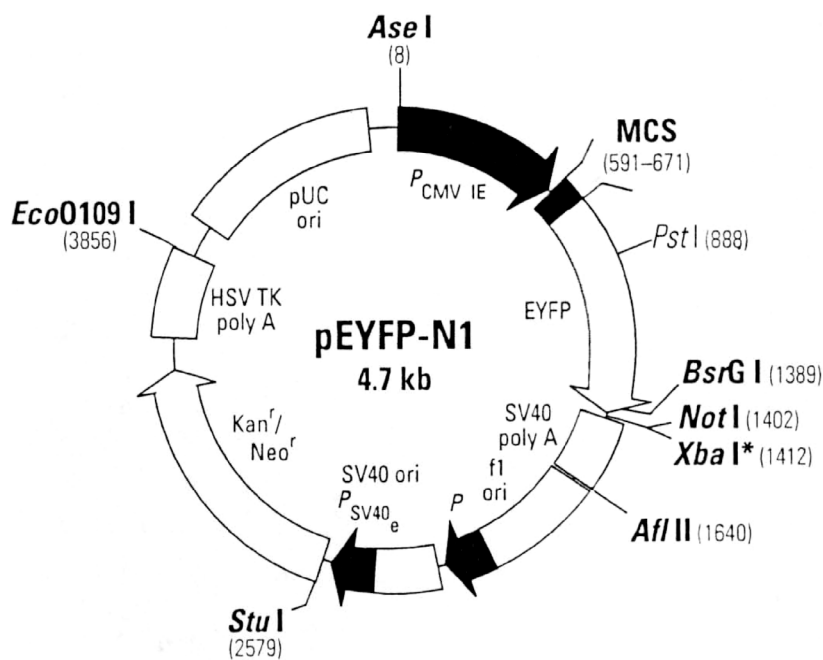


**Fig.10:** Vector map of pEYFP-N1 (BD Clontech): Wild type full length human *hABCA3* cDNA without stop codon was cloned into *EcoRI*/*AgeI* sites of pEYFP-N1 plasmid to obtain pEYFP-N1-WT vector for expression of C-terminal ABCA3-YFP protein fusions.

#### 4.6 Antibodies

Primary antibodies for Western Blotting or immunofluorescence were either purchased from Santa Cruz (Santa Cruz, CA, USA), Chemicon (Billerica, MA, USA), Clontech (Mountain View, CA, USA), Stressgene (Hamburg, Germany), Dianova (Hamburg, Germany), Cell Signaling (Danvers, MA, USA), R&D System (Abingdon, England) or Sigma-Aldrich (München, Germany) (Table 6).

**Table 6:** List of primary antibodies used for Western Blotting (WB) or immunofluorescence (IF).

Primary Antibodies	Source	Type, Host	Dilutions for WB and IF
anti- $\beta$ -actin – HRP conjugate	Santa Cruz (Santa Cruz, CA, USA)	monoclonal, mouse	WB 1:10 000
anti-calnexin	Santa Cruz (Santa Cruz, CA, USA)	polyclonal, goat	WB 1:500; IF 1:200
anti-Hsp 90	Santa Cruz (Santa Cruz, CA, USA)	monoclonal, mouse	WB 1:500
anti-human CD 63 (LAMP3)	Chemicon (Billerica, MA, USA)	monoclonal, mouse	IF: 1:200
anti-EEA-1	Santa Cruz (Santa Cruz, CA, USA)	polyclonal, rabbit	IF: 1:200
anti-GM130	Santa Cruz (Santa Cruz, CA, USA)	polyclonal, goat	IF: 1:50
anti-GFP: Living Colors R A.v. (IL-8)	Clontech (Mountain View, CA, USA)	monoclonal, mouse	WB: 1:500
anti- caspase 4	Stressgene (Hamburg, Germany)	monoclonal, mouse	WB: 1:500
anti- caspase 3	Dianova (Hamburg, Germany)	monoclonal, mouse	WB: 1:133
anti- BiP	Cell Signaling (Danvers, MA, USA)	monoclonal, rabbit	WB: 1:1000
anti- E-cadherin	R&D System (Abingdon, England)	monoclonal, mouse	WB: 1:250
anti- vimentin	Sigma- Aldrich (München, Germany)	monoclonal, mouse	WB: 1:2000
anti-HA-tag	Roche (Basel, Schweiz)	monoclonal, rat	IF: 1:200

Secondary antibodies used for IF were purchased from Invitrogen (Freiburg, Germany) (Table 7).

**Table 7:** List of secondary antibodies used for IF.

Antibody	Excitation (nm)	Emission (nm)	Filter
anti-goat IgG - Alexa 555(donkey)	555	565	III (CY3)
anti-mouse IgG - Alexa 555(goat)	555	565	III (CY3)
anti-rabbit IgG - Alexa 555(goat)	555	565	III (CY3)
anti-rat IgG - Alexa 488(donkey)	495	519	III (green)
anti-rat IgG - Alexa 555	555	565	III (CY3)

Secondary antibodies used for WB were purchased from Invitrogen (Freiburg, Germany), Biozol (Eching, Germany) or Sigma- Aldrich (München, Germany) (Table 8).

**Table 8:** List of secondary antibodies used for WB.

Secondary antibody	Source	Type, Host	Dilution
anti-goat IgG –HRP conjugate	Biozol (Eching, Germany)	Polyclonal, rabbit	WB 1:10 000
anti-mouse: WesternBreeze® - alkaline phosphatase conjugated	Invitrogen (Freiburg, Germany)	Not published	Not published
anti-rabbit IgG – HRP conjugate	Sigma- Aldrich (München, Germany)	Polyclonal, goat	WB 1:10 000

Antibodies for flow cytometry were purchased from BD Biosciences (San Jose, CA, USA) (Table 9).

**Table 9:** List of antibodies used for flow cytometry.

Antibody	Source	Channel
anti-annexinV Cy5	BD Pharmingen TM	III
anti-active-caspase 3 PE conjugated	BD Biosciences	II
PI	BD Pharmingen TM	II

#### 4.7 Bacterial strains and cell lines

*Escherichia coli* DH5  $\alpha$  were obtained from Invitrogen (Freiburg, Germany). Human lung carcinoma epithelial cell line A54p (ACC 107) was obtained from German Collection of Microorganisms and Cell Cultures (DMSZ, Braunschweig, Germany).

## 5. Methods

### 5.1. Molecular biological methods

#### 5.1.1 Cloning strategy: Generation of pUB6-ABCA3-HA vector

In order to generate puB6-hABCA3-HA vector with hemagglutinin tag (HA-tag) fused to C-terminus of the ABCA3 gene, puB6/lacZ vector and pJet1/hABCA3-HA vector were transformed into *E.coli* DH5  $\alpha$  competent cells. Plasmid-DNA of both was isolated, restricted through KpnI and XhoI and separated by gel electrophoresis. The following restriction products were extracted with the help of QIAquick Gel Extraction Kit and Millipore Ultrafree-DA: a 5320 bp KpnI and xhoI fragment containing puB6 vector and a 5150 bp KpnI and xhoI fragment containing hABCA3-HA gene. DNA was precipitated by ethanol and resuspended

in water. For ligation, vector and insert, in 3:1 ratio, were incubated with T4 ligase and corresponding reaction buffer first for 60 min at room temperature and second for 10 min at 65 °C. Products of ligation reaction were multiplied by transformation into *E.coli* DH5  $\alpha$  competent cells. Two negative controls, the first one without insert and the second one without insert and T4 ligase, were generated. When no bacterial colonies have grown in these negative controls, plasmid DNA of the positive clones was isolated and their sequence was confirmed by conventional sequencing.

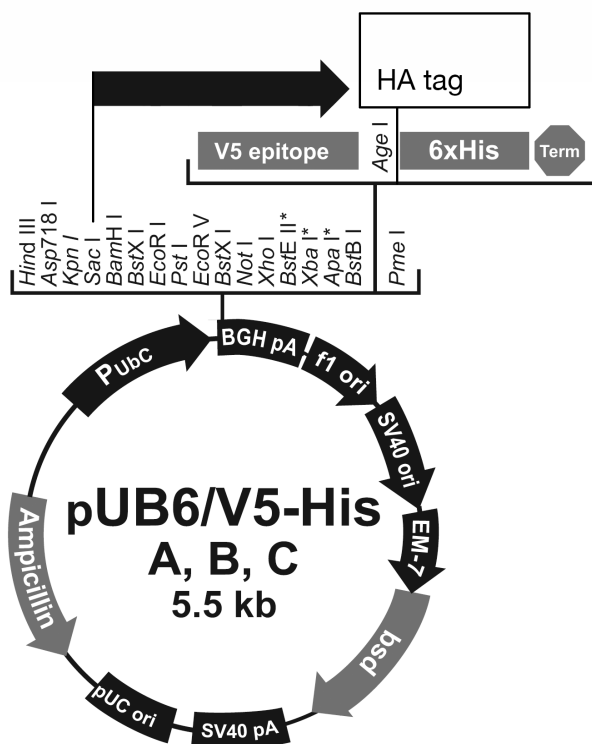


**Fig.11:** Vector map of pUB6/V5-His: Plasmid vector puB6-hABCA3-HA for expression of C-terminal fusions of ABCA3 with hemagglutinin tag (HA-tag) was produced by modification of pUB6/V5-His vector. Own illustration according to a model from Dr. Suncana Kern.

### 5.1.2 Site-directed point mutagenesis

Site-directed point mutagenesis was performed with the help of QuickChange Site-directed Mutagenesis Kit (Stratagene, La Jolla, California, USA) as recommended by the manufacturer. The following cycling parameters as shown in Table 10 were used for the introduction of point mutations into pEYFP-ABCA3- and pUB6-ABCA3-vectors.

**Table 10:** Optimal conditions for PCR in this study. Annealing temperature for introduction of the mutation L101P into pEYFP-ABCA3- vector was 52°C.

Time	Temperature	Cycles
5 min	95 °C	1
30 sec.	95 °C	12
1 min	52 °C	12
20 min	68 °C	12
10 min	68 °C	1

Point-mutagenesis products were digested with DpnI at 37 °C for 1 hour. DpnI is an endonuclease that specifically digests methylated and hemimethylated DNA, which is exclusively present in parental and non-mutated DNA template from bacterial strains (115). This specific digestion permits selection of mutation-containing synthesized DNA and prevents transformation of non-mutated DNA into *E.coli* DH5  $\alpha$ . Point-mutagenesis products were subjected to a 0.8 % agarose gel.

### 5.1.3 DNA-sequencing

DNA-sequencing was conducted by Metabion International AG (Martinsried, Germany).

### 5.1.4 *E.coli* DH5 culture

DH5  $\alpha$  strain were grown on LB-Agar or in LB-Bouillon at 37°C. Media were supplemented with 30 mg/ml of kanamycin or 100 mg/ml of ampicillin when necessary. For subsequent plasmid-DNA isolation, 5 ml of cells were grown in LB-Bouillon at 37 °C with continuous shaking overnight. 1 ml of the preculture was inoculated into 100 ml of LB-Bouillon and was grown further to optical density OD 600: 0.5-0.6. 1 ml of this overnight culture supplemented with 33 % of glycerin was stored as a stock solution at -80 °C.

### 5.1.5 Generation of competent *E.coli* DH5

*E.coli* DH5  $\alpha$  competent cells were generated by CaCl<sub>2</sub> -method. 5 ml of cells were grown in as an overnight preculture at 37 °C with continuous shaking. 1 ml of the preculture

was inoculated into 100 ml of LB-Bouillon and grown further to optical density OD 600: 0.5-0.6. For further procedure, DH5  $\alpha$  cells were incubated on ice. After 5 min of inoculation on ice, cells were collected at 4 °C and 5000 xg for 10 min. The cell pellet was resuspended in 40 ml of ice cold Tfb I buffer (100 mM RbCl<sub>2</sub>, 50 mM MnCl<sub>2</sub>, 30 mM K-acetat, 10 mM CaCl<sub>2</sub>-2H<sub>2</sub>O, 15% glycerin, pH 5) and incubated on ice for further 30 min. Cells were collected at 4 °C and 5000 xg for 10 min, the pellet was dissolved in ice cold Tfb II buffer (10 mM MOPS, 10 mM RbCl<sub>2</sub>, 75 mM CaCl<sub>2</sub>-2H<sub>2</sub>O, 15 % glycerin, pH 6.8), was frozen in liquid nitrogen and stored at -80 °C.

### **5.1.6 Transformation in *E.coli* DH5**

First, 15  $\mu$ l of point-mutagenesis products were added to DH5  $\alpha$  cells and kept on ice for 30 min. Second, cells were heat-treated at 42 °C for 2 min and immediately cooled down on ice for 2 min. Third, cells were inoculated into 900  $\mu$ l of LB medium and grown at 37 °C for 1 hour. Fourth, cells were collected at 5000 xg for 2 min. Cell pellet was dissolved in 100  $\mu$ l of media and cells were grown on LB agar with supplemented antibiotics at 37 °C overnight. One sample with not transformed DH5  $\alpha$  cells was used as a negative control. When no colonies were detectable in negative controls, plasmid-DNA of transformed DH5  $\alpha$  cells was isolated, restricted, subjected to 0.8 % agarose gel and sequence was confirmed by conventional sequencing.

### **5.1.7 Plasmid-DNA isolation**

After transformation of pEYFP-ABCA3 or pUB6-ABCA3-HA vectors into DH5  $\alpha$  strain an overnight culture of DH5  $\alpha$  strain was prepared. DNA was isolated out of DH5  $\alpha$  strain culture either with the help of QIAprep Spin Miniprep Kit or with NucleoBond Xtra Midi EF according to the protocol provided by the manufacturer.

### **5.1.8 Restriction**

Restriction was performed with 500 ng of DNA, 1 U of enzyme/1  $\mu$ g of DNA and 10x corresponding reaction buffer were used. Mixtures were incubated at 37 °C for a minimum of three hours. Results were subjected to a 0.8 % agarose gel.

## 5.2. Mamalian cell culture

### 5.2.1 Media and growth conditions

A549 cells were incubated at 37 °C, 5 % of CO<sub>2</sub> and grown in RPMI+ 10% FBS. In order to keep the lines in culture, cells were regularly split every third day in 1:10 ratio. Cells were used up to 20 passages. Where necessary, 10 ng/ml of tunicamycin (TM), 25 ng/ml of TNF- $\alpha$  and 0.05 ng/ml, 0.5 ng/ml or 5.0 ng/ml of TGF- $\beta$  were added to media.

### 5.2.2 Mycoplasma testing

Mycoplasma testing was performed regularly with the help of Venor GEM-Mycoplasma Detection Kit according to manufacturer's recommendations.

### 5.2.3 Transfection of A549 cells

A549 cells were grown up to 60-70 % confluence. Transfection was performed with ExGen 500 and optimized based on the protocol provided by the manufacturer (Fermentas, Burlington, Canada). 48 hours after transfection, immunofluorescence signal was recognized (Fig.12) and cells were collected for further experiments.

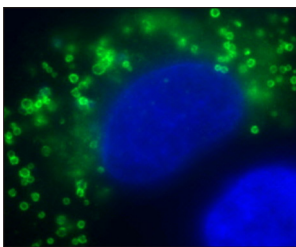


Fig.12: Transfection of A549 cell line with pEYFP-ABCA3-WT.

## 5.3. Biochemical methods

### 5.3.1 Whole cell lysates preparation

To prepare whole cell lysates, A549 cells were trypsinized and subsequently incubated with RIPA- buffer (containing: 0.15M NaCl, 1% Triton-X-100, 0.5% Sodium

deoxycholate, 0.1% SDS, 50 mM Tris, 5 mM EDTA, supplied with Complete protease inhibitor cocktail) for 30 min followed by sonication for 15 sec and incubation on ice for further 15 min. To remove nuclei and cell debris, samples were centrifuged at 4 °C and 1000 xg for 30 min. Supernatant was frozen at – 80 °C.

### **5.3.2 Crude membrane preparation**

A549 cells were grown to confluence, once washed with PBS, covered with 1 ml of ice-cold homogenization buffer (PBS supplemented with 1 mM EDTA and Complete protease inhibitor cocktail from Roche) and subsequently scraped off with a cell scraper on ice. Cells were broken in a 2 ml glass Potter Elvehjem homogenizer with 30 strokes while keeping the homogeniser constantly on ice. The homogenised sample was transferred in a fresh 1.5 ml tube and was sonicated for 30 sec. To remove nuclei and cell debris, samples were centrifuged at 4 °C and 700 xg for 10 min. The post-nuclear supernatant was centrifuged at 4 °C and 100.000 xg for one hour to obtain the crude membrane fraction in form of a pellet. This pellet was resuspended in 20 ml of ice cold resuspension buffer (25 mM HEPES/NaOH pH 7.0, Complete protease inhibitor cocktail) and stored at -20 °C.

### **5.3.3 Determination of protein concentration**

Protein concentration of isolated membrane fraction and whole cell lysates were determined by Bradford protein assay with the help of Bio-Rad Protein Assay Kit (Bio-Rad Laboratories, München, Germany).

### **5.3.4 Deglycosylation-assay**

5 µg of crude membrane fraction was incubated either with PNGase F or with Endo H and corresponding reaction buffers according to protocol provided by the manufacturer (NewEngland BioLabs, Ipswich, USA). After incubation, proteins were subjected to precast SDS-polyacrylamide gels.

### 5.3.5 SDS-Polyacrylamide Gel Electrophoresis (SDS-PAGE)

First, 30 µg of cell lysates or 5 µg of crude membrane fraction were resuspended in a sample buffer, containing 10 % DTT and 1x GF® LDS Sample Buffer (4x). Second, samples were incubated at 70 °C for 10 min. Third, proteins were separated in precast SDS-polyacrylamide gels with 10%, 3-8 % or 7 % of acrylamide concentrations (NuPage® 10 % Bis-Tris Gel, NuPage® 3-8 % Tris-Acetate Gel and 7 % Tris-Acetate Gel from Invitrogen), depending on the protein size of interest (see table 12), in combination with one of the following running buffers: NuPage® MOPS SDS Running Buffer (20x), NuPage® MES SDS Running Buffer (20x) and NuPage® Tris-Acetate SDS Running Buffer (20x) from Invitrogen. Running time for gel electrophoresis varied, depending on protein size of interest, gel and running buffer (Table 11).

**Table 11:** Gels with different acrylamide concentration were used for SDS-PAGE depending on protein size of interest.

10% gels	3-8 % gels	7 % gels
Detection of BiP, HSP90, Calnexin, Caspase 3 and 4 in whole cell lysates	Detection of ABCA3 protein in whole cell lysates	Detection of ABCA3 protein in crude membrane fraction including deglycosylation assay

### 5.3.6 Western Blotting

Western Blotting was performed according to the wet-blotting method that permits reliable transfer of bigger and hardly transportable proteins.

First, PVDF-membranes were activated with methanol for 10 sec followed by washing in distilled water for 30 sec. Second, outer chambers of a wet blotting system were cooled with ice and the inner chamber was filled with transfer buffer (10 % methanol, 80 % distilled water and 10 % Transfer Buffer (20x) from Invitrogen). Proteins were transferred to PVDF-membranes at 220 mA in two hours. Third, depending on primary antibodies, washing and blocking buffers were prepared specifically as recommended by the manufacturer. WesternBreeze® kit was used for detection of GFP-protein.

Fourth, after protein transfer membranes were washed three times for 10 min in a washing solution (PBS, TBS or WesternBreeze® depending on the primary antibody). Fifth, membranes were blocked for one hour in blocking buffer, prepared specifically as recommended by the manufacturer (blocking buffer I: 10% skin milk powder, PBS or TBS; blocking buffer II: 10 % BSA, PBS or TBS) at room temperature followed by an overnight incubation at 4 °C in primary antibody diluted in blocking buffer. Sixth, the membranes were

washed again three times for 10 min in washing solution, incubated for one hour in a secondary antibody in blocking solution at room temperature and washed again three times for 10 min in washing solution.

Seventh, for the chemiluminescent visualization, ELC<sub>TM</sub> Western Blotting Analyses System was applied as recommended by the manufacturer. Chemiluminescence detection was performed with Diana III camera system.

### **5.3.7 Liposome preparation and NBD-lipid uptake**

Liposome preparation and NBD-lipid uptake were performed following previously published protocols (57). Liposomes (~100 nm) containing C<sub>12</sub>-NBD-PC or C<sub>12</sub>-NBD-PE were prepared by mixing lipids in chloroform in the following molar ratios: L- $\alpha$ DPPC : C<sub>12</sub>-NBD-PC : egg PC : egg PG : cholesterol = 5:5:5:3:2 and L- $\alpha$ DPPC : egg PC : egg PG : cholesterol : C<sub>12</sub>-NBD-PE = 10:5:3:2:2. Cells grown on coverslips were transfected with pUB6-HA vectors expressing ABCA3 WT or one of the three mutations. 48 h later cells were incubated for 2 h with liposomes so that the final concentration of C<sub>12</sub>-NBD-PC or C<sub>12</sub>-NBD-PE in the medium was 150  $\mu$ M. Cells were washed three times with PBS and prepared for immunofluorescence with primary monoclonal rat anti-HA-tag antibody (1:200, Roche) and secondary anti-rat IgG Alexa Fluor 555 antibody (1:200, Invitrogen). NBD-lipid uptake was examined with an Olympus FluoView FV 1000 confocal microscope.

### **5.3.8 RNA isolation from A549 cells**

A549 cells were grown to  $2.4 \times 10^5$  cells/ 6 well and were transfected 8 hours later. Where necessary, incubation with 10  $\mu$ g/ml of tunicamycin (TM) was started 24 hours after transfection. 48 hours after transfection, RNA was isolated with the help of High Pure RNA Isolation Kit and DNase I, RNase free according to manufacturer's recommendation. Isolated RNA was stored at - 80 °C and when necessary, thawed on ice.

### **5.3.9 RT-PCR**

SuperScript<sup>TM</sup>III First Strand Synthesis System for RT-PCR was used to generate cDNA on total RNA template isolated from A549 cells. Reactions, containing 1 $\mu$ g of total RNA and oligo (dT)-primers, were performed according to the manufacturer's protocol. To

exclude genomic DNA contamination of RNA template a negative control without addition of reverse transcriptase (RT) was performed for each sample. To amplify gene of interest, PCR was conducted with gene specific primers and 5 µl of DNA-product. Table 12 shows optimal parameters for RT-PCR.

**Table 12:** Optimal cycling parameters for RT-PCR in this study.

Time	Temperature	Cycles
5 min	95 °C	1
20 sec.	95 °C	35
20 sec.	65 °C	35
45 sec.	72 °C	35
5 min	72 °C	1
∞	4 °C	1

To obtain the level of basal protein expression, PCR was also performed with a housekeeping specific primer. PCR products were subjected to a 3% agarose gel. The results were considered positive and were statistically evaluated, when no PCR-bands appeared in reactions without addition of RT.

### 5.3.10 Densitometric analysis of the intensity of protein and DNA bands

First, chemiluminescence detection of proteins separated by Western Blotting was performed with Diana III camera system (Raytest). Second, the amount of proteins or the amount of DNA separated on agarose gels was evaluated by densitometry with the help of the software AIDA. The relative band intensity of the protein or DNA band was obtained through normalization to the intensity of a housekeeping protein or gene.

### 5.3.11 Immunofluorescence

Cells were grown on coverslips and after 24 hours these cells were transfected either with pEYFP-*ABCA3*- or with pUB6-*ABCA3-HA*- vector. 48 hours after transfection, cells were fixed and permeabilized by methanol incubations at room temperature for 10 min and were washed three times with D-PBS buffer. Unspecific binding sites were blocked by blocking buffer (containing D-PBS, 3 % BSA and 10 % FBS) for 30 min. Cells were incubated in

primary antibody (Table 6) diluted in blocking buffer for one hour. After incubation, samples were washed three times with D-PBS and incubated in secondary antibody, either a green- or red-fluorescent antibody (Table 7), in blocking buffer for 30 min. All further steps were performed in dark. After incubation, samples were washed again three times and coverslips were fixed on a microscope slide with Vectashield Hard and Set Mounting Media (Vector Laboratories, Burlingame, USA), containing DAPI that stains DNA and is a brilliant blue-fluorescent marker for cell nuclei.

For immunofluorescence analysis samples were evaluated with the help of Fluorescence microscope Axiovert 135 with filter sets R/B/G and filter set FRET and with the software AxioVision Release 4.7.1.

### **5.3.12 FACS analyses**

A549 cells were transfected with pEYFP-ABCA3-Wt, -R43L, -R280C or -L101P and were grown to 70 % confluence. Cells were gated in the FL-1 channel (YFP-positive population of cells). Apoptosis was determined using different approaches. Early apoptosis was assayed by 1) measuring intracellular glutathione (GSH) levels with the cell-permeable monochlorobimane (Sigma) method and 2) by annexin V<sup>+</sup>/propidium iodide (PI) staining (Cy5-conjugated anti-annexin V and PI; BD Pharmingen), and late apoptosis was determined via intracellular active caspase 3 levels (PE-conjugated anti-active-caspase 3; BD Pharmingen) in cells permeabilized with the IntraPrep kit (Beckman Coulter, Krefeld, Germany) according to manufacturer's protocol. To exclude unspecific binding isotype controls for caspase 3 and negative controls for glutathione and annexin V/PI staining were applied. BD FACSCanto II Flow Cytometer was used for the assay and FACSDiva v6.1.3 for data analyses (BD Bioscience).

### **5.3.13 Statistical analyses**

Statistical analysis was performed by one-way ANOVA and Bonferroni's test using GraphPad Prism version 4.0 (GraphPad Software Inc., San Diego, CA). All results were presented as means  $\pm$ SEM of minimum four experiments and p-values < 0.05 were considered significant.

## 6. Results

### 6.1 Creating a model system to analyse the effect of ABCA3 mutations on alveolar type II cells' homeostasis

In attempt to elucidate how the overexpression of R43L, R280C and L101P mutant ABCA3 protein impair homeostasis of human type II pneumocytes, the first part of the study was concentrated on creation of a plasmid vector carrying WT ABCA3 cDNA, on introduction of point mutations and on generating a cell system that can be easily transfected with a high efficiency.

#### 6.1.1 Generation of pUB6-hABCA3 vector and site-directed point mutagenesis

With intention to detect and exclude any effect of YFP-protein expression on intracellular ABCA3 protein localization, another plasmid vector carrying WT ABCA3 cDNA was created and subsequent used for transfection into A549 cells and for immunofluorescence studies. For this purpose, pJet1/hABCA3-HA, carrying HA-tag fused to C-terminal of the ABCA3 gene, was used as a starting vector from which ABCA3-HA cDNA was cloned into puB6/lacZ (Fig.13, 14).

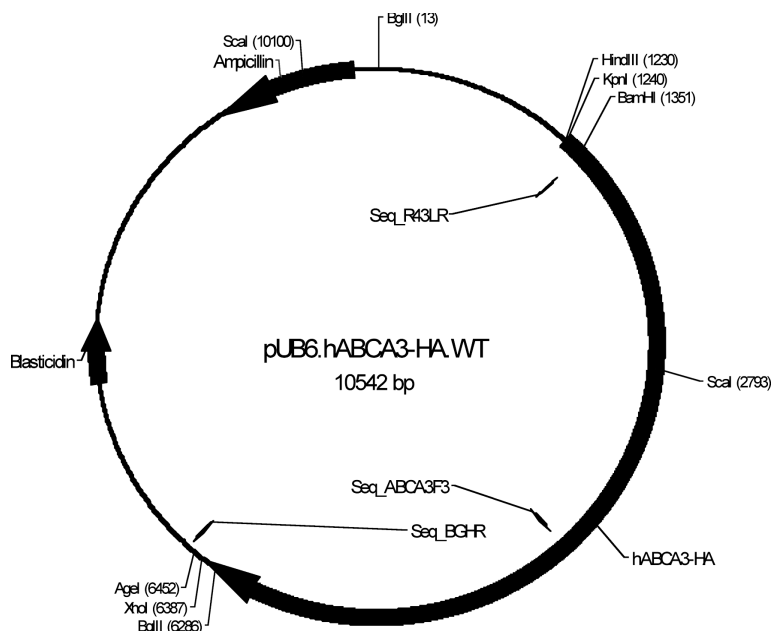
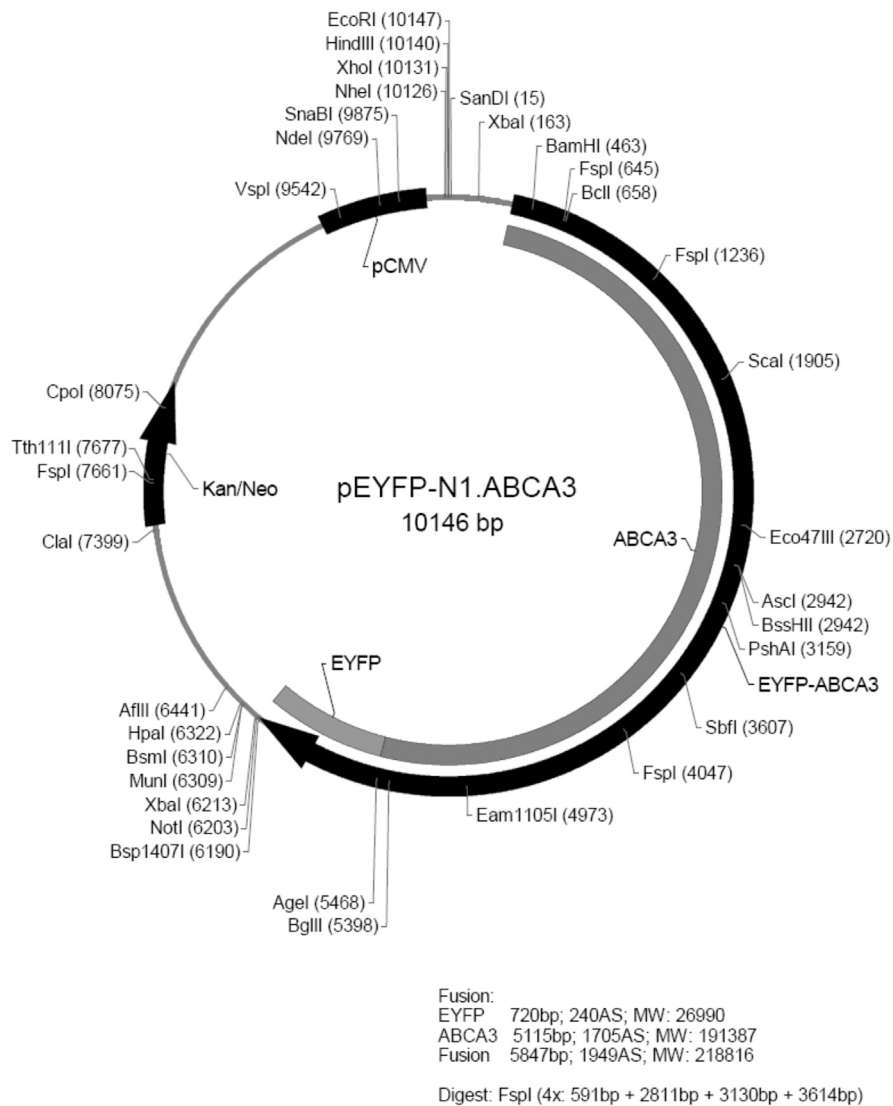
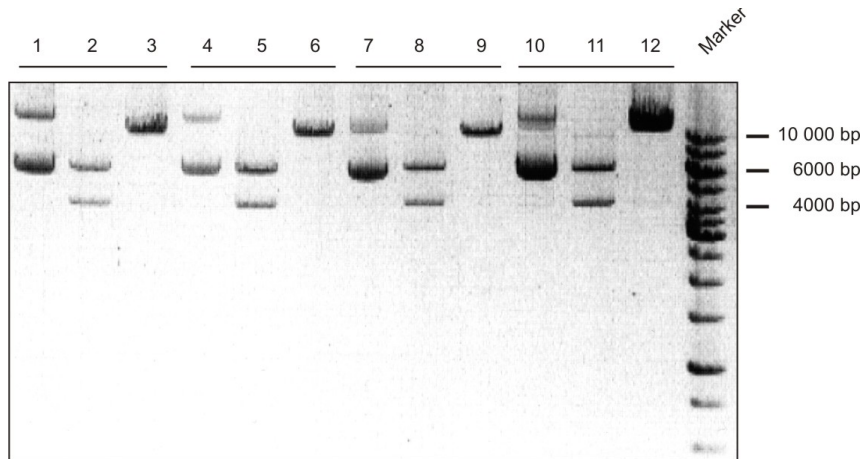


Fig.13: Vector map of pUB6-hABCA3-HA-WT



**Fig.14:** Vector map of pEYFP-ABCA3-WT

To investigate the effect of R43L, R280C and L101P mutant proteins on human alveolar type II pneumocytes, these point mutations were created by site-directed point mutagenesis into pUB6-hABCA3-HA and pEYFP-ABCA3 vectors. The results of cloning and subsequent site-directed point mutagenesis were confirmed by enzymatic restriction and sequencing (Fig.15 and 16).



**Fig.15:** Analysis of pUB6/h*ABCA3*-*HA*-WT, -R43L, R280C and -L101P plasmids. Analysis of pUB6/h*ABCA3*-*HA*-WT in lane 1-3, of pUB6/h*ABCA3*-*HA*-R43L in lane 4-6, of pUB6/h*ABCA3*-*HA*-R280C in lane 7-9 and of pUB6/h*ABCA3*-*HA*-L101P in lane 10-12 on a 0.8 % agarose gel. Plasmid DNA was restricted either with Bgl II (lane 2, 5, 8, 11) giving two chains (6273 bp and of 4269 bp) or with Hind III (lane 3, 6, 9, 12) linearizing the vector (10542 bp). Not restricted vectors are shown in lane 1,4,7,10.

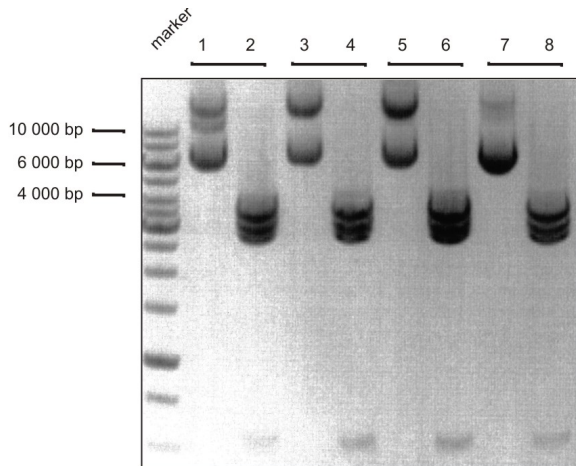


**Fig.16:** Analysis of pEYFP/*ABCA3*-WT, -R43L, R280C and -L101P plasmids. Analysis of pEYFP/*ABCA3*-WT in lane 1 and 2, of pEYFP/*ABCA3*-R43L in lane 3 and 4, of pEYFP/*ABCA3*-R280C in lane 5 and 6 and of pEYFP/*ABCA3*-L101P in lane 7 and 8 on a 0.8 % agarose gel. In lane 1,3,5 and 7 plasmids are not restricted. Plasmid DNA restricted with Fsp I is shown in lane 2,4,6 and 9, giving four chains (3614 bp, 3130 bp, 2811 bp, 591 bp).

### 6.1.2 Optimization of transfection procedure in A549 cell line

Transfection of plasmid DNA into A549 cells was performed with the help of ExGen 500 from Fermentas. To achieve best transfection efficiency, the protocol provided by the manufacturer was varied. For this purpose, four ExGen/ DNA ratios from 1:5 - 1:8 were tested. Transfection efficiency of vectors carrying *ABCA3* cDNA was examined in parallel to transfection efficiency of a small reference vector pmax-GFP from AMAXA. Best results were achieved with an ExGen/ DNA ratio of 1:6 and subsequent incubation. After the mixture was incubated at room temperature for 10 min and was added to the cells, the plate with cells was not centrifuged, as originally recommended by the manufacturer. For pmax-GFP, transfection efficiency was 80 %, whereas for pEYFP-*ABCA3* and pUB6-h*ABCA3*-*HA* it was

20 % at most. The low transfection efficiency can be explained by difficulties in transfection of the huge vector size accompanied by the huge size of the *ABCA3* gene. Transfection efficiency was controlled at different time points. 12, 24, 48 and 72 hours after transfection, *ABCA3*-WT protein localization was determined to lamellar bodies (LB). For further experiments, cells were collected 48 hours after transfection to ensure enough time for general protein turnover in presence and influence of mutant *ABCA3* proteins (Fig.17).

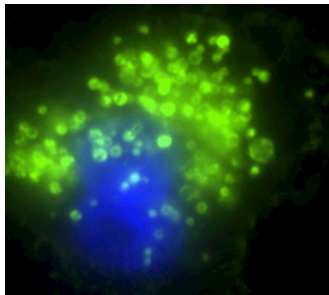


**Fig.17:** Immunofluorescence studies in A549 cell line, transiently transfected with pEYFP-*ABCA3*-WT.

## **6.2 General characterization of R43L, R280C and L101P *ABCA3* mutations**

In the first part of the study, important preliminary work was accomplished: a vector containing WT *ABCA3* cDNA tagged with HA was created and introduction of point mutations into pUB6-h*ABCA3*-HA and pEYFP-*ABCA3* vectors was performed. In addition, a protocol for transient transfection of A549 cells was established, being an essential precondition for the following investigation of type II pneumocytes' homeostasis influenced by *ABCA3* mutant proteins.

Three clinically relevant *ABCA3* mutations identified in patients with neonatal surfactant deficiency (R43L and L101P) and chronic pILD (R280C) were chosen for the study. While cell biology of R43L and R280C mutations has not been studied yet, L101P mutation was previously described as a trafficking/folding defect resulting in the ER retention of L101P protein. L101P mutation was deliberately chosen for this study as a cause for the *ABCA3* ER retention. As so far Matsumura and colleagues (61) have described two categories of mutations, general characterization of the new mutations R43L and R280C was assessed by determination of the intracellular protein localization and analysis of protein expression, processing and glycosylation.

### 6.2.1 Localization and trafficking

Previous studies showed localization of the ABCA3 transporter to the limiting membrane of lamellar bodies (LBs) in lung alveolar type II-cells (41). In order to investigate ABCA3 protein localization or possibly impaired protein trafficking in A549 cells, staining of different cell compartments was performed in parallel with staining of the ABCA3 protein. Following compartments were analysed: First, LBs were stained with the marker LAMP3, an integral part of membranes of LBs. Second, the ER, important for protein processing and quality controlling, was marked by calnexin, an ER-bound chaperone that is involved in quality control of protein folding within the UPR system (see “*Introduction*”), in order to elucidate if ABCA3 mutant proteins might be retained in the ER due to processing or folding defect. Third, as the Golgi apparatus is an integral part of processing, sorting and modification of proteins delivered from the ER, ABCA3 mutant protein localization to this cell compartment was assessed as well via the marker GM130. GM130 codes for a protein that participates in forming and maintaining cis-Golgi and that supports vesicular transport. Fourth, early endosomes were detected via EEA-1, a protein that binds phosphatidylinositol-3-phosphate in endosomes membranes. Endosomes are formed via endocytosis and plasma membrane invagination and transport proteins to lysosomes for subsequent digestion.

To double confirm ABCA3 protein localization in A549 cells and to rule out possible influence and effect of YFP-expression, colocalization studies were performed in parallel with pEYFP-ABCA3 vector and pUB6-hABCA3-HA vector. Effects that could have been expected in case of YFP-ABCA3 expression were protein aggregation, impaired protein trafficking and protein degradation. The intracellular protein localization of ABCA3 protein was determined 48 hours after transfection. Fluorescence microscopy of A549 cells expressing either type of ABCA3 protein fusions showed no differences in protein behavior depending on the type of the vector or the size of the protein tag. YFP-ABCA3 WT protein was completely localized to LBs (Fig.18). ABCA3 WT protein appeared as a ring-like and dot-like structure in immunofluorescence (Fig.18). The colocalization of WT with the ER protein calnexin, GM130 and EEA1 was not present (Fig.18B, 19, 20). Similar was observed in the case of R43L mutant, which gave a vesicular signal that overlapped with LAMP3 fluorescence (Fig.18A) and showed no colocalization with calnexin, GM130 and EEA1 (Fig.18B, 19, 20). R280C protein colocalized frequently with LAMP3, however the colocalization was not absolute, often showing cytoplasmic distribution that overlapped with the fluorescence of calnexin (Fig.18, A and B). L101P mutation did not show any vesicular signal at all (Fig.18A) but it presented with a net-like cytoplasmic fluorescence colocalizing with the ER protein calnexin (Fig.18B). Further immunofluorescence studies showed no localization of L101P mutant protein with markers for Golgi apparatus or early endosomes (Fig.19, 20).

This suggests correct localization of the WT and R43L transporters in the LAMP3-positive (LAMP3<sup>+</sup>) vesicles and retention of the L101P mutant in the ER, possibly as a result of protein misfolding. Dual localization of R280C protein might be a sign of hindrance in the processing and folding of this mutant which slows down but does not abolish its progress through the ER, Golgi and toward LAMP3<sup>+</sup> vesicles. As no differences in the intracellular ABCA3 protein localization were found in A549 cells transfected with plasmid vectors expressing ABCA3-YFP (pEYFP-N1/ABCA3) or ABCA3-HA-tag (pUB6-HA/ABCA3), further experiments were performed with pEYFP-ABCA3 vector because it was easier to control the transfection efficiency with this self-fluorescent vector prior to further experiments.

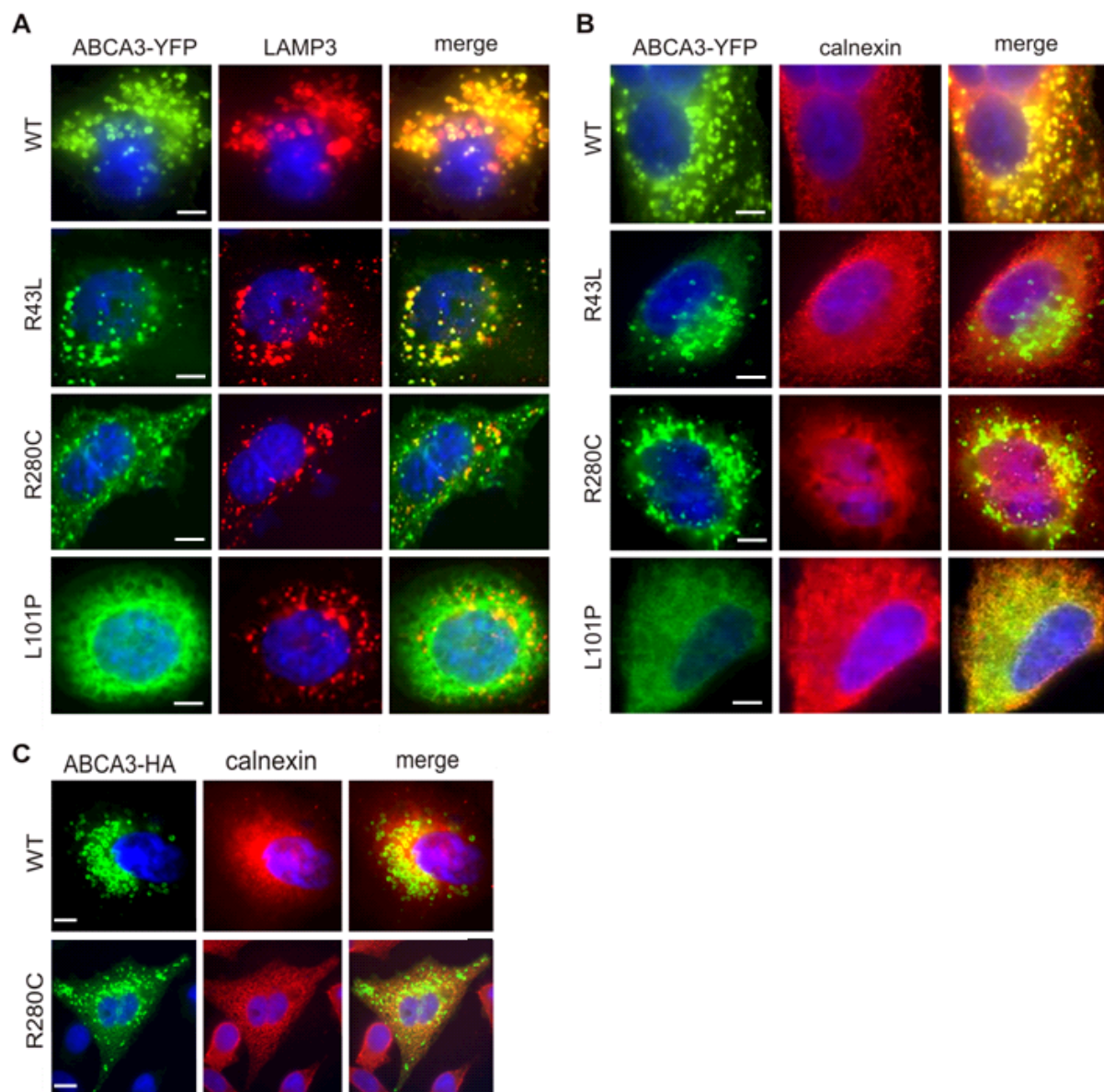


**Fig.18:** Intracellular localization of the WT and mutant R43L, R280C and L101P ABCA3 proteins (I). A549 cells were transiently transfected with pEYFP-N1/ABCA3 vectors expressing WT or one of the three mutations. YFP fluorescence of ABCA3-YFP fusions (*green*) was used to detect ABCA3 WT and R43L, R280C and L101P proteins. Colocalization of the ABCA3-YFP signal with immunofluorescence of (A) lysosomal/lamellar body protein LAMP3 and (B) ER protein calnexin (*both red*) are shown. WT and R43L localized in LAMP3<sup>+</sup> vesicles, R280C in LAMP3<sup>+</sup> vesicles and partially in the ER and L101P completely in the ER. C. Partial ER localization of HA-tagged R280C in A549 cells transfected with pUB6-HA-R280C plasmid confirms the R280C ER retention as independent of the type of plasmid or protein tag. Representative pictures are shown. Scale bars: 5 μm.

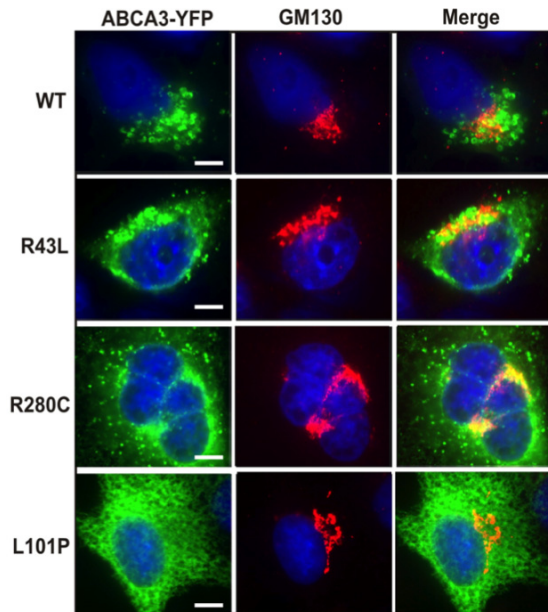


**Fig.19:** Intracellular localization of the WT and mutant R43L, R280C and L101P ABCA3 proteins (II). A549 cells were transiently transfected with pEYFP-N1/ABCA3 vectors expressing WT or one of the three mutations. YFP fluorescence of ABCA3-YFP fusions (*green*) was used to detect ABCA3 WT and R43L, R280C and L101P proteins. Golgi apparatus was marked with GM130 (*red*). Colocalization of the ABCA3-YFP signal with immunofluorescence of the Golgi apparatus was not present in WT or mutants. Representative pictures are shown. Scale bars: 5  $\mu$ m.

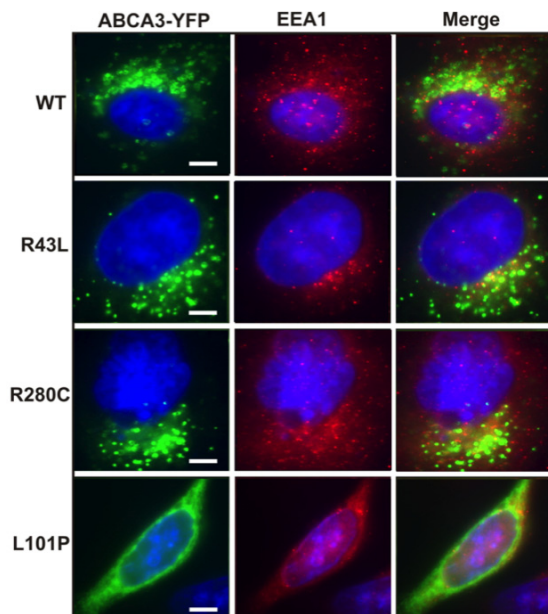


**Fig.20:** Intracellular localization of the WT and mutant R43L, R280C and L101P ABCA3 proteins (III). A549 cells were transiently transfected with pEYFP-N1/ABCA3 vectors expressing WT or one of the three mutations. YFP fluorescence of ABCA3-YFP fusions (*green*) was used to detect ABCA3 WT and R43L, R280C and L101P proteins. Colocalization of the ABCA3-YFP signal with EEA1, the immunofluorescence signal of early endosomes (*red*), was not present in WT or mutants. Representative pictures are shown. Scale bars: 5  $\mu$ m.

Several authors report localization of ABCA3 WT protein in LBs. To provide an additional confirmation of ABCA3 WT protein localization to LBs, it was tested if ABCA3 WT protein colocalizes with surfactant protein C (SP-C) that is stored within LBs. For this

purpose, A549 cells were cotransfected with pcDNA4-To-ABCA3-HA-WT and pEGFP-N1-SPC-WT vectors and immunofluorescence studies were performed. As a result, almost complete colocalization of ABCA3 WT protein and SP-C WT protein was found forming dot-like structures (Fig.21). This result confirms that ABCA3 WT and SP-C WT proteins do colocalize to LAMP3 positive dot-like structures in alveolar type II cells.

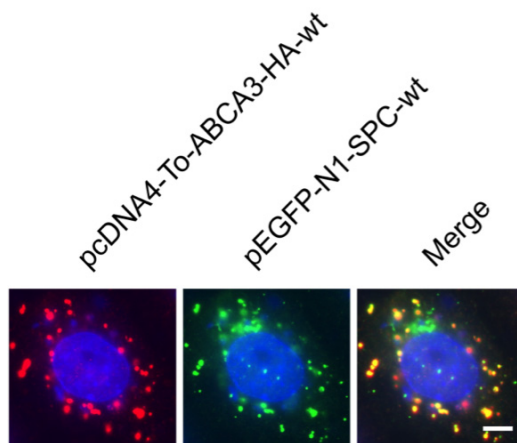


**Fig.21:** Intracellular colocalization of ABCA3 WT and SP-C WT protein. A549 cells were transiently cotransfected with pcDNA4-TO-ABCA3-HA-WT and pEGFP-N1-SPC-WT vectors. GFP fluorescence of SP-C fusions (*green*) was used to detect SP-C WT. Absolute colocalization of the SP-C-GFP signal with immunofluorescence of HA-tagged ABCA3-WT (*red*) is shown confirming the ABCA3 localization to lamellar bodies. Scale bars: 5  $\mu$ m.

### 6.2.2 ABCA3 WT and mutant protein processing and maturation in A549 cells

Since incomplete LB-localization of R280C mutant and absolute ER-storage of L101P mutant, indicating a strong misfolding and processing defect, further investigation on ABCA3 protein expression was performed. In immunoblots, two protein bands (180 kDa and 220 kDa), 30 kDa bigger than previously observed in not labeled ABCA3 constructs (57, 61) due to the presence of the 30 kDa yellow fluorescent protein (YFP), were immunodetected in ABCA3 WT, R43L and R280C by anti YFP/GFP antibody in transiently transfected A549 cells (Fig.22A). The processing of ER retained L101P protein was different showing complete lack of the 180 kDa band, in line with published data (57, 61, Fig.22A). However, it can be concluded that absence of 180 kDa protein band in L101P mutant protein is a strong indicator for impaired protein processing, suggesting that ABCA3 cleavage is an essential step for ABCA3 protein maturation and subsequent trafficking. New data showed that the 150 kDa protein band is possibly the mature ABCA3 transporter and necessary for its functionality (34). Generation of the lower 150 kDa band in R43L and R280C mutants as observed in ABCA3 WT is necessary for at least partial ABCA3 function.

### 6.2.3 Glycosylation of ABCA3 protein

After Western Blotting analysis of cell lysates from cells expressing ABCA3 protein, demonstrating that ABCA3 WT, R43L and R280C mutant proteins are expressed as 220 kDa and 180 kDa forms, whereas 180 kDa protein is not detectable in L101P mutant (Fig.22A), further investigation on ABCA3 processing was performed.

Glycosylation is an enzymatic process within the ER and Golgi, which links saccharides to immature proteins to produce glycans. ABCA3 is a glycoprotein that obtains high-mannose oligosaccharides inside of the ER and complex oligosaccharides by modification of high-mannose oligosaccharides in the Golgi. Processing of oligosaccharides and protein progress down the ER-Golgi maturation pathway was analyzed by deglycosylation of the membrane fractions from the A549 cells expressing WT and three mutations with two endoglycosidases EndoH (cleaves only high-mannose sugars) and PNGaseF (cleaves high-mannose and complex sugars) (Fig. 22B). Immunoblotting with anti-GFP antibody revealed absence of complex sugars in L101P protein that was susceptible to both enzymes, PNGaseF and EndoH, resulting in both cases in a single shifted deglycosylated 210 kDa band and no 220 kDa band. Both sugar types were present in WT, R43L and R280C proteins, as visible by the resistance of a portion of the 220 kDa band to the EndoH treatment. The 180 kDa band was resistant to deglycosylation (Fig.22B). These results also additionally confirm the localization studies showing retention of the L101P mutant in the ER and ability of WT, R43L and R280C to progress further from the ER to the Golgi.

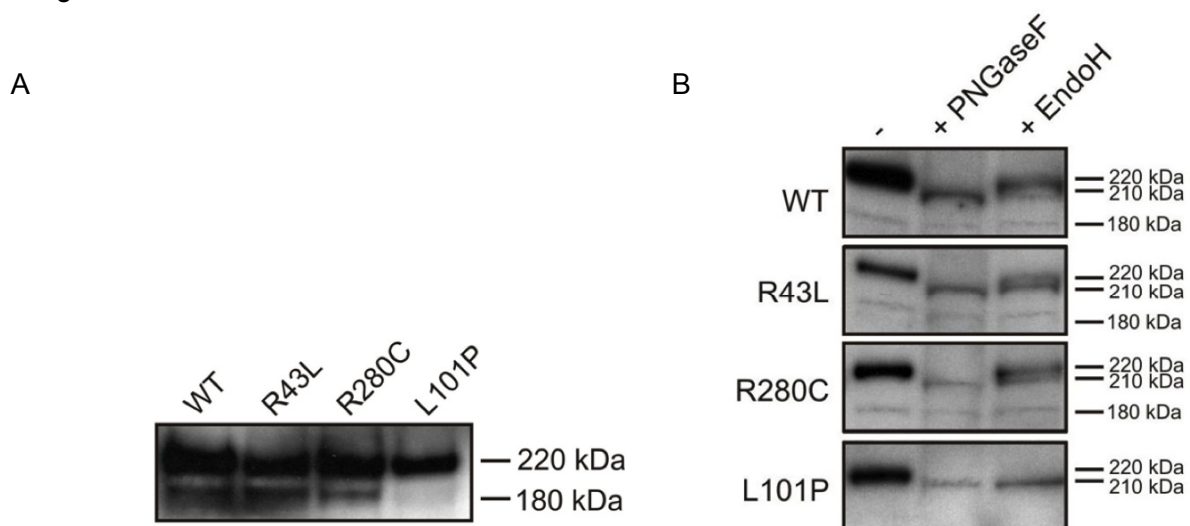


**Fig.22: Processing of the WT and mutant R43L, R280C and L101P ABCA3.** (A) Immunodetection with anti-GFP antibody showed two ABCA3 protein bands (180 kDa and 220 kDa) in whole cell lysates of A549 cells expressing WT and R43L and R280C mutations, and only one protein band in the cells expressing L101P mutation. (B) Deglycosylation assay with PNGaseF and EndoH on the membrane fractions from A549 cells transfected with pEYFP-N1/ABCA3 plasmids and subsequent ABCA3-YFP immunodetection with anti-GFP antibody showed presence of high-mannose and complex oligosaccharides in WT, R43L and R280C proteins, as well as only high-mannose and no complex oligosaccharides in the L101P mutant resulting from the L101P ER retention.

#### 6.2.4 Functional assay

Trafficking/ folding defect and ER accumulation of L101P protein exclude the ABCA3 function in the case of this mutant. However, R43L and R280C mutation are mostly (R280C) or completely (R43L) correctly localized and potentially functional (Fig.18, A and B). Therefore, a functional study of uptake of fluorescently NBD-labeled lipids into the lamellar-body-like vesicles in A549 cells transfected with pUB6-HA/ABCA3 plasmids was performed (Fig.23). Liposomes containing NBD-labeled major surfactant phospholipid phosphatidylcholine (C<sub>12</sub>-NBD-PC) and NBD-labeled minor surfactant phospholipid phosphatidylethanolamine (C<sub>12</sub>-NBD-PE) were incubated with A549 cells expressing WT, R43L, R280C and L101P HA-tagged proteins. L101P mutant was used to monitor the situation with nonfunctional ABCA3 protein. Colocalization of the fluorescent signal of C<sub>12</sub>-NBD-PC and C<sub>12</sub>-NBD-PE (green) with ABCA3-HA-positive vesicles (red), which normally colocalized with LAMP3 (Fig.18, A and B), was monitored by confocal microscopy.

Interestingly, uptake of fluorescent liposomes into A549 cells was prominent in all cells, including those expressing L101P mutants (Fig.23) and therefore without ABCA3 function and untransfected A549 (data not shown), showing numerous NBD-positive vesicular structures dispersed throughout the cytoplasm (Fig.23). This confirms that lipid/liposome uptake into the cytoplasm through the plasma membrane does not depend on functional ABCA3, and that ABCA3 is solely an intracellular vesicular lipid transporter.

WT-ABCA3-HA signal formed ring-like structures, consistent with the localization of ABCA3 in the limiting membrane of lamellar bodies. Both NBD-PC and NBD-PE fluorescent signals were often visible as a punctual signal merging with this ring-like border of WT-ABCA3-HA vesicles (Fig.23, A-C). Also, accumulation of the weaker diffuse green NBD signal was frequently observed within the inner space of WT-ABCA3-HA vesicles (Fig.23C and Fig.23, A and B - small sections). NBD is a fluorophore characterized by extremely fast photobleaching and we suppose that uptake and packing of a bigger amount of this fluorescent dye into the WT-ABCA3-HA vesicles might cause self-quenching of the fluorescence. Another possible reason for this effect is a diffuse distribution of the limited amount of NBD-phospholipids within the vesicles, which makes the signal less pronounced. Similar colocalization of NBD fluorescence with ABCA3-HA vesicles was extremely rarely observed in the cells expressing R43L and R280C mutations (Fig.23, A and B). This indicates ability of WT-ABCA3-HA vesicles to take up and accumulate both fluorescent lipids, while R280C-ABCA3-HA and R43L-ABCA3-HA vesicles did not show such ability.

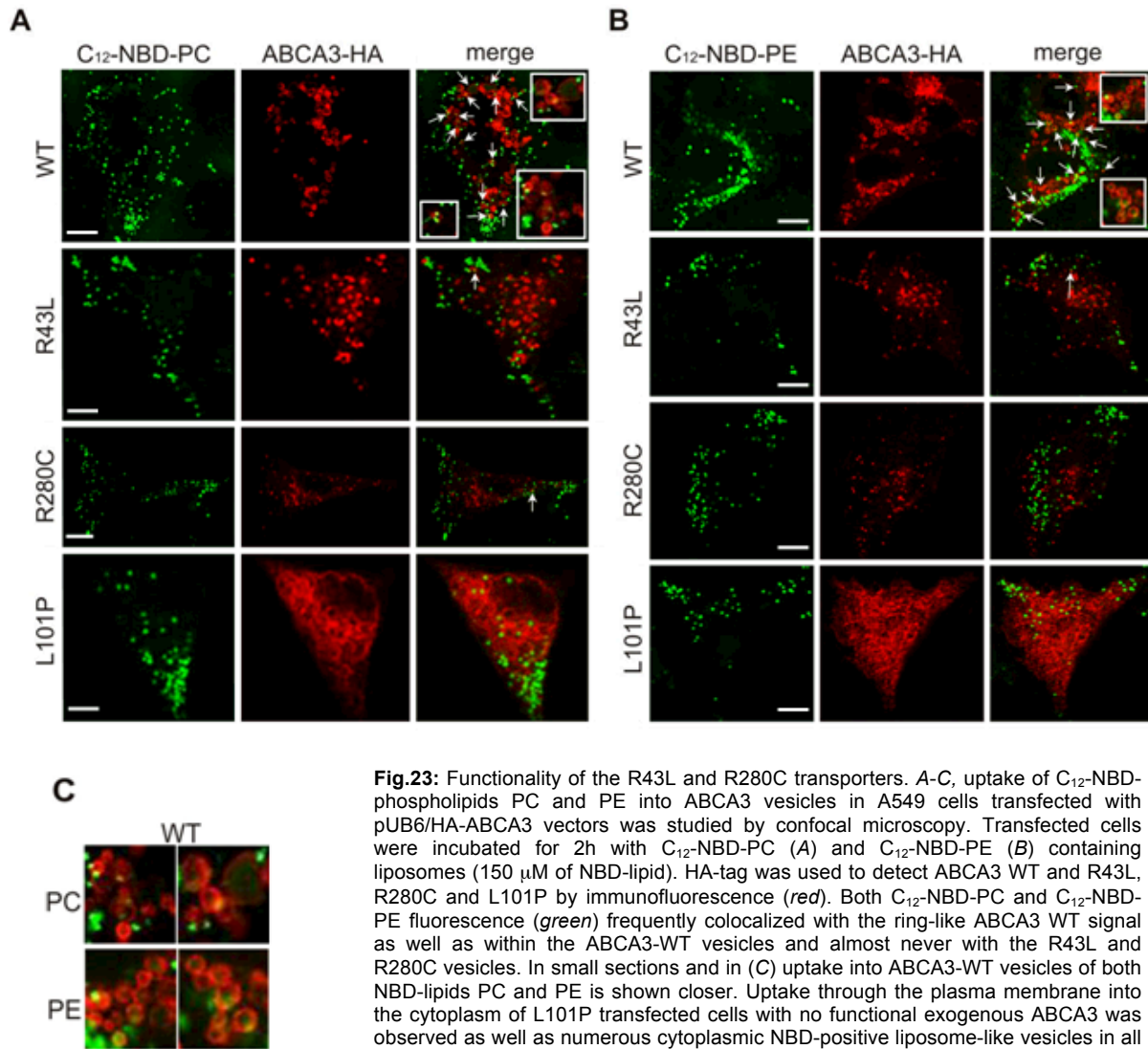


**Fig.23:** Functionality of the R43L and R280C transporters. A-C, uptake of C<sub>12</sub>-NBD-phospholipids PC and PE into ABCA3 vesicles in A549 cells transfected with pUB6/HA-ABCA3 vectors was studied by confocal microscopy. Transfected cells were incubated for 2h with C<sub>12</sub>-NBD-PC (A) and C<sub>12</sub>-NBD-PE (B) containing liposomes (150 μM of NBD-lipid). HA-tag was used to detect ABCA3 WT and R43L, R280C and L101P by immunofluorescence (red). Both C<sub>12</sub>-NBD-PC and C<sub>12</sub>-NBD-PE fluorescence (green) frequently colocalized with the ring-like ABCA3 WT signal as well as within the ABCA3-WT vesicles and almost never with the R43L and R280C vesicles. In small sections and in (C) uptake into ABCA3-WT vesicles of both NBD-lipids PC and PE is shown closer. Uptake through the plasma membrane into the cytoplasm of L101P transfected cells with no functional exogenous ABCA3 was observed as well as numerous cytoplasmic NBD-positive liposome-like vesicles in all A549 cells independent of the ABCA3 mutation (A and B). Scale bars: 5 μm

### 6.2.5 Biogenesis of LAMP3<sup>+</sup> vesicles induced by ABCA3-WT protein expression

Expression of WT or three mutations exhibited different effects on biogenesis of the LAMP3<sup>+</sup> vesicles in A549 cells. To elucidate the effect of ABCA3 expression on LB biogenesis in AT II cells, the amount of LBs was assessed in ABCA3 Wt and mutants. A549 cells normally show a low number of small LAMP3<sup>+</sup> vesicles, but expression of WT-ABCA3 induced biogenesis of many big vesicles with ring-like signals of ABCA3 fluorescence (equally from pEYFP-N1 or pUB6-HA vectors). Expression of R43L, R280C and L101P mutations exhibited a negative effect on vesicle formation and induced a lower number of smaller compact LAMP3<sup>+</sup> vesicles, with the most drastic effect in L101P mutant (Fig.24). This again proves the role of ABCA3 in lamellar body biogenesis as previously described (55, 57, 58). Decreased uptake of NBD fluorescence in lamellar bodies and impact on lamellar body biogenesis together suggest functional impairment of the R43L and R280C proteins.

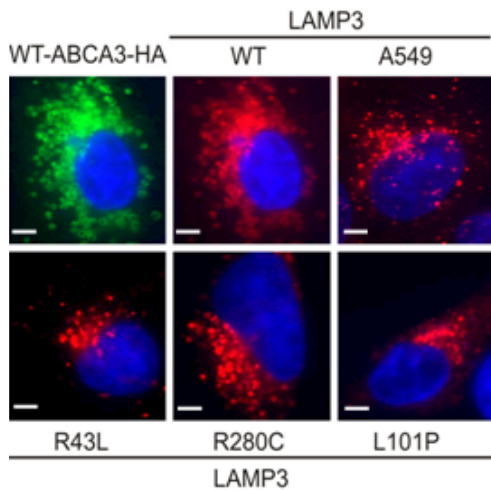


**Fig.24:** Influence of WT ABCA3 and three mutations on biogenesis of LAMP3<sup>+</sup> vesicles in A549 transfected with pUB6/HA-ABCA3. WT ABCA3 (*green*) induced biogenesis of LAMP3<sup>+</sup> vesicles (*red*) increasing their number and size in A549 cells, while R43L, R280C and L101P proteins showed no such effect (the same was observed in A549 pEYFP-N1/ABCA3 transfected cells - not shown). Representative pictures are shown. Scale bars: 5  $\mu$ m.

### 6.3 Induction of ER stress by mutant ABCA3 expression

In the first two parts of this study, general characterization of the clinical relevant mutations R43L, R280C and L101P was performed by identification of the intracellular protein localization to LBs or ER (Fig.18) and analysis of glycosylation pattern of ABCA3 WT and mutant proteins (Fig.22B). Since these ABCA3 mutations caused a decrease of LB numbers, further studies were performed to elucidate how these mutants disturb cell homeostasis of AT II cells.

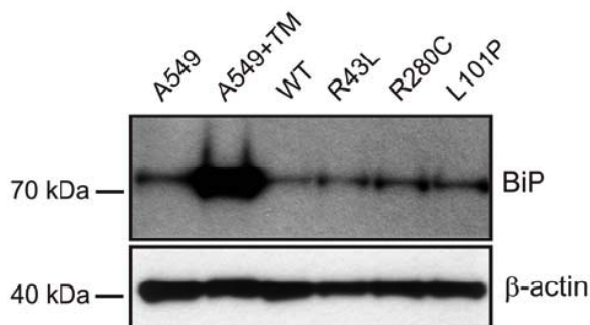
However, a model, in which misfolded proteins cause cell injury and cell death through disruption of the quality control system (see *“Introduction”*), was supported by a study on misfolded SP-C. It was shown that ER protein accumulation and cytosolic aggregate formation of some SP-C mutations induced ER stress and subsequent apoptotic cell death (106). Based on these results, the aim of this study was to analyse cellular response to mutant ABCA3 protein expression as previously demonstrated for SP-C mutations, especially in terms of ER chaperones and apoptotic markers.

### 6.3.1 L101P and R280C mutation upregulate ER stress marker BiP

BiP/Grp78 is an essential ER chaperone of Hsp70 family, which assists translocation of a nascent protein chain into the ER and its subsequent folding. When misfolded proteins accumulate in the ER, BiP upregulation is one of the first signals of the ER stress and allows further UPR activation (116). The effect of ABCA3 mutations on chaperones is especially interesting since until now ER stress-induction has not been investigated in ABCA3 mutants.

Immunoblotting of whole cell lysates from A549 cells expressing ABCA3-WT and three mutants revealed upregulation of BiP chaperone in the case of the L101P and R280C mutations in comparison to WT (Fig.25, A and B), caused by complete (L101P) and partial (R280C) ER retention of these two mutated ABCA3 transporters (Fig.18). No significant BiP increase was detectable between WT and correctly localized R43L mutation. While treatment of A549 cells with a potent ER stress-causing antibiotic tunicamycin (TM) caused drastic BiP upregulation in A549 cells, differences measured between WT and three mutations were more subtle differences.

A



B

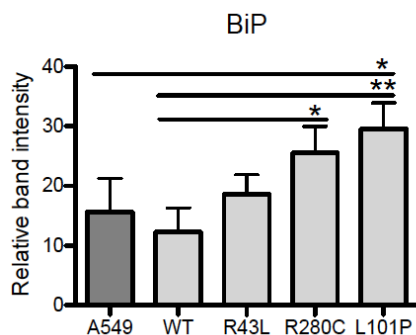
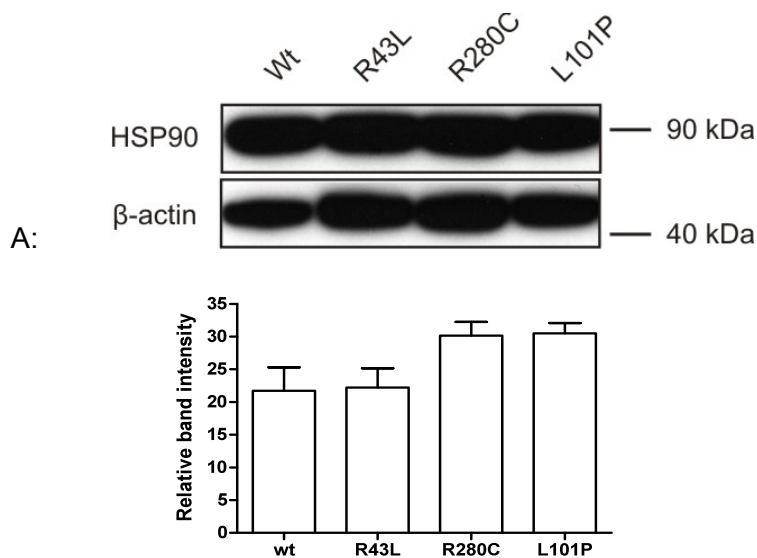


**Fig.25:** ER stress chaperone BiP. A, A549 cells with ER retained L101P mutant or partially ER retained R280C protein showed upregulation of the immunodetected ER chaperone BiP in comparison to WT and A549 cells. BiP was drastically upregulated after 14h treatment of A549 cells with 10ug/ml of ER stressor tunicamycin (TM). B, intensity of each protein band was densitometrically quantified and normalized to the corresponding  $\beta$ -actin band. Densitometric quantification of the BiP protein level of four independent experiments, without inclusion of drastic effect of TM treatment, is presented; \*  $p < 0.05$ , \*\*  $p < 0.01$ .

### 6.3.2 ABCA3 mutants influence expression of Hsp90

Heat shock protein family provides an intracellular response for general protection against protein aggregation in the cytosol. These proteins promote the conformational maturation of a large variety of proteins into three-dimensional structures. Hsp90 is the most prominent of the heat shock proteins in the cell with 1-2 % of all cytosol proteins.

The intracellular amount of Hsp90 was analysed in whole cell lysates of A549 cells transiently transfected with pEYFP-ABCA3-WT, -R43L, -R280C and -L101P by immunoblotting. The amount of Hsp90 in R43L mutant was comparable to that in WT, whereas in both R280C and L101P mutants, stronger protein band intensity was obtained (Fig.26). Fine differences between WT and mutations can be explained by only 20 % transfection rate. But the increase of Hsp90 protein expression in R280C and especially in L101P, together with increased BiP protein expression, suggest that these ABCA3 mutants have significant impact on cell homeostasis and initiate the UPR system.



B:

**Fig.26:** ER stress chaperone Hsp 90. A, A549 cells with ER retained L101P mutant or partially ER retained R280C protein showed slight upregulation of the immunodetected ER chaperone Hsp90 in comparison to WT and A549 cells. In R43L mutant, Expression of ER-chaperone Hsp90 was as low as in WT. B, intensity of each protein band was densitometrically quantified and normalized to the corresponding  $\beta$ -actin band. Densitometric quantification of the Hsp90 protein level of four independent experiments is presented.

### 6.3.3 No influence on calnexin expression by ABCA3 mutations

Moreover, together with a number of other chaperones, calnexin facilitates protein folding by catalyzing intra- and inter-molecular disulfide bond formation to prevent trafficking of unfolded proteins to Golgi apparatus and further downstream in the secretory pathway,

rather retained in the ER lumen. In attempt to elucidate any effect of mutant ABCA3 protein on calnexin expression, the whole cell lysates of A549 cells transiently transfected with pEYFP-ABCA3-WT, R43L, R280C or L101P were prepared and analyzed by immunoblotting using an anti-calnexin antibody (Fig.27A). As a result, calnexin expression did not change significantly between WT and mutations. Having only 20 % transfection rate possibly influenced the measurements of fine differences and smaller changes as well.

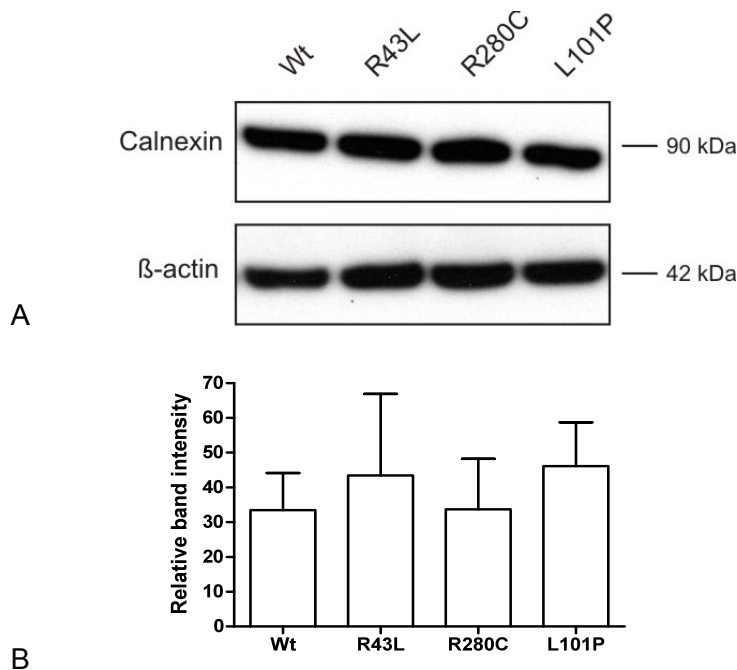


**Fig.27:** ER stress chaperone calnexin. *A*, A549 cells with ABCA3 WT and three mutations showed no upregulation of the immunodetected ER chaperone calnexin. *B*, intensity of each protein band was densitometrically quantified and normalized to the corresponding β-actin band. Densitometric quantification of the calnexin protein level of four independent experiments is presented.

### 6.3.4 L101P and R280C mutation increase susceptibility of A549 cells to the ER stress

In this study it was recognized that ABCA3 mutant proteins disturb cell homeostasis in A549 cell line via induction of ER stress assessed by chaperone BiP, particularly in case of partially (R280C) and complete (L101P) ER-retained mutations (Fig.25). Upon ER accumulation of misfolded proteins BiP dissociates from the luminal domain of IRE1, allows IRE1 dimerization and synthesis of active XBP1 protein, a UPR transcription factor, which regulates expression of ER stress proteins including BiP. XBP1 activation is regulated on the level of splicing of 26 nt intron from the *XBP1* mRNA by endoribonuclease activity of the IRE1 dimer (82-84).

To confirm the observations made on the ER chaperone level, splicing of the *XBP1* mRNA was assayed by RT-PCR as described by Hybiske and colleagues (117). Two approaches were applied to analyze XBP1 splicing. In a first experiment, 48 hours after transfection, A549 cells were analyzed for XBP1 splicing via RT-PCR and in a second experiment to intensify the stress, transfected cells were additionally incubated with 10 ng/ml of tunicamycin (TM) for 13 hours.

First, the ratio of spliced (s; ~500 bp – 26 bp) and unspliced (u; ~500 bp) XBP1 RT-PCR bands was determined, prior and after the treatment of the PCR products with *Pst*I restriction endonuclease, as a measuring control. Slower migrating hybrid (h) band of unspliced and spliced single-stranded DNAs produced during PCR, and thus equally contributing to unspliced and spliced bands, was observed as well after the long-run separation on 3 % agarose (84, Fig.28A). Tunicamycin treatment strongly increased the intensity of the spliced PCR band in A549 cells in comparison to untreated A549 (Fig.28B). In A549 cells with either WT or one of the three mutations, increase of XBP1 splicing was measured only in the case of L101P mutation (Fig.28A). Probably because of the robustness of the method and 20 % transfection rate, finer differences between WT and R43L and R280C were not observable, and the effect was measurable only in the case of the L101P as the strongest defect (Fig.28A).

Second, in attempt to imitate that in nature lungs are not exclusively affected by ABCA3 mutations but also exposed to outside stress factors such as viral infection and smoking, and to investigate the susceptibility of cells with ABCA3 mutations to external ER stress-causing agents, transfected cells were exposed to 10 mg/ml of tunicamycin, an inhibitor of N-linked glycosylation (Fig.28, D and E). The outcome of such double internal genetic and external tunicamycin pressure on XBP1 splicing was examined. Tunicamycin treatment strongly induced XBP1 splicing with the comparable effect in A549 and WT cells (Fig.28D). However, after exposure to tunicamycin XBP1 splicing was considerably more pronounced in R280C and L101P mutations if compared to A549 cells with WT and R43L mutations (Fig.28, D and E). Obviously, although XBP1 splicing was measurable only for the strongest L101P defect under non-stimulated condition, cells with L101P and R280C mutations were significantly more prone to further elevation of ER stress upon exposure to an external stressor (Fig.28, D and E).

These results demonstrate that through mimicking outer stress, ABCA3 mutants do change normal protein cell biology and disturb cell homeostasis of AT II cells more significantly by raising the level of intracellular stress and susceptibility to it. Furthermore, these results suggest that presence of outside stress factors has an additional impact on cellular response to ABCA3 mutants in AT II cells.

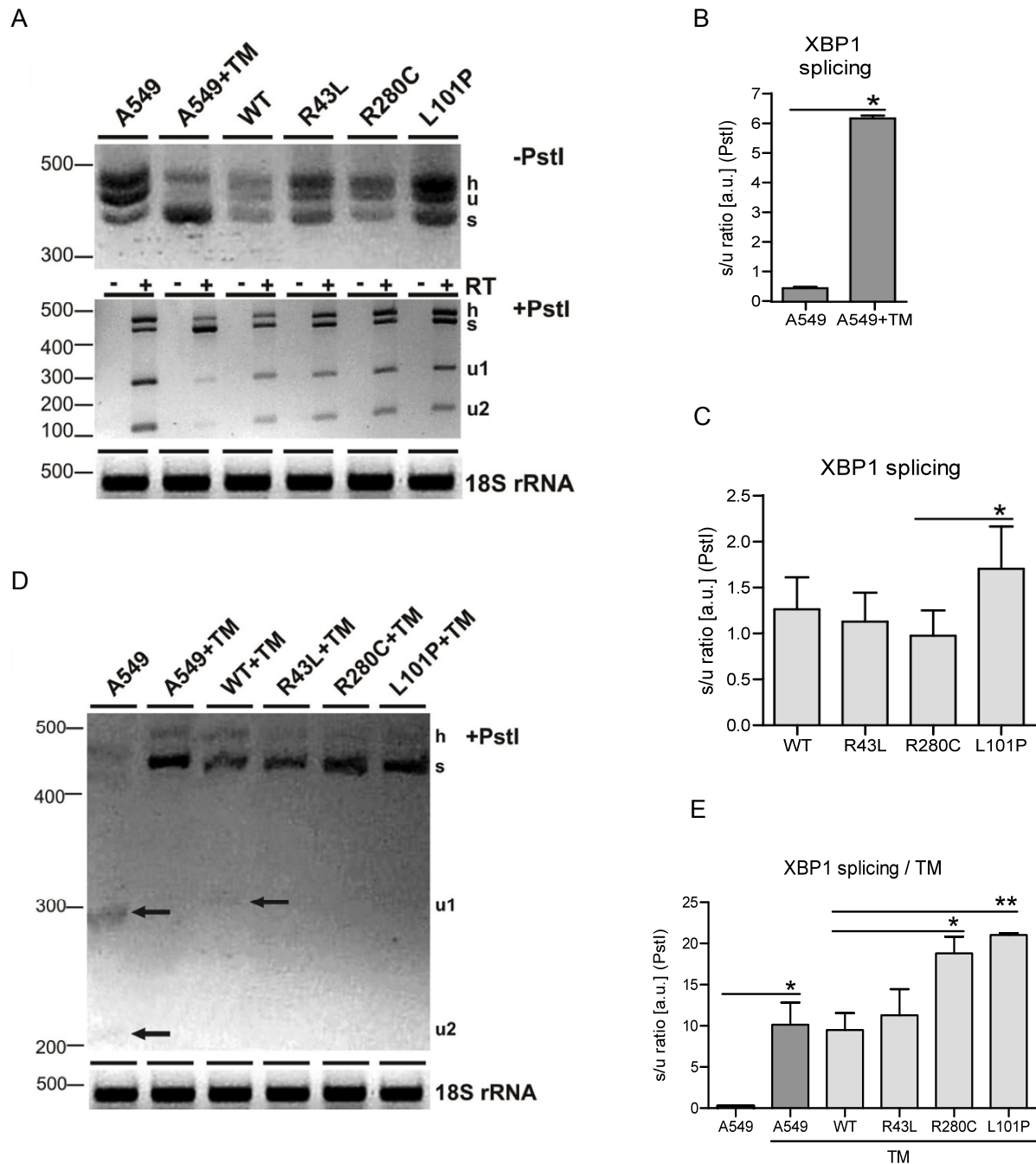


**Fig.28:** Susceptibility of A549 cells with *ABCA3* mutations to ER stress measured by XBP1 splicing. XBP1 activation during UPR is regulated on the level of splicing of a 26 nt intron from the *XBP1* mRNA. **A**, XBP1 splicing in untransfected A549 cells with and without tunicamycin (TM) treatment (10 mg/ml, 14 h) and in A549 cells with R43L, R280C and L101P mutations. Two PCR products were detected by RT-PCR: u - unspliced and s - spliced XBP1 bands. h denotes a hybrid band between unspliced and spliced ssDNA produced during PCR and observed after long-run separation on 3 % agarose (*upper panel*) (21). For easier densitometric evaluation and to ensure good separation between unspliced and hybrid band, half of the PCR products were cut by *PstI* endonuclease which cuts only unspliced (u) band giving two bands u1 and u2 (*middle panel*). Control reactions without reverse transcriptase (+/-RT) and 18S rRNA (*lower panel*) are shown as well. **B** and **C**, densitometric quantification of the bands (s, u) from the upper panel (no *PstI*) and the middle panel (shown in the graph; *PstI* digest), presented as the ratio s/u (no *PstI*) or the ration s/u1+u2 (*PstI* digest). TM highly elevated XBP1 splicing in A549 cells (**A**). Lower effect of L101P mutation on XBP1 splicing in A549 cells and no effect in A549 with WT and R43L and R280C mutations were observed (**B** and **C**). **D** and **E**, as in **A-C**: TM treatment of all A549 cells expressing *ABCA3* mutations (10 mg/ml, 14 h) strongly induced XBP1 splicing in all cells, with the most significant increase in A549 expressing R280C and L101P mutations in comparison to the WT+TM or A549+TM. After exposure to TM almost no unspliced bands (u1 and u1) were observed, only increase in spliced (s) bands in R280C and L101P mutations. Shown are the 3 % agarose after the *PstI* digestion of the RT-PCR products (*upper panel*) and 18S rRNA (*lower panel*) (**D**) and the densitometric evaluation of the bands (**E**). Presented graphs are the densitometric quantification of four independent experiments; \* p<0.05, \*\* p<0.01.

## 6.4 L101P and to a lesser extent R280C mutation induce apoptosis of A549 cells

Constant accumulation of defect proteins within the ER and activation of the UPR system affect significantly cell homeostasis: As demonstrated, R280C- and L101P-expressing cells revealed elevated BiP levels and XBP1 splicing, particularly in the presence of additional ER stressor, indicating that these mutants perturb homeostasis of A549 cells by raising the level of the intracellular stress and susceptibility to it (Fig.25, 28). Prolonged and unresolved ER stress accompanied by constant UPR activation and its failure can lead to increased degradation of defect proteins, reduced general protein synthesis or initiating of pro-apoptotic pathway (see *“Introduction”*). Since it was shown that SP-C mutations, accumulated in the ER or cytosol, induce ER stress and subsequent apoptotic cell death (94, 106), it was interesting if ABCA3 mutations impair this fatal stress/apoptosis/cell-dysfunction axis as well. Activation of the apoptotic pathway in cells expressing ABCA3 mutants was assessed by early and late apoptotic markers: annexin V/PI staining, GSH decrease and caspase 3 activation.

### 6.4.1. Annexin V/PI staining

In apoptosis, pro-apoptotic activation of caspase 3 can change characteristics of the plasma membrane and leads to externalization of phosphatidylserines (PS) (97). The exact mechanism how caspase 3 interacts with phospholipid translocation is not completely understood to the date. However, the expression of PS on the cell surface of dying cells is a signal for macrophages to capture these cells for phagocytosis (118). Annexin V specifically binds to the surface-exposed PS of apoptotic cells and is used as a marker of early apoptosis. Besides, a marker for late apoptosis and necrosis is propidium iodide (PI) that binds to double-stranded DNA, but only in non-viable cells that have lost membrane integrity. In order to experimentally investigate whether both early apoptosis and necrosis might be induced by ABCA3 mutants, flow cytometry was performed to analyse annexin V staining of cells expressing ABCA3 defect proteins and to analyse PI staining within these cells.

For this purpose, A549 cells were transiently transfected with pEYFP-ABCA3-WT - R43L, -R280C or L101P and 48 hours after transfection, samples were prepared for flow cytometry. Flow cytometry assay of Cy5-coupled Annexin V surface binding showed an increase in the number of annexin V<sup>+</sup>/PI<sup>-</sup> cells in transfected YFP<sup>+</sup> cells in the case of R280C and L101P mutations when compared to WT and R43L indicating early apoptotic state of those cells (Fig. 30A).

#### **6.4.2. GSH decrease**

Glutathione is an essential low-molecular-weight thiol and a major component of the cell antioxidant system. Loss of intracellular GSH is an early hallmark of apoptosis progression and a part of early changes for generation of a permissive environment for the activation of apoptotic enzymes (119). For this purpose, A549 cells were transiently transfected with pEYFP-ABCA3-WT -R43L, -R280C or L101P and 48 hours after transfection, samples were prepared for flow cytometry. YFP fluorescence was utilized to determine the population of transfected cells (YFP<sup>+</sup>) and to measure the apoptotic markers exclusively in those cells. Intracellular GSH level, measured by flow cytometry of monochlorobimane binding to GSH and generation of a fluorescent adduct, was significantly decreased in the YFP<sup>+</sup> cells with L101P protein compared to YFP<sup>+</sup> WT, and to a lower extent compared to R43L and to R280C (Fig.30B).

#### **6.4.3. Caspase 3 activation**

Pro-apoptotic pathway is initiated by active caspases, a family of highly conserved proteases present in the cell as inactive precursors and activated through a cascade of regulated proteolytic cleavages leading to controlled cell death (91, 120). Among 15 known members in mammalian species, caspase 3 is one of the executioner caspases activated at the end of the cascade. Therefore, activation of caspase 3 is a late apoptotic marker. For this purpose, two approaches were applied and active caspase 3 was measured by Western Blotting as well as by flow cytometry.

First, an increase of caspase 3 activation in cells expressing the ER-retained L101P mutant in comparison to WT and R43L was observed via flow cytometry assay of intracellular active caspase 3 (Fig. 30C). R280C values showed steady increase in caspase 3 activation, however with lower significance than L101P (Fig. 30C).

Second, to confirm this observation, active caspase 3 was additionally measured by immunoblotting. A549 cells were transiently transfected with pEYFP-ABCA3-WT, -R43L, -R280C and -L101P and after 48 hours the whole cell lysates were prepared and analyzed by immunoblotting using an antibody, that detects the pro-form of caspase 3 (32 kDa) as well as the active forms of caspase 3 (19 and 17 kDa). Cells, expressing R43L, R280C or L101P mutant proteins, revealed clearly elevated levels of active caspase 3. Especially in L101P expressing cells the amount of active caspase 3 was significant higher than in WT (Fig.29). These results confirm data obtained by FACS.

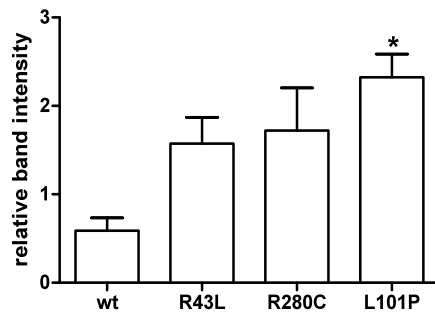
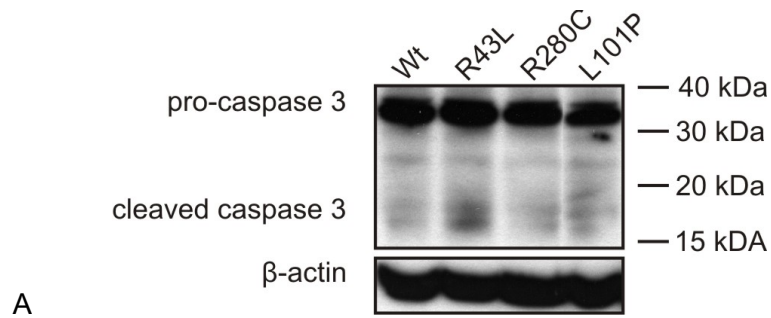
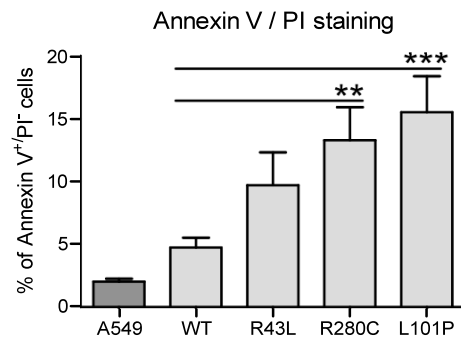
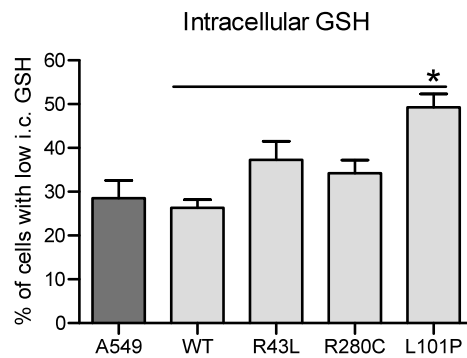


**Fig.29:** Early apoptosis marker caspase 3. *A*, A549 cells with ER retained L101P mutant showed upregulation of the immunodetected active caspase 3 in comparison to WT. *B*, intensity of each protein band was densitometrically quantified and normalized to the corresponding β-actin band. Densitometric quantification of the active caspase 3 protein level of three independent experiments is presented; \*  $p < 0.05$ .

A



B



C

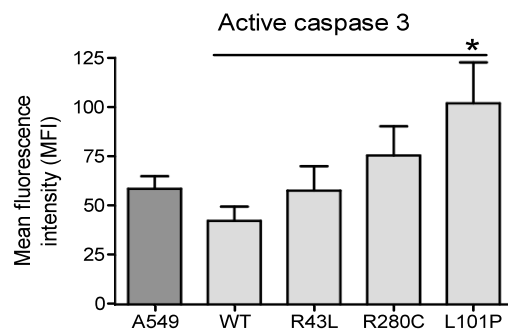


**Fig.30** Apoptosis in A549 cells expressing L101P and R280 mutations. A549 cells were transfected with pEYFP-N1/ABCA3 plasmids and apoptotic markers were analysed by FACS in transfected (YFP<sup>+</sup>) population of cells and A549 cells by assaying (A) annexin V<sup>+</sup>/propidium iodide (PI) staining and (B) intracellular (i.c.) glutathione (GSH) level with coupling of monochlorobimane with GSH, to determine early apoptosis, and (C) intracellular active caspase 3 level (MFI), to detect late apoptosis. Elevated early and late apoptotic markers were detectable in cells expressing L101P mutation, and one early marker (Annexin V) in cells expressing R280C mutation. Results were calculated from six independent experiments; \* p<0.05, \*\* p<0.01, \*\*\* p<0.001.

In summary, while R43L mutation did not raise apoptotic signaling above the A549 or WT level, R280C mutation increased one early apoptotic marker and ER-localized L101P mutations significantly elevated early and late apoptotic markers, indicating injury of the cells with L101P protein.

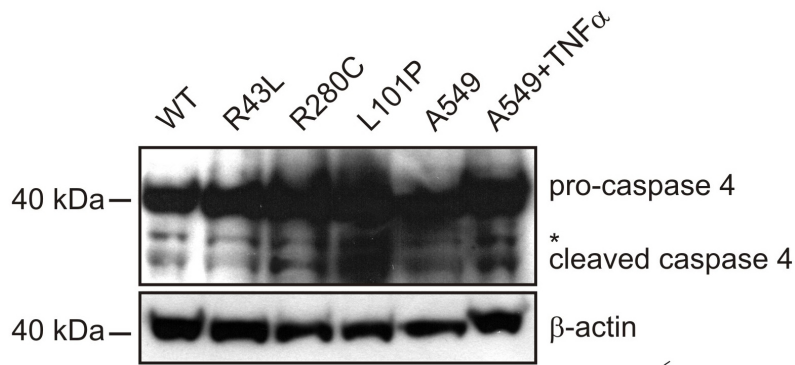
#### **6.4. Prolonged ER stress leads to apoptosis through caspase 4 activation in cells expressing R280C and L101P mutations**

To examine if initiation of apoptosis in cells with *ABCA3* mutations is indeed a consequence of the ER stress signaling, cleavage of caspase 4, which is activated by ER stress specific stimuli in a mitochondria and cell death receptor-independent way (93, 94), was assessed. Cleavage of caspase 4 leads to proteolytic activation of executioner caspase 3 and to cell elimination (95). Therefore, activation of caspase 4 identifies ER stress as an apoptosis trigger.

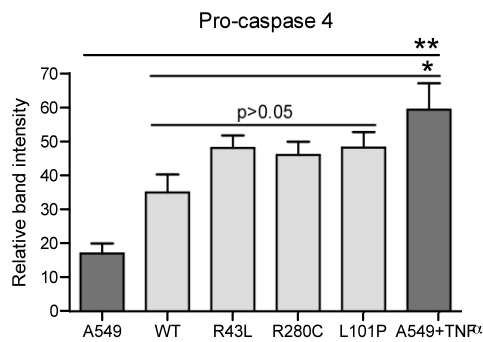
In attempt to elucidate if these *ABCA3* mutants induce pro-apoptotic pathway in an ER stress depending manner, caspase 4 was analyzed in whole cell lysates of A549 cells transiently transfected with pEYFP-*ABCA3*-WT, -R43L, -R280C and -L101P by immunoblotting. The anti-caspase 4 antibody detected the pro-form at 42 kDa and two cleaved forms.

Treatment of A549 cells with apoptosis inducing cytokine  $\text{TNF}\alpha$  resulted in the cleavage of caspase 4 (Fig.31, A-C). Immunoblotting of whole cell lysates from the cells expressing WT or R43L, R280C or L101P mutations showed insignificant changes in pro-caspase 4 level between WT and mutations, but the level of pro-caspase 4 was somewhat higher in transfected cells than in A549 cells (Fig.31B). In contrast, cleaved caspase 4 in R280C and L101P mutants increased significantly in comparison to WT. Changes measured between R43L and WT were not significant (Fig.31C). This shows that caspase 4 is involved in apoptotic signaling in cells with L101P and R280C mutations and that activation of the apoptotic pathway can be a consequence of the ER stress caused by complete or partial ER retention of the *ABCA3* protein.

A



B



C

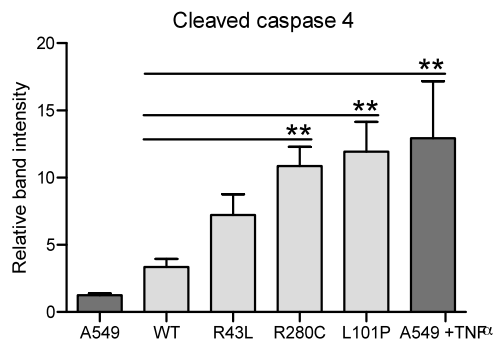


**Fig.31:** Apoptotic signaling in cells with L101P and R280C mutations is activated by ER stress. A, immunoblotting on whole cell lysates from A549 cells transfected with pEYFP-N1/ABCA3 and densitometric analyses of (B) pro-caspase 4 and (C) cleaved caspase 4 demonstrated increased caspase 4 cleavage in cells expressing L101P and R280C mutations, as well as after TNF $\alpha$  treatment of A549 (25 ng/ml, 16 h) in comparison to WT and untreated A549. No significant changes in the pro-caspase 4 level in transfected cells with WT, R43L, R280C and L101P mutations were detected but pro-caspase 4 was slightly increased in transfected cell compared to A549 (B). \* - unknown unspecific band. Intensity of each protein band was densitometrically quantified and normalized to the corresponding  $\beta$ -actin band. Six independent experiments were used for densitometric evaluation; \*  $p < 0.05$ , \*\*  $p < 0.01$ .

## 6.5 Epithelial-mesenchymal transition in A549 cells expressing ABCA3 defect proteins

Increasing evidence indicates a connection of fibrogenesis and epithelial apoptosis in the pathogenesis of interstitial lung disease (103, 107, 108). When lung tissue is injured, the consequent lung repair requires an additional source of myofibroblasts and fibroblasts (110, 121, see "Introduction"). However, it was discovered that epithelial alveolar type II cells can undergo epithelial-mesenchymal transition (EMT), thereby changing their morphology and

cell characteristics towards myofibroblast like cells and contributing to fibrogenesis via TGF- $\beta$  and cytokine secretion (109, 114).

To the date, it was not yet investigated if alveolar type II cells with defect ABCA3 protein contribute significantly to fibrogenesis in the lungs. Therefore, it was interesting, to test if AT II cells expressing R43L, R280C and L101P mutants that were identified to cause unresolved ER stress (Fig.25, 28) and to induce apoptosis (Fig.29-31) undergo EMT in AT II cells.

### **6.5.1 Induction of epithelial-mesenchymal transition in A549 cell line**

It is well known that some key factors like Tissue Growth factor  $\beta$ 1 (TGF- $\beta$ 1) are responsible for transition of epithelial cells to myofibroblasts and fibroblasts and effect cell characteristics and morphology *in vitro* (109, 114). In order to characterize and confirm the transition to mesenchymal phenotype in AT II cells, the effect of TGF- $\beta$ 1 on A549 cell line was analyzed by two approaches: first, analysis of the mesenchymal marker vimentin and second, analysis of the epithelial marker E-cadherin.

First, A549 cells were incubated with different concentrations of TGF- $\beta$ 1 to determine optimal concentrations of TGF- $\beta$ 1 to induce EMT in this cell line. For vimentin analysis, A549 cells were cultured in RPMI+ 10 %FBS for 24 hours as usual. Treatment with various concentrations of TGF- $\beta$ 1 (0.05 ng/ml –5.0 ng/ml) was performed in serum free RPMI for additional 24 hours. In whole cell lysates, expression of vimentin was examined by immunoblotting. As a result, in not treated as well as in treated A549 cells, vimentin was detected. Through TGF- $\beta$ 1 concentrations of 0.05 ng/ml, 0.5 ng/ml and 5.0 ng/ml, there was an steady increase in vimentin expression in comparison to not treated A549 cells (Fig.32), whereas vimentin levels were at their highest at 5.0 ng/ml of TGF- $\beta$ .

Second, ECAD only appeared in A549 cells that were cultured under standard conditions (Fig.33). In cell lysates of A549 cells treated with 0.05 and 0.5 ng/ml of TGF- $\beta$ 1 and cultured in serum free media, ECAD disappeared (Fig.32). These results demonstrate that EMT can take place in alveolar type II cells and suggest that TGF- $\beta$  activated alveolar type II cells may contribute to pulmonary fibrogenesis.

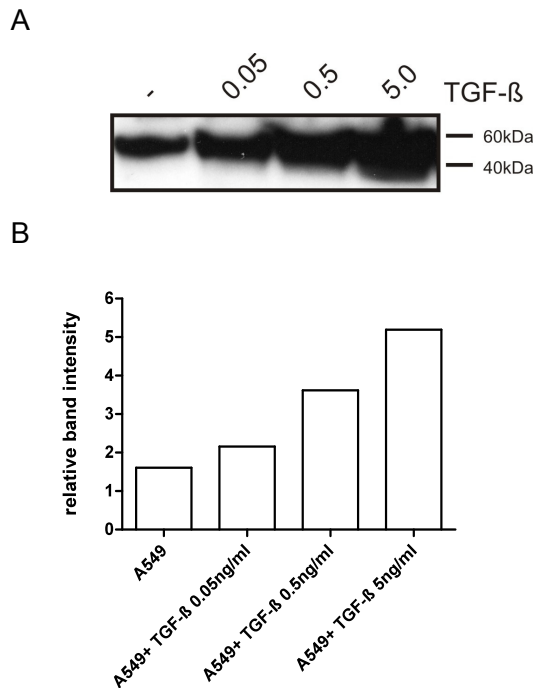


**Fig.32:** Induction of EMT in A549 cell line through different concentrations of TGF-β1. *A*, A549 cells showed upregulation of the immunodetected marker of myofibroblasts vimentin through increasing TGF-β1 concentrations. *B*, densitometric quantification of the vimentin protein level is presented.

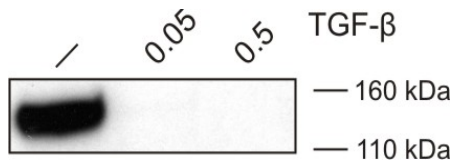


**Fig.33:** ECAD in A549 cell line in absence and presence of TGF β1. A549 cells showed lost of immunodetected ECAD under TGF β1-treatment.

### 6.5.2 Induction of epithelial-mesenchymal transition in A549 expressing ABCA3 defect protein

Given that fibrosis is a common manifestation in genetic ILDs and that alveolar type II cells contribute significantly to fibrogenesis, it was interesting to investigate if R43L, R280C and L101P ABCA3 mutations make alveolar type II cells more prone for transdifferentiation into myofibroblast like cells, thereby contributing to fibrogenesis in the lung. For this reason, vimentin and ECAD were analyzed in the whole cell lysates of A549 cells, transiently transfected with pEYFP-ABCA3-WT, -R43L, -R280C or -L101P by immunoblotting.

As a result, in cells expressing ABCA3 WT, R43L, R280C or L101P mutants, the epithelial marker ECAD was present (Fig.34). Furthermore, as shown for untransfected A549 cells (Fig.32), vimentin appeared in ABCA3 WT expressing cells as well as in mutants.

However, vimentin revealed no difference in cells with ABCA3 WT or with the three mutations (Fig.34). This result can be explained by the low transfection efficiency and less time for transfected cells to undergo EMT. However, these data are indicators that in stable transfected cells, alveolar type II cells might undergo EMT in response to disturbed cell homoeostasis perturbed by ABCA3 defect protein.

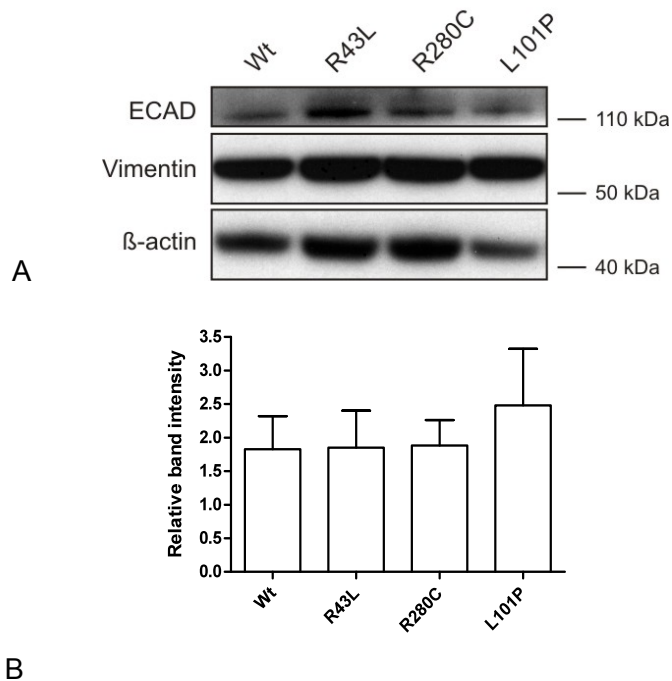
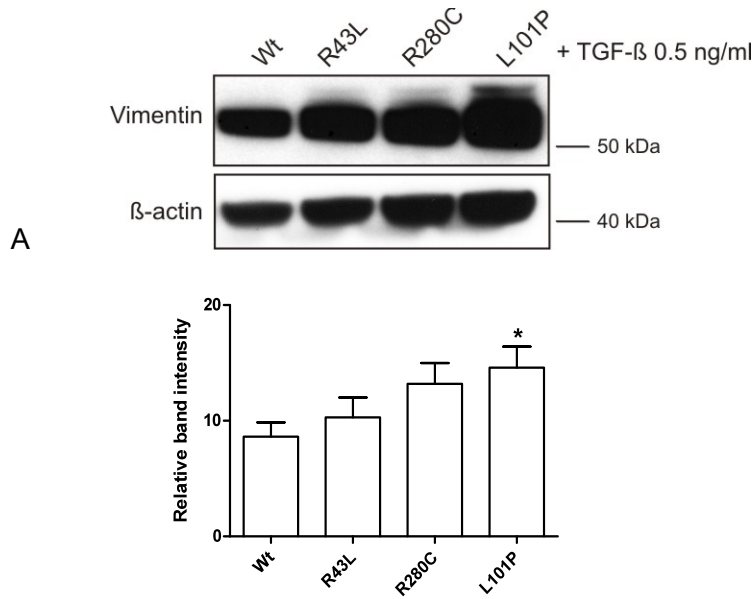


**Fig.34:** ECAD and vimentin in A549 cells expressing ABCA3 WT or mutant proteins. *A*, A549 cells showed no differences in immunodetected vimentin and ECAD in WT or the three mutations. *B*, intensity of each protein band was densitometrically quantified and normalized to the corresponding β-actin band. Densitometric quantification of the vimentin protein level of three independent experiments is presented.

Considering the fact that alveolar epithelial cells release various profibrotic cytokines and growth factors (see “Introduction”) thereby contributing to the induction of EMT in epithelial lung cells and fibrogenesis, it was experimentally tested if ABCA3 mutants induce EMT in AT II cells under additional stimulation with TGF-β1.

Therefore, A549 cells were transiently transfected with pEYFP-ABCA3- WT, -R43L, -R280C or -L101P and 24 hours after transfection, these cells were additionally incubated with 0.5 ng/ml of TGF-β1 for further 24 hours. The whole cell lysates were prepared and analysed via immunoblotting using an anti-vimentin antibody. As a result, vimentin was slightly increased in cells with R43L and R280C mutations and being at its highest in L101P mutation (Fig.35).



B

**Fig.35:** Marker of myofibroblasts vimentin in A549 cells expressing ABCA3 WT or mutant proteins under additional stimulation with 0.5 ng/ml of TGF- $\beta$ 1. A, A549 cells with ER retained L101P mutant showed upregulation of the immunodetected marker of myofibroblasts vimentin in comparison to WT. B, intensity of each protein band was densitometrically quantified and normalized to the corresponding  $\beta$ -actin band. Densitometric quantification of the vimentin protein level of three independent experiments is presented; \*  $p < 0.05$ .

In conclusion, under additional stimulation with TGF- $\beta$ 1, imitating autocrine or paracrine cellular stimulation in the lungs, vimentin was upregulated in alveolar type II cells with ABCA3 defect proteins, especially in A549 cells with ER-retained L101P defect protein. These results suggest that these mutations push cells toward transdifferentiation into myofibroblasts contributing to fibrogenesis in the lungs and pathogenesis of ILD.

## 7. Discussion

*ABCA3* mutations cause surfactant deficiency and fatal respiratory distress syndrome in full-term neonates and chronic ILD of children (21, 22, 63-73). The cellular pathomechanisms of *ABCA3*-related chronic ILD are probably complex including influence of *ABCA3* mutations on surfactant homeostasis but possibly also on the fitness and function of alveolar type II cells as cells for surfactant production, lung repair and immunological defense (122).

In this study the influence of three *ABCA3* mutations, R43L, R280C and L101P, on intracellular stress and induction of apoptosis in cultured lung epithelial A549 cells was investigated. All three mutations were found in children with *ABCA3*-associated lung disease being either fatal neonatal respiratory distress syndrome (L101P (22) and R43L (28, 48)) or chronic ILD (R280C (48, own unpublished data) (Table 2). While cell biology of R43L and R280C mutations was studied here for the first time, L101P mutation was used as a known example of the trafficking/folding defect leading to the ER retention of *ABCA3* with no information on ER stress (57, 61).

### 7.1 General characterization of the three *ABCA3* mutations R43L, R280C and L101P

The general characterization of R43L, R280C and L101P *ABCA3* mutant proteins included the analysis of the intracellular localization, of protein processing and glycosylation and an uptake assay of NBD-labeled phospholipids PC and PE. To the date, *ABCA3* mutations are either known for a functional defect and for impaired protein trafficking (61).

Improper protein folding, failed trafficking and mislocalization are well recognized in other diseases associated with mutations in ABC transporters. For example in Tangier Disease, a genetic HDL- deficiency, caused by defect *ABCA1* transporter, the *ABCA1* mutations R587W and Q597R are mainly retained in the ER instead of being transported to the plasma membrane accompanied by impaired processing of oligosaccharides (123). Moreover, in Cystic Fibrosis caused by mutations in the *ABCC7* gene encoding an ABC transporter, named cystic fibrosis transmembrane conductance regulator (CFTR) (124), the most common mutant  $\Delta F508$  is retained and destroyed in the ER by the ER quality control system and failed trafficking to plasma membrane (125).

Initial characterization in A549 cells demonstrated that each of the mutations analyzed in this study affect the *ABCA3* transporter in a different way. It was shown the correct localization of WT and R43L proteins in LAMP3<sup>+</sup> vesicles and dual localization of

R280C protein in LAMP3<sup>+</sup> vesicles and calnexin<sup>+</sup> ER compartment (Fig.18-20), indicating less efficient but not abolished R280C trafficking. Similar dual localization is known in the case of other ABCA3 mutants as G122S (57). However, L101P mutant protein appeared as a net-like structure without any vesicle structures and LAMP3 colocalization but complete storage in the ER (Fig.18), as previously described (61).

Previous studies have analyzed ABCA3 localization to LBs by using LAMP3 staining as well (59). In attempt to confirm additionally the localization of ABCA3 WT protein to LBs and to show normal alveolar type II physiology in A549 cells used in this study, the colocalization of ABCA3 WT protein and SP-C WT protein, that is stored within LBs, was demonstrated in A549 cells expressing both proteins simultaneously (Fig.21).

ABCA3 protein expression was analyzed in alveolar type II cells by immunoblotting of whole cell lysates and of the crude membrane fractions. Previously, ABCA3 protein expression was described in human and mice tissues as well as in different cell lines. The appearance of ABCA3 as one or two protein bands by immunoblotting depended on the species and antibody, which were used (28, 58, 59). But recently, the lower protein band was recognized as the mature one (34). In this study, when a yellow fluorescent protein (YFP) of 30 kDa was fused to ABCA3 protein, both protein bands, cleaved and noncleaved forms, were present in cell cultures when ABCA3 WT was overexpressed (Fig.22). Similar processing was observed for R43L and R280C proteins (Fig.22). Considering the fact of correct LB localization of R43L mutant protein assessed by immunofluorescence studies, it was not surprising to find WT-processing and presence of complex oligosaccharides (Fig.22). In the case of YFP-R280C mutant protein, when dual localization to LAMP3<sup>+</sup> vesicles and ER compartment was found, it was interesting to detect similar protein processing and presence of complex oligosaccharides in this mutation as before in WT and R43L mutation (Fig.22), confirming their ability to proceed from the ER to the Golgi.

In contrast, L101P protein remained in the ER, having therefore no complex sugars, and no smaller 180 kDa protein form (Fig.22), as previously published (57, 61). This data demonstrate a strong processing and glycosylation defect in L101P mutant protein.

In summary, these results suggesting the presence of oligosaccharides in ABCA3 WT and R43L are consistent with proper immunofluorescence localization studies. However, in terms of R280C mutation, the similarity of ABCA3 processing and protein glycosylation to WT and R43L mutation makes a functional defect most likely, being in line with immunofluorescence studies when R280C was mainly localized to LBs. In case of L101P mutant, absent oligosaccharides are consistent with failed trafficking and the ER-localization demonstrated in this immunofluorescence studies as well as with strong processing deficiency confirmed through absent cleaved form in Western Blotting. It can be speculated that L101P mutant increases ER stress due to its processing defect and ER-storage.

Following this prediction ER stress was assessed in all mutants.

While ER retention of L101P excludes ABCA3 function, the function of R43L and R280C transporters was studied additionally. As ABCA3 is involved in lamellar body biogenesis in lung cells (22, 55, 60), which normally have a low number of compact LAMP3<sup>+</sup> vesicles, expression of ABCA3-WT induced biogenesis of LAMP3<sup>+</sup> vesicles by increasing their number and size in A549 cells (59, Fig.24). In addition, ABCA3-WT signal was observed as ring-like structures consistent with the ABCA3 presence in the limiting membrane of lamellar bodies (41, Fig.18, 24). In contrast to the WT, expression of ABCA3 mutations, especially L101P, impaired biogenesis of LAMP3<sup>+</sup> vesicles by reducing their number and size (Fig.24). This can be a consequence of the inability of these mutated transporters to effectively load lipids into the nascent lamellar bodies.

The uptake assay of NBD-labeled phospholipids PC and PE into ABCA3-HA-positive vesicles demonstrated frequent overlap of the NBD signal, both PC and PE coupled, with the ring-like ABCA3-WT fluorescence and its accumulation in the inner space of the WT-ABCA3 vesicles (Fig.23). In the case of R43L and R280C mutations such colocalization was rarely observed suggesting functional impairment of R43L and R280C proteins. Similar uptake experiments have been previously described (57). In contrast to those data, which showed diffuse distribution of NBD-PC and NBD-PE fluorescence throughout the cytoplasm, numerous distinct NBD-positive vesicles were detected (Fig.23, A and B). The uptake and number of NBD-vesicles observed in the cytoplasm was similar for both phospholipids in A549 cells and in transfected A549, and was also independent of the ABCA3 mutation, including L101P. This confirms that for the liposome/lipid uptake through the plasma membrane into the cytoplasm ABCA3 function is dispensable and ABCA3 is solely an intracellular vesicular transporter. Furthermore, we observed an impact of ABCA3 mutations on the uptake of both PC and PE. This parallels data published in Cheong *et al.* (2007) (55) which demonstrated decreased incorporation of radiolabeled PC and PE into the lamellar bodies and surfactant of the ABCA3 heterozygote mouse, consistent with a role of ABCA3 in the transport of both phospholipid species. However, this is also in contrast to Cheong *et al.* (2006) (57) showing no uptake of NBD-PE into the lysosome-like vesicles in A549 cells. Therefore, it is questionable if the PE transport through functional ABCA3 actually happens *in vivo* or only in *in vitro* system after exposing cultured A549 cells to 150  $\mu$ M of NBD lipid.

## 7.2 Induction of ER stress and UPR system by ABCA3 mutants

Continuous overload of the ER compartment with misfolded proteins is harmful for the cell and leads to activation of the UPR system (126). Misfolding and ER retention of other lipid ABC transporters is well known (123, 125). The most common mutation  $\Delta$ F508 of the ABCC7-transporter, leading to cystic fibrosis, is not only misfolded and therefore retained in the ER, it also raises ER stress and activates UPR (127). Also in SP-C deficiency, the mutations  $\Delta$ exon4 and L188Q, which are retained in the ER or form aggregates in the cytoplasm, induce UPR activation (94). But also in other organs than the lung, accumulation of mutant protein in the ER cause toxic effects and cellular injury via ER stress, particularly via BiP upregulation, as in liver and lung disease caused by  $\alpha$ 1-AT deficiency (128) and neuronal degenerating diseases (129).

According to recent *in vitro* studies on cells expressing mutant ABCA3 proteins it could have been speculated that dysfunction of the ATP-dependent lipid transporter resulting in modified composite of surfactant components may give evidence for the mechanism how mutant ABCA3 proteins disturb cell homeostasis and causes RDS or pILD (56, 59, 60). In contrast, this study on human lung epithelial cell line A549 overexpressing mutant ABCA3 protein showed previously not examined cellular dysfunction, including raised level of intracellular stress, susceptibility to it and induction of pro-apoptotic pathway:

Since L101P protein accumulates in the ER, it was not surprising to find significant increase of the ER stress (Fig.25-28). Upregulation of chaperones is in line with ER localization and defect protein glycosylation, indicating a strong misfolding defect and a strong effect on induction of ER stress. Especially, splicing of XBP1 mRNA goes along with subsequent upregulation of BiP caused by the misfolding defect of L101P mutant protein. The ER stress caused by R280C mutation was lower. This might be a consequence of a dual nature of this protein, which could be less harmful for the cell than complete ER retention, and/or possible dependency of the magnitude of its intracellular effects on small unmanageable inconsistencies of an experimental system. Correctly localized R43L mutation, despite its influence on the ABCA3 function and lamellar body biogenesis, had almost no impact on ER stress under any conditions above the range of the WT values (Fig.25-28), being in line with proper localization and processing studies and indicating less cellular disturbance. However, the low increase of ER stress in cells with R43L or R280C defect proteins might be due to low transfection efficiency of 20 % and to the robustness of the method.

Since in nature, lungs are not exclusively affected by mutant ABCA3 protein but also by environmental conditions such as dust, smoking, infection and hypoxemia that cause

additional intracellular stress, ER stress and UPR activation, examined via XBP1 splicing, were enhanced by exposure of transfected cells to tunicamycin, an ER stressor (Fig. 28, D and E). In this way the stress pressure imposed on the cells was doubled: 1) genetic background of the *ABCA3* mutations and 2) exposure to the stress-causing agent. The cells with mutations R280C and L101P, which impair *ABCA3* trafficking, were more prone to further XBP1 splicing than the WT or A549 (Fig.28D). This is interesting if known that viral infections (e.g. RSV, herpes virus) or cigarette smoke are common outside factors, which, as tunicamycin, elevate ER stress (130, 131). Also clinical experts report from the onset of *ABCA3*-associated ILD in children following exposure to cigarette smoke (68) and describe a teenage patient with a late onset of *ABCA3*-related disease with fibrosis following the beginning of cigarette consumption (71). If *ABCA3* mutations raise susceptibility of alveolar type II cells to external stress, additional exposure to outside stressors as respiratory viral infections or smoke might contribute to or even trigger genetic ILD.

### **7.3 Induction of apoptotic cell death by *ABCA3* mutations**

Constant accumulation of defect proteins within the ER lumen and activation of the UPR system disturb cell homeostasis, cause cell toxicity and disruption of cell function. Furthermore, prolonged and unresolved ER can trigger apoptotic cell death (see “Introduction”). Recently, upon accumulation of mutant SP-C protein in the ER and also in model systems for other conformational diseases like Parkinson’s disease, the mechanism of ER stress and subsequent apoptotic cell death was found *in vitro* (106, 132). However, in patients with IPP/IFP alveolar epithelial cells were identified to undergo apoptosis, whereas apoptosis was absent in control lungs (133, 134).

In this study, the connection between the overexpression of *ABCA3* mutations and induction of apoptotic cell death was analysed by three lines of evidence: activation of caspase 3, either via immunoblot or via FACS, PI and annexin V staining. Since L101P protein accumulation in the ER increased stress response elements, early and late apoptosis markers were also recognized in the cells with this mutation (Fig.29, 30). The ER stress caused by R280C mutation was lower and therefore surface staining with annexin V, as an early apoptosis sign, was the only apoptotic marker detected in R280C cells. Correctly localized R43L mutation, despite its influence on the *ABCA3* function and lamellar body biogenesis, had almost no impact on stress and apoptosis under any conditions above the range of the WT values (Fig.29, 30).

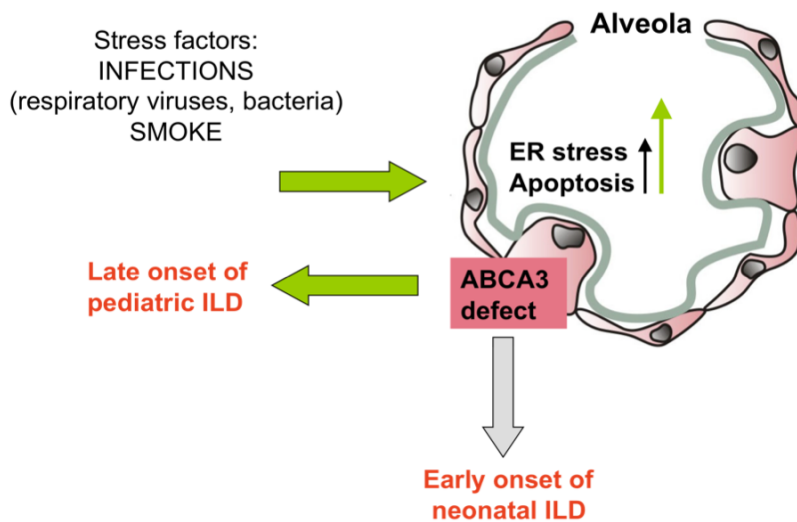


**Fig.36:** Hypothesis of early and late onset of lung disease caused by *ABCA3* mutations. Impaired *ABCA3* transporter function is accompanied by disturbed surfactant composition and acute respiratory distress syndrome in newborns. Late onset of pediatric ILD might be caused by increased intracellular stress and apoptosis, exacerbated by outer stressors as infection or cigarette smoke. The author of this model is Dr. Suncana Kern, she provided it to our research group and I use it with her permission.

Prolonged accumulation of misfolded proteins and unresolved ER stress are connected with the activation of apoptotic pathway in a caspase 4-dependent way (see “Introduction”, (94)). The link between ER stress and induction of apoptosis in cells, overexpressing *ABCA3* mutations, was established through the upregulation of caspase 4 in the case of both L101P and R280C mutations (Fig. 31). As expression of R43L mutant protein shows no impact on ER stress, correctly localized R43L mutation, was not associated with caspase 4 cleavage above the range of the WT values (Fig.31).

Given to the low transfection efficiency of 20%, the relative induction of apoptosis in A549 cells, overexpressing mutant R280C and L101P *ABCA3* protein, is highly significant in mutants compared to WT. Overexpression of R280C and L101P *ABCA3* proteins perturb homeostasis of A11 by raising the level of the intracellular stress and susceptibility to it and can push them toward apoptotic pathway. This might impair normal function of A11 in lung repair, immunological defense and surfactant production and the resulting cell injury may contribute to pathogenesis of pILD (Fig.36).

#### 7.4 EMT in alveolar type II cells overexpressing *ABCA3* mutations

In lungs of patients with *ABCA3* deficiency related disease, pathologists found features of fibrosis (21, 68, 71). Lung disease with fibrotic foci is believed to be a consequence of chronic alveolar epithelial injury and abnormal alveolar repair (107, 110). Fibroblastic foci are characterized by mesenchymal cells as fibroblast and myofibroblasts as

well as by abnormal extracellular proteins (see “*Introduction*”). However, pathogenesis of pulmonary fibrosis is still poorly understood, but alveolar type II cells seem to have a key role in this process (135). Recent studies not only on fibrotic lung disorders, but also on renal and liver diseases, showed that epithelial cells can undergo EMT and that TGF- $\beta$  plays a key role in transition of epithelial cells into mesenchymal cells (114, 136, 137). Epithelial lung cells that have undergone EMT may contribute to the development of fibroblastic foci in various ways: as a new source of fibroblasts or by the activation and migration of fibroblasts and by the release of cytokines and growth factors. However, the precise mechanism of the formation of fibroblastic foci and the origin of mesenchymal cells are both incompletely understood.

In this study, it was demonstrated for the first time that A549 cells overexpressing ABCA3 mutant proteins, especially L101P cells, gain a mesenchymal phenotype with increased expression of vimentin, particularly in presence of TGF- $\beta$ 1 (Fig.34, 35). It can be speculated that the examined ABCA3 mutations make AT II cells more prone to undergo EMT. Furthermore, induction of ER stress and apoptosis in these ABCA3 mutations, particularly the ER-retained L101P mutation, is associated with induction of EMT in AT II. Role of ER stress and apoptosis in lung disease has also been studied by other groups, showing that ER stress- and apoptosis- markers occur at sites of fibrosis in alveolar type II cells (103, 104, 133, 134). These results suggest that ER stress may contribute to lung fibrosis through induction of EMT in ABCA3 related lung disease. Further experiments are necessary to support these notions. This mechanism is also believed to underlie in SP-C-related lung disease (138). SP-C and ABCA3 are both ATII-expressed proteins essential for surfactant homeostasis and both lead to genetic ILD equally variable in the age of onset, severity and pathology. Therefore, it is interesting to see that common mechanisms underlying both types of genetic ILD must exist and this data show that they probably encompass the ER stress and apoptosis of AT II cells mediating EMT. Therefore, AT II cells with ABCA3 deficiency may have a critical role for development of fibrosis in pILD (Fig.37).

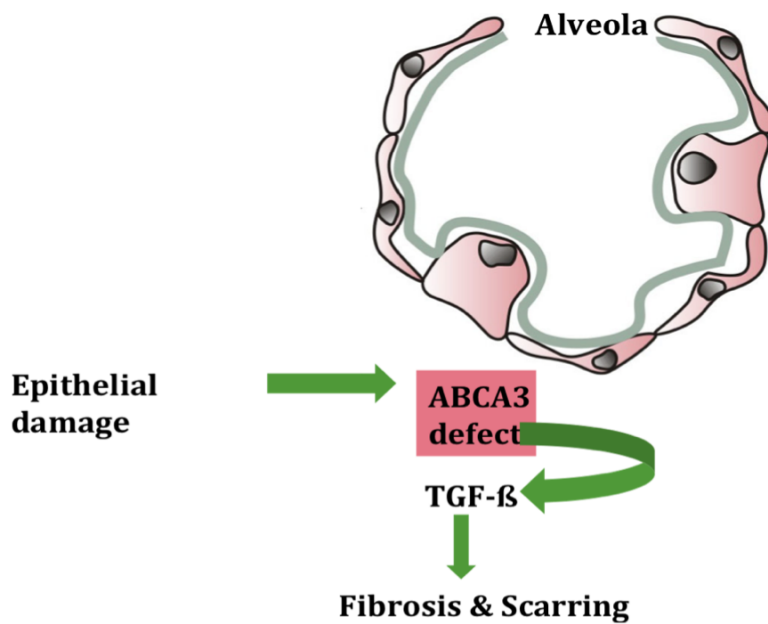


**Fig 37:** EMT in ATII might be a possible mechanism of lung fibrogenesis in children with *ABCA3* mutation. *ABCA3* mutations disturb cell homeostasis and induce ER stress and apoptosis. The resulting cell injury might be a stimulus for endocrine or autocrine TGF- $\beta$  secretion. TGF- $\beta$  stimulates fibroblasts migration and EMT in ATII, thereby promoting pulmonary fibrogenesis. Own illustration according to a model of Dr. Suncana Kern.

## 7.5 Conclusion

Apparently, the effect of *ABCA3* mutations on homeostasis of lung epithelial cells depends on the type of *ABCA3* protein defect. With this study it was shown for the first time, that the clinical relevant *ABCA3* mutations with partial or complete *ABCA3* trafficking defect raise intracellular stress and susceptibility to it, and induce apoptotic cell death signaling. Induction of ER stress and apoptosis as a result of overexpression of some *ABCA3* mutations is accompanied with findings consistent with EMT. Similar as proposed for SP-C deficiency, intracellular stress and apoptosis of alveolar type II cells might play a role in pathogenesis of *ABCA3*-related lung disease.

## 7.6 Future directions

This study demonstrated mechanisms, which may contribute to the pathogenesis of ABCA3 related lung disease thereby raising new questions that should be addressed in future work.

First, studies on induction of ER stress and apoptosis in ATII cells expressing ABCA3 mutations should be supplemented by further experiments. Studies on the most common E292V mutation, a type II mutation located to LBs with reduced functional activity, would also be helpful to confirm findings of ER retained mutation in this study.

Second, more work is necessary to verify if ER stress and apoptosis of AT II cells are indeed present in (fibrotic) lung tissue of patients with ABCA3 mutations. Studies on lung tissue from children with ABCA3 mutations could also provide more information on ATII cells and their role in pathogenesis of pILD, e.g. in terms of morphology, surfactant homeostasis and cytokine and growth factor release.

Third, exposure to outside stressor should become a subject of future experiments. RSV-infection could be a helpful instrument. Further investigations on the precise pathway of how ABCA3 mutant proteins can lead to fibrogenesis and studies on the role of TGF- $\beta$  are needed.

This might help to understand or even predict the disease course, or consider new therapy options (as protein rescue with chaperones) depending on the type of the ABCA3 protein defect. Since to date no causative therapy is available for the treatment of pILD, the role of chemical chaperones should be tested *in vitro* for ER-retained ABCA3 mutations.

## 8. References

1. Fan LL, Deterding RR, Langston C. Pediatric interstitial lung disease revisited. *Pediatric pulmonology*. 2004Nov;38(5):369-78.
2. Griese M, Haug M, Brasch F, et al. Incidence and classification of pediatric diffuse parenchymal lung diseases in Germany. *Orphanet Journal of Rare Diseases*. 2009;426.
3. Fan LL, Mullen AL, Brugman SM, Inscore SC, Parks DP, White CW. Clinical spectrum of chronic interstitial lung disease in children. *The Journal of pediatrics*. 1992Dec;121(6):867-72.
4. Dinwiddie R, Sharief N, Crawford O. Idiopathic interstitial pneumonitis in children: a national survey in the United Kingdom and Ireland. *Pediatric pulmonology*. 2002Jul;34(1):23-9.
5. Coultas DB, Zumwalt RE, Black WC, Sobonya RE. The epidemiology of interstitial lung diseases. *American journal of respiratory and critical care medicine*. 1994Oct;150(4):967-72.
6. Xaubet A, Ancochea J, Morell F, et al. Report on the incidence of interstitial lung diseases in Spain. Sarcoidosis vasculitis and diffuse lung diseases official journal of WASOG World Association of Sarcoidosis and Other Granulomatous Disorders. 2004;21(1):64-70.
7. López-Campos JL, Rodríguez-Becerra E. Incidence of interstitial lung diseases in the south of Spain 1998-2000: the RENIA study. *European journal of epidemiology*. 2004Jan;19(2):155-61.
8. Clement A. Task force on chronic interstitial lung disease in immunocompetent children. *The European respiratory journal : official journal of the European Society for Clinical Respiratory Physiology*. 2004Oct;24(4):686-97.
9. McFetridge L, McMorrow A, Morrison PJ, Shields MD. Surfactant Metabolism Dysfunction and Childhood Interstitial Lung Disease (chILD). *The Ulster medical journal*. 2009Jan;78(1):7-9.
10. Deutsch GH, Young LR, Deterding RR, et al. Diffuse Lung Disease in Young Children: Application of a Novel Classification Scheme. *American Journal of Respiratory and Critical Care Medicine*. 2007;176(11):1120-8.
11. Johansson J, Curstedt T, Robertson B. The proteins of the surfactant system. *The European respiratory journal official journal of the European Society for Clinical Respiratory Physiology*. 1994;7(2):372-391.
12. Mason RJ, Voelker DR. Regulatory mechanisms of surfactant secretion. *Biochimica et Biophysica Acta*. 1998;1408(2-3):226-240.
13. Rooney SA. Regulation of surfactant secretion. *Comparative biochemistry and physiology Part A Molecular integrative physiology*. 2001;129(1):233-243.
14. Andreeva AV, Kutuzov MA, Voyno-Yasenetskaya TA. Regulation of surfactant secretion in alveolar type II cells. *American journal of physiology Lung cellular and molecular physiology*. 2007;293(2):L259-L271.
15. Schmitz G, Müller G. Structure and function of lamellar bodies, lipid-protein complexes involved in storage and secretion of cellular lipids. *Journal Of Lipid Research*. 1991;32(10):1539-1570.
16. Thouvenin G, Abou Taam R, Flamein F, et al. Characteristics of disorders associated with genetic mutations of surfactant protein C. *Archives of Disease in Childhood*. 2010;95(6):449-454.
17. Guillot L, Epaud R, Thouvenin G, et al. New surfactant protein C gene mutations associated with diffuse lung disease. *Journal of Medical Genetics*. 2009;46(7):490-494.
18. Cameron HS, Somaschini M, Carrera P, et al. A common mutation in the surfactant protein C gene associated with lung disease. *The Journal of pediatrics*. 2005;146(3):370-375.
19. Nogee LM, Dunbar AE, Wert S, Askin F, Hamvas A, Whitsett JA. Mutations in the surfactant protein C gene associated with interstitial lung disease. *Chest*. 2002;121(3 Suppl):20S-21S.
20. Nogee LM, Wert SE, Proffitt SA, Hull WM, Whitsett JA. Allelic heterogeneity in hereditary surfactant protein B (SP-B) deficiency. *American Journal of Respiratory and Critical Care Medicine*. 2000;161(3 Pt 1):973-981.
21. Bullard JE, Wert SE, Whitsett JA, Dean M, Nogee LM. ABCA3 mutations associated with pediatric interstitial lung disease. *American Journal of Respiratory and Critical Care Medicine*. 2005;172(8):1026-1031.
22. Shulenin S, Nogee LM, Annilo T, Wert SE, Whitsett JA, Dean M. ABCA3 gene mutations in newborns with fatal surfactant deficiency. *The New England Journal of Medicine*. 2004;350(13):1296-1303.
23. Nogee LM, Garnier G, Dietz HC, et al. A mutation in the surfactant protein B gene responsible for fatal neonatal respiratory disease in multiple kindreds. *Journal of Clinical Investigation*. 1994;93(4):1860-1863.
24. Schuerman FABA, Griese M, Gille JP, Brasch F, Noorduynd LA, Van Kaam AH. Surfactant protein B deficiency caused by a novel mutation involving multiple exons of the SP-B gene. *European Journal Of Medical Research*. 2008;13(6):281-286.
25. Somaschini M, Wert S, Mangili G, Colombo A, Nogee L. Hereditary surfactant protein B deficiency resulting from a novel mutation. *Intensive Care Medicine*. 2000;26(1):97-100.

26. Tredano M, Griese M, De Blic J, et al. Analysis of 40 sporadic or familial neonatal and pediatric cases with severe unexplained respiratory distress: relationship to SFTPB. *American journal of medical genetics Part A*. 2003;119A(3):324-339.
27. Garmany TH, Moxley MA, White FV, et al. Surfactant composition and function in patients with ABCA3 mutations. *Pediatric Research*. 2006;59(6):801-805.
28. Brasch F, Schimanski S, Mühlfeld C, et al. Alteration of the pulmonary surfactant system in full-term infants with hereditary ABCA3 deficiency. *American Journal of Respiratory and Critical Care Medicine*. 2006;174(5):571-580.
29. Clement A, Nathan N, Epaud R, Fauroux B, Corvol H. Interstitial lung diseases in children. *Orphanet Journal of Rare Diseases*. 2010;522.
30. Hartl D, Griese M. Interstitial lung disease in children – genetic background and associated phenotypes. *Respiratory Research*. 2005;6(1):32.
31. Whitsett JA, Wert SE, Weaver TE. Alveolar Surfactant Homeostasis and the Pathogenesis of Pulmonary Disease. *Annual Review of Medicine*. 2010;61:105-119.
32. Dean M, Hamon Y, Chimini G. The human ATP-binding cassette (ABC) transporter superfamily. *Journal Of Lipid Research*. 2001;42(7):1007-17.
33. Klugbauer N, Hofmann F. Primary structure of a novel ABC transporter with a chromosomal localization on the band encoding the multidrug resistance-associated protein. *FEBS Letters*. 1996;391(1-2):61-65.
34. Engelbrecht S, Kaltenborn E, Griese M, Kern S. The surfactant lipid transporter ABCA3 is N-terminally cleaved inside LAMP3-positive vesicles. *FEBS Letters*. 2010;584(20):4306-12.
35. Schmitz G, Kaminski WE. ABC transporters and cholesterol metabolism. *Frontiers in bioscience a journal and virtual library*. 2001;6D505-D514.
36. Hayden MR, Clee SM, Brooks-Wilson A, Genest J, Attie A, Kastelein JJ. Cholesterol efflux regulatory protein, Tangier disease and familial high-density lipoprotein deficiency. *Current Opinion in Lipidology*. 2000;11(2):117-122.
37. Tsybovsky Y, Molday RS, Palczewski K. The ATP-binding cassette transporter ABCA4: structural and functional properties and role in retinal disease. *Advances in experimental medicine and biology*. 2010;703:105-125.
38. Dean M. The genetics of ATP-binding cassette transporters. *Methods in Enzymology*. 2005;400:409-429.
39. Oram JF. Tangier disease and ABCA1. *Biochimica et Biophysica Acta*. 2000;1529(1-3):321-330.
40. Sun H, Nathans J. ABCR: rod photoreceptor-specific ABC transporter responsible for Stargardt disease. *Methods in Enzymology*. 2000;315:879-897.
41. Mulugeta S, Gray JM, Notarfrancesco KL, et al. Identification of LBM180, a lamellar body limiting membrane protein of alveolar type II cells, as the ABC transporter protein ABCA3. *The Journal of Biological Chemistry*. 2002;277(25):22147-22155.
42. Yamano G, Funahashi H, Kawanami O, et al. ABCA3 is a lamellar body membrane protein in human lung alveolar type II cells. *FEBS Letters*. 2001;508(2):221-225.
43. Stahlman MT, Besnard V, Wert SE, et al. Expression of ABCA3 in developing lung and other tissues. *The journal of histochemistry and cytochemistry official journal of the Histochemistry Society*. 2007;55(1):71-83.
44. Yoshida I, Ban N, Inagaki N. Expression of ABCA3, a causative gene for fatal surfactant deficiency, is up-regulated by glucocorticoids in lung alveolar type II cells. *Biochemical and Biophysical Research Communications*. 2004;323(2):547-555.
45. Connors TD, Van Raay TJ, Petry LR, Klinger KW, Landes GM, Burn TC. The cloning of a human ABC gene (ABC3) mapping to chromosome 16p13.3. *Genomics*. 1997;39(2):231-234.
46. Bruder E, Hofmeister J, Aslanidis C, et al. Ultrastructural and molecular analysis in fatal neonatal interstitial pneumonia caused by a novel ABCA3 mutation. *Modern pathology an official journal of the United States and Canadian Academy of Pathology Inc*. 2007;20(10):1009-1018.
47. Bullard JE, Wert SE, Nogee LM. ABCA3 deficiency: neonatal respiratory failure and interstitial lung disease. *Seminars in Perinatology*. 2006;30(6):327-334.
48. Somaschini M, Nogee LM, Sassi I, et al. Unexplained neonatal respiratory distress due to congenital surfactant deficiency. *The Journal of pediatrics*. 2007;150(6):649-653, 653.e1.
49. Stahlman MT, Gray MP, Falconieri MW, Whitsett JA, Weaver TE. Lamellar body formation in normal and surfactant protein B-deficient fetal mice. *Laboratory investigation a journal of technical methods and pathology*. 2000;80(3):395-403.
50. DeMello DE, Heyman S, Phelps DS, et al. Ultrastructure of lung in surfactant protein B deficiency. *American Journal of Respiratory Cell and Molecular Biology*. 1994;11(2):230-239.
51. Brasch F, Griese M, Tredano M, et al. Interstitial lung disease in a baby with a de novo mutation in the SFTPC gene. *The European respiratory journal official journal of the European Society for Clinical Respiratory Physiology*. 2004;24(1):30-39.

52. Hamvas A, Nogee LM, White FV, et al. Progressive lung disease and surfactant dysfunction with a deletion in surfactant protein C gene. *American Journal of Respiratory Cell and Molecular Biology*. 2004;30(6):771-776.
53. Stevens PA, Pettenazzo A, Brasch F, et al. Nonspecific interstitial pneumonia, alveolar proteinosis, and abnormal proprotein trafficking resulting from a spontaneous mutation in the surfactant protein C gene. *Pediatric Research*. 2005;57(1):89-98.
54. Fitzgerald ML, Xavier R, Haley KJ, et al. ABCA3 inactivation in mice causes respiratory failure, loss of pulmonary surfactant, and depletion of lung phosphatidylglycerol. *Journal Of Lipid Research*. 2007;48(3):621-632.
55. Cheong N, Zhang H, Madesh M, et al. ABCA3 is critical for lamellar body biogenesis in vivo. *The Journal of Biological Chemistry*. 2007;282(33):23811-23817.
56. Hammel M, Michel G, Hoefler C, et al. Targeted inactivation of the murine Abca3 gene leads to respiratory failure in newborns with defective lamellar bodies. *Biochemical and Biophysical Research Communications*. 2007;359(4):947-951.
57. Cheong N, Madesh M, Gonzales LW, et al. Functional and trafficking defects in ATP binding cassette A3 mutants associated with respiratory distress syndrome. *The Journal of Biological Chemistry*. 2006;281(14):9791-9800.
58. Nagata K, Yamamoto A, Ban N, et al. Human ABCA3, a product of a responsible gene for abca3 for fatal surfactant deficiency in newborns, exhibits unique ATP hydrolysis activity and generates intracellular multilamellar vesicles. *Biochemical and Biophysical Research Communications*. 2004;324(1):262-268.
59. Matsumura Y, Sakai H, Sasaki M, Ban N, Inagaki N. ABCA3-mediated choline-phospholipids uptake into intracellular vesicles in A549 cells. *FEBS Letters*. 2007;581(17):3139-3144.
60. Ban N, Matsumura Y, Sakai H, et al. ABCA3 as a lipid transporter in pulmonary surfactant biogenesis. *The Journal of Biological Chemistry*. 2007;282(13):9628-9634.
61. Matsumura Y, Ban N, Ueda K, Inagaki N. Characterization and classification of ATP-binding cassette transporter ABCA3 mutants in fatal surfactant deficiency. *The Journal of Biological Chemistry*. 2006;281(45):34503-34514.
62. Matsumura Y, Ban N, Inagaki N. Aberrant catalytic cycle and impaired lipid transport into intracellular vesicles in ABCA3 mutants associated with nonfatal pediatric interstitial lung disease. *American journal of physiology Lung cellular and molecular physiology*. 2008;295(4):L698-L707.
63. Prestridge A, Wooldridge J, Deutsch G, et al. Persistent tachypnea and hypoxia in a 3-month-old term infant. *The Journal of pediatrics*. 2006;149(5):702-706.
64. Saugstad OD, Hansen TWR, Rønnestad A, et al. Novel mutations in the gene encoding ATP binding cassette protein member A3 (ABCA3) resulting in fatal neonatal lung disease. *Acta paediatrica*. 2007;96(2):185-190.
65. Bullard JE, Nogee LM. Heterozygosity for ABCA3 mutations modifies the severity of lung disease associated with a surfactant protein C gene (SFTPC) mutation. *Pediatric Research*. 2007;62(2):176-179.
66. Yokota T, Matsumura Y, Ban N, Matsubayashi T, Inagaki N. Heterozygous ABCA3 mutation associated with non-fatal evolution of respiratory distress. *European Journal of Pediatrics*. 2008;167(6):691-693.
67. Kunig AM, Parker TA, Nogee LM, Abman SH, Kinsella JP. ABCA3 deficiency presenting as persistent pulmonary hypertension of the newborn. *The Journal of pediatrics*. 2007;151(3):322-324.
68. Doan ML, Guillerman RP, Dishop MK, et al. Clinical, radiological and pathological features of ABCA3 mutations in children. *Thorax*. 2008;63(4):366-373.
69. Karjalainen MK, Haataja R, Hallman M. Haplotype analysis of ABCA3: association with respiratory distress in very premature infants. *Annals of Medicine*. 2008;40(1):56-65.
70. Garmany TH, Wambach JA, Heins HB, et al. Population and disease-based prevalence of the common mutations associated with surfactant deficiency. *Pediatric Research*. 2008;63(6):645-649.
71. Young LR, Nogee LM, Barnett B, Panos RJ, Colby TV, Deutsch GH. Usual interstitial pneumonia in an adolescent with ABCA3 mutations. *Chest*. 2008;134(1):192-195.
72. Ciantelli M, Ghirri P, Presi S, et al. Fatal respiratory failure in a full-term newborn with two ABCA3 gene mutations: a case report. *Journal of perinatology official journal of the California Perinatal Association*. 2011;31(1):70-72.
73. Anandarajan M, Paulraj S, Tubman R. ABCA3 Deficiency: an unusual cause of respiratory distress in the newborn. *The Ulster medical journal*. 2009;78(1):51-52.
74. Anelli T, Sitia R. Protein quality control in the early secretory pathway. *The European Molecular Biology Organization Journal*. 2008;27(2):315-327.
75. Ma Y, Hendershot LM. ER chaperone functions during normal and stress conditions. *Journal of Chemical Neuroanatomy*. 2004;28(1-2):51-65.
76. Ron D, Walter P. Signal integration in the endoplasmic reticulum unfolded protein response. *Nat Rev Mol Cell Biol*. 2007;8(7):519-529.

77. Malhotra JD, Kaufman RJ. The endoplasmic reticulum and the unfolded protein response. *Seminars in Cell Developmental Biology*. 2007;18(6):716-731.
78. Meusser B, Hirsch C, Jarosch E, Sommer T. ERAD: the long road to destruction. *Nature Cell Biology*. 2005;7(8):766-772.
79. Oyadomari S, Yun C, Fisher EA, et al. Cotranslocational degradation protects the stressed endoplasmic reticulum from protein overload. *Cell*. 2006;126(4):727-739.
80. Rao RV, Ellerby HM, Bredesen DE. Coupling endoplasmic reticulum stress to the cell death program. *Cell Death and Differentiation*. 2004;11(4):372-380.
81. Bertolotti A, Zhang Y, Hendershot LM, Harding HP, Ron D. Dynamic interaction of BiP and ER stress transducers in the unfolded-protein response. *Nature Cell Biology*. 2000;2(6):326-332.
82. Yoshida H, Matsui T, Yamamoto A, Okada T, Mori K. XBP1 mRNA is induced by ATF6 and spliced by IRE1 in response to ER stress to produce a highly active transcription factor. *Cell*. 2001;107(7):881-891.
83. Uemura A, Oku M, Mori K, Yoshida H. Unconventional splicing of XBP1 mRNA occurs in the cytoplasm during the mammalian unfolded protein response. *Journal of Cell Science*. 2009;122(Pt 16):2877-2886.
84. Back SH, Lee K, Vink E, Kaufman RJ. Cytoplasmic IRE1 $\alpha$ -mediated XBP1 mRNA splicing in the absence of nuclear processing and endoplasmic reticulum stress. *The Journal of Biological Chemistry*. 2006;281(27):18691-18706.
85. Yoshida H, Oku M, Suzuki M, Mori K. pXBP1(U) encoded in XBP1 pre-mRNA negatively regulates unfolded protein response activator pXBP1(S) in mammalian ER stress response. *The Journal of Cell Biology*. 2006;172(4):565-575.
86. Yoshida H, Matsui T, Hosokawa N, Kaufman RJ, Nagata K, Mori K. A time-dependent phase shift in the mammalian unfolded protein response. *Developmental Cell*. 2003;4(2):265-271.
87. Hollien J, Lin JH, Li H, Stevens N, Walter P, Weissman JS. Regulated Ire1-dependent decay of messenger RNAs in mammalian cells. *The Journal of Cell Biology*. 2009;186(3):323-331.
88. Adachi Y, Yamamoto K, Okada T, Yoshida H, Harada A, Mori K. ATF6 is a transcription factor specializing in the regulation of quality control proteins in the endoplasmic reticulum. *Cell Structure and Function*. 2008;33(1):75-89.
89. Liu CY, Kaufman RJ. The unfolded protein response. *Journal of Cell Science*. 2003;116(Pt 10):1861-1862.
90. Tardif KD, Waris G, Siddiqui A. Hepatitis C virus, ER stress, and oxidative stress. *Trends in Microbiology*. 2005;13(4):159-163.
91. Thornberry NA. Caspases: Enemies Within. *Science*. 1998;281(5381):1312-1316.
92. Li P, Nijhawan D, Budihardjo I, et al. Cytochrome c and dATP-Dependent Formation of Apaf-1 / Caspase-9 Complex Initiates an Apoptotic Protease Cascade. *Cell*. 1997;91:479-489.
93. Nakagawa T, Zhu H, Morishima N, et al. Caspase-12 mediates endoplasmic-reticulum-specific apoptosis and cytotoxicity by amyloid- $\beta$ . *Nature*. 2000;403(6765):98-103.
94. Mulugeta S, Maguire JA, Newitt JL, Russo SJ, Kotorashvili A, Beers MF. Misfolded BRICHOS SP-C mutant proteins induce apoptosis via caspase-4- and cytochrome c-related mechanisms. *American journal of physiology Lung cellular and molecular physiology*. 2007;293(3):L720-L729.
95. Hitomi J, Katayama T, Taniguchi M, Honda A, Imaizumi K, Tohyama M. Apoptosis induced by endoplasmic reticulum stress depends on activation of caspase-3 via caspase-12. *Neuroscience Letters*. 2004;357(2):127-130.
96. Morishima N, Nakanishi K, Takenouchi H, Shibata T, Yasuhiko Y. An endoplasmic reticulum stress-specific caspase cascade in apoptosis. Cytochrome c-independent activation of caspase-9 by caspase-12. *The Journal of Biological Chemistry*. 2002;277(37):34287-94.
97. Balasubramanian K, Mirnikjoo B, Schroit AJ. Regulated Externalization of Phosphatidylserine at the Cell Surface. *Journal of Biological Chemistry*. 2007;282(25):18357-18364.
98. Blankenberg FG. Imaging the molecular signatures of apoptosis and injury with radiolabeled annexin V. *Proceedings of the American Thoracic Society*. 2009;6(5):469-476.
99. Laufer EM, Winkens HM, Corsten MF, Reutelingsperger CPM, Narula J, Hofstra L. PET and SPECT imaging of apoptosis in vulnerable atherosclerotic plaques with radiolabeled Annexin A5. *The quarterly journal of nuclear medicine and molecular imaging official publication of the Italian Association of Nuclear Medicine AIMN and the International Association of Radiopharmacology IAR and Section of the Society of*. 2009;53(1):26-34.
100. Wu J, Kaufman RJ. From acute ER stress to physiological roles of the Unfolded Protein Response. *Cell Death and Differentiation*. 2006;13(3):374-384.
101. Marciniak SJ, Ron D. Endoplasmic reticulum stress signaling in disease. *Physiological Reviews*. 2006;86(4):1133-1149.

102. Kim I, Xu W, Reed JC. Cell death and endoplasmic reticulum stress: disease relevance and therapeutic opportunities. *Nature Reviews Drug Discovery*. 2008;7(12):1013-1030.
103. Korfei M, Ruppert C, Mahavadi P, et al. Epithelial endoplasmic reticulum stress and apoptosis in sporadic idiopathic pulmonary fibrosis. *American Journal of Respiratory and Critical Care Medicine*. 2008;178(8):838-46.
104. Drakopanagiotakis F, Xifteri A, Polychronopoulos V, Bouros D. Apoptosis in lung injury and fibrosis. *The European respiratory journal official journal of the European Society for Clinical Respiratory Physiology*. 2008;32(6):1631-1638.
105. Lawson WE, Crossno PF, Polosukhin VV, et al. Endoplasmic reticulum stress in alveolar epithelial cells is prominent in IPF: association with altered surfactant protein processing and herpesvirus infection. *American journal of physiology Lung cellular and molecular physiology*. 2008;294(6):L1119-L1126.
106. Mulugeta S, Nguyen V, Russo SJ, Muniswamy M, Beers MF. A Surfactant Protein C Precursor Protein BRICHOS Domain Mutation Causes Endoplasmic Reticulum Stress, Proteasome Dysfunction, and Caspase 3 Activation. *American Journal of Respiratory Cell and Molecular Biology*. 2005;32(6):521-530.
107. Selman M, King TE, Pardo A. Idiopathic pulmonary fibrosis: prevailing and evolving hypotheses about its pathogenesis and implications for therapy. In: *Annals of Internal Medicine*. 2001. p.136-151.
108. Gauldie J, Kolb M, Sime PJ. A new direction in the pathogenesis of idiopathic pulmonary fibrosis? *Respiratory Research*. 2002;3(1):1.
109. Kim JH, Jang YS, Eom K-S, et al. Transforming Growth Factor  $\beta$ 1 Induces Epithelial-to-Mesenchymal Transition of A549 Cells. 2007;22(5):898-904.
110. Corvol H, Flamein F, Epaud R, Clement A, Guillot L. Lung alveolar epithelium and interstitial lung disease. *International Journal of Biochemistry*. 2009;41(8-9):1643-51.
111. Kapanci Y, Desmouliere A, Pache JC, Redard M, Gabbiani G. Cytoskeletal protein modulation in pulmonary alveolar myofibroblasts during idiopathic pulmonary fibrosis. Possible role of transforming growth factor beta and tumor necrosis factor alpha. *American Journal of Respiratory and Critical Care Medicine*. 1995;152(6 Pt 1):2163-2169.
112. Bals R, Hiemstra PS. Innate immunity in the lung: how epithelial cells fight against respiratory pathogens. *The European respiratory journal official journal of the European Society for Clinical Respiratory Physiology*. 2004;23(2):327-333.
113. Kelly M, Kolb M, Bonniaud P, Gauldie J. Re-evaluation of fibrogenic cytokines in lung fibrosis. *Current Pharmaceutical Design*. 2003;9(1):39-49.
114. Kasai H, Allen JT, Mason RM, Kamimura T, Zhang Z. TGF- $\beta$ 1 induces human alveolar epithelial to mesenchymal cell transition (EMT). *Respiratory Research*. 2005;6(1):56.
115. Nelson M, McClelland M. Use of DNA methyltransferase/endonuclease enzyme combinations for megabase mapping of chromosomes. *Methods in Enzymology*. 1992;216:279-303.
116. Buck TM, Wright CM, Brodsky JL. The activities and function of molecular chaperones in the endoplasmic reticulum. *Seminars in cell developmental biology*. 2007;18(6):751-761.
117. Hybiske K, Fu Z, Schwarzer C, et al. Effects of cystic fibrosis transmembrane conductance regulator and DeltaF508CFTR on inflammatory response, ER stress, and Ca<sup>2+</sup> of airway epithelia. *American journal of physiology Lung cellular and molecular physiology*. 2007;293(5):L1250-L1260.
118. Balasubramanian K, Schroit AJ. Aminophospholipid asymmetry: A matter of life and death. *Annual Review of Physiology*. 2003;65(1):701-734.
119. Franco R, Schoneveld OJ, Pappa A, Panayiotidis MI. The central role of glutathione in the pathophysiology of human diseases. *Archives of Physiology and Biochemistry*. 2007;113(4-5):234-258.
120. Kumar S. Caspase function in programmed cell death. *Cell Death and Differentiation*. 2007;14(1):32-43.
121. Iwano M, Plieth D, Danoff TM, Xue C, Okada H, Neilson EG. Evidence that fibroblasts derive from epithelium during tissue fibrosis. *Journal of Clinical Investigation*. 2002;110(3):341-350.
122. Mason RJ. Biology of alveolar type II cells. *Respirology Carlton Vic*. 2006;11 Suppl(s1):S12-S15.
123. Tanaka AR, Abe-Dohmae S, Ohnishi T, et al. Effects of mutations of ABCA1 in the first extracellular domain on subcellular trafficking and ATP binding/hydrolysis. *The Journal of Biological Chemistry*. 2003;278(10):8815-9.
124. Pilewski JM, Frizzell RA. Role of CFTR in airway disease. *Physiological Reviews*. 1999;79(1 Suppl):S215-S255.
125. Cheng SH, Gregory RJ, Marshall J, et al. Defective intracellular transport and processing of CFTR is the molecular basis of most cystic fibrosis. *Cell*. 1990;63(4):827-834.
126. Xu C, Bailly-Maitre B, Reed JC. Endoplasmic reticulum stress: cell life and death decisions. *Journal of Clinical Investigation*. 2005;115(10):2656-2664.
127. Bartoszewski R, Rab A, Jurkuvenaite A, et al. Activation of the unfolded protein response by deltaF508 CFTR. *American Journal of Respiratory Cell and Molecular Biology*. 2008;39(4):448-457.

128. Lawless MW, Greene CM, Mulgrew A, Taggart CC, O'Neill SJ, McElvaney NG. Activation of endoplasmic reticulum-specific stress responses associated with the conformational disease Z alpha 1-antitrypsin deficiency. *The Journal of Immunology*. 2004;172(9):5722-5726.
129. Lindholm D, Wootz H, Korhonen L. ER stress and neurodegenerative diseases. *Cell Death and Differentiation*. 2006;13(3):385-392.
130. He B. Viruses, endoplasmic reticulum stress, and interferon responses. *Cell Death and Differentiation*. 2006;13(3):393-403.
131. Jorgensen E, Stinson A, Shan L, Yang J, Gietl D, Albino AP. Cigarette smoke induces endoplasmic reticulum stress and the unfolded protein response in normal and malignant human lung cells. *BMC Cancer*. 2008;8:229.
132. Smith WW, Jiang H, Pei Z, et al. Endoplasmic reticulum stress and mitochondrial cell death pathways mediate A53T mutant alpha-synuclein-induced toxicity. *Human Molecular Genetics*. 2005;14(24):3801-3811.
133. Barbas-Filho J, Ferreira M, Sesso A, Kairalla R, Carvalho C, Capelozzi V. Evidence of type II pneumocyte apoptosis in the pathogenesis of idiopathic pulmonary fibrosis (IFP)/usual interstitial pneumonia (UIP). *Journal of Clinical Pathology*. 2001;54(2):132-138.
134. Uhal BD, Joshi I, Hughes WF, Ramos C, Pardo A, Selman M. Alveolar epithelial cell death adjacent to underlying myofibroblasts in advanced fibrotic human lung. *American Journal of Physiology*. 1998;275(6 Pt 1):L1192-L1199.
135. Selman M, Pardo A. Role of epithelial cells in idiopathic pulmonary fibrosis: from innocent targets to serial killers. *Proceedings of the American Thoracic Society*. 2006;3(4):364-372.
136. Desmoulière A, Darby IA, Gabbiani G. Normal and pathologic soft tissue remodeling: role of the myofibroblast, with special emphasis on liver and kidney fibrosis. *Laboratory investigation a journal of technical methods and pathology*. 2003;83(12):1689-1707
137. Marmai C, Sutherland R, Kim K, Dolganov G, Fang X, Kim S, Jiang S, Golden J, Hoopes C, Matthay M, Chapman H, Wolters P. Alveolar Epithelial Cells Express Mesenchymal Proteins in Patients With Idiopathic Pulmonary Fibrosis. *Am J Physiol Lung Cell Mol Physiol* April 15, 2011 ajpgung.00212.2010
138. Zhong Q, Zhou B, Ann D, Minoo P, Liu Y, Banfalvi A, Krishnaveni M, Dubourd M, Demaio L, Willis B, Kim K, duBois R, Crandall E, Beers M and Borok Z. Role of ER Stress in EMT of Alveolar Epithelial Cells: Effects of Misfolded Surfactant Protein. *Am. J. Respir. Cell Mol. Biol.* 2010; 0: 2010-0347OCv1

## 9. List of tables

Table 1: Overview of <i>ABCA3</i> mutations examined in previous studies <i>in vitro</i> .....	10
Table 2: Characteristics of patients with <i>ABCA3</i> mutations analyzed in this study.....	14
Table 3: List of primers for point mutagenesis or sequencing.....	23
Table 4: List of primers for RT-PCR.....	23
Table 5: List of vectors .....	24
Table 6: List of primary antibodies used for Western Blotting (WB) or immunofluorescence (IF).....	26
Table 7: List of secondary antibodies used for IF .....	26
Table 8: List of secondary antibodies used for WB .....	27
Table 9: List of antibodies used for flow cytometry .....	27
Table 10: Optimal conditions for PCR in this study.....	29
Table 11: Gels with different acrylamide concentration were used for SDS-PAGE depending on protein size of interest .....	33
Table 12: Optimal cycling parameters for RT-PCR in this study.....	35

## 10. List of figures

Fig.1: Distribution of pediatric ILD in Germany.....	3
Fig.2: Classification of diffuse lung disease in children.....	4
Fig.3: A representative electron micrograph of a lamellar body in A549 cells .....	5
Fig.4: Structure of an ABC-transporter.....	7
Fig.5: Structure of the ABCA3 transporter in a lipid bilayer membrane .....	8
Fig.6: Localization of the <i>ABCA3</i> mutations R43L, R280C and L101P within the <i>ABCA3</i> transporter.....	13
Fig.7: Schematic representation of the splicing of XBP1 mRNA.....	16
Fig.8: Overview of the UPR system and its elements .....	16
Fig.9: Scheme of the mechanism how ER stress causes apoptotic cell death .....	18
Fig.10: Vector map of pEYFP-N1.....	25
Fig.11: Vector map of pUB6/V5-His .....	28
Fig.12: Transfection of A549 cell line with pEYFP- <i>ABCA3</i> -WT .....	31
Fig.13: Vector map of pUB6- <i>hABCA3-HA</i> -WT.....	37
Fig.14: Vector map of pEYFP- <i>ABCA3</i> -WT.....	38
Fig.15: Analysis of pUB6/ <i>hABCA3-HA</i> -WT, -R43L, R280C and -L101P plasmids .....	39
Fig.16: Analysis of pEYFP/ <i>ABCA3</i> -WT, -R43L, R280C and -L101P plasmids .....	39
Fig.17: Immunofluorescence studies in A549 cell line, transiently transfected with pEYFP- <i>ABCA3</i> -WT.....	40
Fig.18: Intracellular localization of the WT and mutant R43L, R280C and L101P <i>ABCA3</i> proteins (I).....	42
Fig.19: Intracellular localization of the WT and mutant R43L, R280C and L101P <i>ABCA3</i> proteins (II) .....	43
Fig.20: Intracellular localization of the WT and mutant R43L, R280C and L101P <i>ABCA3</i> proteins (III).....	43
Fig.21: Intracellular colocalization of <i>ABCA3</i> WT and SP-C WT protein .....	44
Fig.22: Processing of the WT and mutant R43L, R280C and L101P <i>ABCA3</i> .....	45

Fig.23: Functionality of the R43L and R280C transporters .....	47
Fig.24: Influence of WT ABCA3 and three mutations on biogenesis of LAMP3 <sup>+</sup> vesicles in A549 transfected with pUB6/HA-ABCA3.....	48
Fig.25: ER stress chaperone BiP .....	49
Fig.26: ER stress chaperone Hsp 90 .....	50
Fig.27: ER stress chaperone calnexin .....	51
Fig.28: Susceptibility of A549 cells with ABCA3 mutations to ER stress measured by XBP1 splicing .....	53
Fig.29: Early apoptosis marker caspase 3 .....	56
Fig.30 Apoptosis in A549 cells expressing L101P and R280 mutations .....	57
Fig.31: Apoptotic signaling in cells with L101P and R280C mutations is activated by ER stress.....	59
Fig.32: Induction of EMT in A549 cell line through different concentrations of TGF- $\beta$ 1.....	61
Fig.33: ECAD in A549 cell line in absence and presence of TGF $\beta$ 1 .....	61
Fig.34: ECAD and vimentin in A549 cells expressing ABCA3 WT or mutant proteins.....	62
Fig.35: Marker of myofibroblasts vimentin in A549 cells expressing ABCA3 WT or mutant proteins under additional stimulation with 0.5 ng/ml of TGF- $\beta$ 1 .....	63
Fig.36: Hypothesis of early and late onset of lung disease caused by ABCA3 mutations .....	69
Fig 37: EMT in ATII as a possible mechanism of lung fibrogenesis in children with ABCA3 mutation .....	71

## 11. Danksagung

Mein Dank gilt im besonderen meinem Doktorvater Herrn Prof. Dr. Matthias Griese für die Überlassung des Themas, für die ausgezeichnete Betreuung und die wissenschaftlichen Anregungen und Hilfestellungen. Darüber hinaus danke ich ihm für seine warmen und aufbauenden Worte in Borstel, die bis heute in mir nachklingen und mir Mut vor jedem neuen Vortrag machen.

Des Weiteren möchte ich meinen beiden Betreuern im Labor, Frau Dr. S. Kern und Herr Dr. M. Woischnik, für ihre Unterstützung und Ausdauer sowohl bei der Lösung der methodischen Probleme als auch bei der Interpretation der erhobenen Daten, danken, sowie für die Hilfe bei der Anfertigung von Abbildungen und Zeichnungen.

Besonderer Dank gilt der MTA Frau Stefanie Gruschka für ihre Unterstützung bei der Umsetzung der Experimente, ihre Hilfsbereitschaft und ihre Freundschaft.

Meiner Mitdotorandin Eva Kaltenborn danke ich für die gute Zusammenarbeit im Labor und ihre Hilfsbereitschaft und Ausdauer bei der Erstellung unsere Veröffentlichung. Bei meinen Mitdotoranden Steffi Heinrich und Christiane Sparr und unserer technischen Assistentin Andrea Schams möchte ich mich für die gute Zusammenarbeit bedanken.

Vielen Dank auch an unsere beiden Postdocs Herrn Dr. D. Hartl und Herrn Dr. A. Hector für die Unterstützung bei der Planung und Ausführung der durchflusszytometrischen Analysen.

Besonderer Dank gilt meiner Familie und im Besonderen meiner Mutter. Ihre Unterstützung und anhaltende Motivation trugen entscheidend zur Anfertigung der experimentellen Arbeit als auch zur Fertigstellung dieses Manuskripts bei. Weil sie mich berät und mir mit ihrer Erfahrung stets zur Seite steht, bin ich heute dort, wo ich sein möchte.

Meinem Freund Stephan danke ich für seine liebevolle Unterstützung und für die Hilfe bei der Anfertigung der Abbildungen und Tabellen.

## 12. Publication list

**Weichert N**, Kaltenborn E, Hector A, Woischnik M, Schams A, Holzinger A, Kern S and Griese M: Some ABCA3 mutations elevate ER stress and initiate apoptosis of lung epithelial cells. *Respiratory Research* 2011, 12:4

### Posters and presentations

1. *Cellular mechanisms of interstitial lung disease in children caused by mutations of the ABCA3-transporter*  
Presentation: Herbsttreffen der Sektion Zellbiologie der DGP 2009
2. **Nina Weichert**, Eva Kaltenborn, Andreas Hector, Markus Woischnik, Suncana Moslavac, Matthias Griese: *How ABCA3 Mutations disturb the homeostasis of type-II pneumocytes*  
Posterpresentation: Treffen des Forschungskubus der Dr. von Haunerschen Kinderklinik 2009
3. **Nina Weichert**, Eva Kaltenborn, Andreas Hector, Markus Woischnik, Suncana Moslavac, Matthias Griese: *Cellular mechanisms of interstitial lung disease in children caused by mutations of the ABCA3-transporter*  
Posterpresentation: DoktaMed 2009 at LMU München
4. **Nina Weichert**, Eva Kaltenborn, Andreas Hector, Markus Woischnik, Suncana Moslavac, Matthias Griese: *Molekulare und zelluläre Pathomechanismen interstitieller Lungenerkrankungen verursacht durch Mutationen im ABCA3-Transporter*  
Posterpresentation: Herbsttreffen der Sektion Zellbiologie der DGP 2008

### Award:

Poster Award: **Nina Weichert**, Eva Kaltenborn, Andreas Hector, Markus Woischnik, Suncana Moslavac, Matthias Griese: *Cellular mechanisms of interstitial lung disease in children caused by mutations of the ABCA3-transporter*  
DoktaMed 2009 at LMU München